UNIVERZITA PALACKÉHO V OLOMOUCI

Přírodovědecká fakulta

Katedra biotechnologií

Specifické farmakologické modulátory agregace a šíření tau proteinu pro terapii Alzheimerovy choroby

DIPLOMOVÁ PRÁCE

Autor:	**Bc. Martina Pavlíková**
Studijní program:	B0512A130007 Biotechnologie a genové inženýrství
Studijní obor:	Biotechnologie a genové inženýrství
Forma studia:	Prezenční
Vedoucí práce:	**Mgr. Viswanath Das, Ph.D.**
Rok:	2024

PALACKÝ UNIVERSITY IN OLOMOUC

Faculty of Science

Department of Biotechnology

Specific pharmacological modulators of tau aggregation and spreading for Alzheimer's disease therapy

MASTER'S THESIS

Author:	**Bc. Martina Pavlíková**
Study program:	B0512A130007 Biotechnology and Genetic engineering
Branch of study:	Biotechnology and Genetic engineering
Form of study:	Attendant
Supervisor:	**Mgr. Viswanath Das, Ph.D.**
Year:	2024

Prohlašuji, že jsem diplomovou práci vypracovala samostatně pod vedením Mgr. Viswanath Dase, Ph.D. s vyznačením všech použitých pramenů a spoluautorství. Souhlasím se zveřejněním diplomové práce podle zákona č. 111/1998 Sb., o vysokých školách, ve znění pozdějších předpisů. Byla jsem seznámena s tím, že se na moji práci vztahují práva a povinnosti vyplývající ze zákona č. 121/2000 Sb. autorský zákon, ve znění pozdějších předpisů.

V Olomouci dne 30. 4. 2024

.....

Bc. Martina Pavlíková

I declare that I have prepared the master's thesis independently under the supervision of Mgr. Viswanath Das, Ph.D., indicating all sources used and co-authorship. I agree with the publication of the master's thesis according to Act No. 111/1998 Coll., on Higher Education, as amended. As amended, I have been informed that my thesis is subject to the rights and obligations arising from Act No. 121/2000 Coll., Copyright Act.

In Olomouc on 30. 4. 2024

.....

Bc. Martina Pavlíková

Acknowledgements

First, I would like to thank my supervisor, Mgr. Viswanath Das, Ph.D., for his guidance and valuable advice during the preparation of this thesis. I am also indebted to Mgr. Narendran Annadurai, Ph.D., for his assistance with laboratory experiments and for imparting practical skills that have enriched my research endeavours. Additionally, I extend my thanks to Ing. Soňa Gurská, Ph.D., for her help in handling and preparing the drug experiments. I am also grateful to the entire staff of the Institute of Molecular and Translational Medicine for their kind attitude and willingness to help, with special mention to Mgr. Anna Janošťáková for her guidance and expertise in cell culturing techniques.

Lastly, I express my heartfelt appreciation to my family and friends, particularly my parents and my dear friend Milena Antoníčková, for their unwavering moral support and encouragement throughout the preparation of this thesis and my studies.

This work was supported in parts by the infrastructural projects (CZ-OPENSCREEN – LM2023052; EATRIS-CZ – LM2023053), large RI Project (Czech-BioImaging – LM2023050; LM2018129), the projects National Institute for Neurological Research (Program EXCELES, ID Project No. LX22NPO5107) - Funded by the European Union - Next Generation EU from the Ministry of Education, Youth and Sports of the Czech Republic (MEYS), project TN02000109 (Personalized Medicine: From Translational Research into Biomedical Applications is co-financed with the state support of the Technology Agency of the Czech Republic as part of the National Centers of Competence Program), and the Grant Agency of the Czech Republic (Grant # 23-06301J).

Bibliografická identifikace

Jméno a příjmení autora	Bc. Martina Pavlíková
Název práce	Specifické farmakologické modulátory agregace a šíření tau proteinu pro terapii Alzheimerovy choroby
Typ práce	Diplomová
Pracoviště	Ústav Molekulární a Translační Medicíny
Vedoucí práce	Mgr. Viswanath Das, Ph.D.
Rok obhajoby práce	2024

Abstrakt

Neurodegenerativní onemocnění, jako je Alzheimerova choroba (AD), představují v klinické praxi značné výzvy kvůli svému postupnému průběhu a devastujícímu dopadu na kognitivní funkce. AD je charakterizována akumulací tau proteinových agregátů, což vede k tvorbě neurofibrilárních klubek a dysfunkci synapsí. Tato studie si kladla za cíl identifikovat potenciální farmakologické látky schopné modulovat dynamiku agregace tau prostřednictvím screeningu látek uložených v Prestwick Chemical Library®. S využitím tau peptidů jako modelu *in vitro* byly provedeny testy k posouzení účinnosti kandidátů na léčiva při inhibici agregace tau. Buněčné modely byly dále použity k vyhodnocení schopnosti vybraných sloučenin zabránit šíření tau a tvorbě intracelulárních agregátů. Výzkum odhalil Chicago sky blue 6B, Dopamin hydrochlorid a Methacyklin hydrochlorid jako slibné kandidáty s inhibičními účinky na agregaci tau. Tato zjištění přinášejí nové poznatky o strategiích pro modulaci dynamiky agregace tau a nabízejí potenciální cesty pro vývoj cílených terapií zaměřených na zpomalení průběhu onemocnění a zachování kognitivních funkcí u Alzheimerovy choroby.

Klíčová slova	tau protein, Alzheimerova choroba, tauopatie, Thioflavin T, agregace tau proteinu, seeding tau proteinu, šíření tau proteinu, biosensorové buňky, chemická knihovna, léky
Počet stran	64
Počet příloh	1
Jazyk	Anglický

Bibliographical identification

Author's first name and surname	Bc. Martina Pavlíková
Title	Specific pharmacological modulators of tau aggregation and spreading for Alzheimer's disease therapy
Type of thesis	Master
Department	Institute of Molecular and Translational Medicine
Supervisor	Mgr. Viswanath Das, Ph.D.
The year of presentation	2024

Abstract

Neurodegenerative diseases, exemplified by Alzheimer's disease (AD), present formidable challenges in clinical management due to their progressive nature and devastating impact on cognitive function. AD is characterized by the accumulation of tau protein aggregates, resulting in the formation of neurofibrillary tangles and synaptic dysfunction. This study aimed to identify potential pharmacological agents capable of modulating tau aggregation dynamics through screening the Prestwick Chemical Library®. By utilizing tau peptides as an *in vitro* model, the study assessed the efficacy of drug candidates in inhibiting tau aggregation. Cellular models were subsequently employed to evaluate the ability of selected compounds to prevent tau spreading and intracellular aggregate formation. The investigation unveiled Chicago sky blue 6B, Dopamine hydrochloride, and Methacycline hydrochloride as promising candidates with inhibitory effects on tau aggregation. These findings shed light on novel strategies for modulating tau aggregation dynamics, offering potential avenues for the development of targeted therapies aimed at slowing disease progression and preserving cognitive function in Alzheimer's disease.

Keywords	tau protein, Alzheimer's disease, tauopathy, Thioflavin T, tau aggregation, tau seeding, tau spreading, biosensor cells, chemical library, drugs
Number of pages	64
Number of appendices	1
Language	English

Contents

Aims and objectives of the thesis

The study aims to screen the Prestwick Chemical Library® containing diverse approved and literature drugs with known biological activities to identify specific pharmacological modulators of tau aggregation and spreading.

This will be achieved by pursuing the following objectives:

1. Utilizing tau peptides as an *in vitro* model and employing a thioflavin T binding assay and high-content imaging to screen drugs.
2. Using cellular models of tau spreading to test the effects of selected drugs and to identify inhibitors that prevent the formation of tau prion-like aggregates.

1 INTRODUCTION

Alzheimer's disease (AD) represents a formidable challenge to public health, with its prevalence steadily increasing as populations age worldwide. Characterized by progressive cognitive decline and memory loss, AD severely impacts patients' quality of life and presents a significant burden on healthcare systems. Despite extensive research efforts, effective disease-modifying treatments for AD remain elusive, emphasizing the urgent need for innovative therapeutic approaches.

One of the pathological hallmarks of AD is the abnormal aggregation and spreading of tau protein, leading to the formation of neurofibrillary tangles (NFTs) and neuronal dysfunction. Targeting tau aggregation and propagation has emerged as a promising strategy for AD therapy, with the potential to halt disease progression and alleviate symptoms.

This thesis aims to investigate specific pharmacological modulators of tau aggregation and spreading for AD therapy. The study seeks to screen the Prestwick Chemical Library® comprising diverse approved and literature drugs with known biological activities to identify potential candidates capable of modulating tau pathology. Utilizing tau peptides as an *in vitro* model, the study will employ a Thioflavin T binding assay and high-content imaging to screen the library of drugs systematically.

The primary objective of this research is to identify compounds within the Prestwick Chemical Library® that exhibit the ability to modulate tau aggregation and spreading. Subsequently, selected drugs showing promising results will undergo further evaluation in cellular models of tau spreading. By testing these compounds in cellular systems, the study aims to identify inhibitors capable of preventing the formation of tau prion-like aggregates, a critical step toward developing effective AD therapies.

Through a comprehensive screening approach and subsequent validation in cellular models, this thesis endeavors to contribute to the identification of novel pharmacological agents for the treatment of AD. By identifying potential therapeutic compounds, this research aims to facilitate the development of urgently needed disease-modifying treatments.

2 CURRENT STATE OF THE PROBLEM

2.1 Neurodegenerative diseases

2.1.1 Pathogenesis and diagnosis

The group of neurodegenerative diseases (NDs) is characterized by complex disorders that pose significant health challenges for the world's population. The prevalence of these diseases has been steadily increasing due to the rising number of older adults (Heemels 2016; Gitler *et al.* 2017; Dugger and Dickson 2017; Vaquer-Alicea and Diamond 2019). NDs encompass a variety of conditions, with the most common types being amyloidoses, tauopathies, and α-synucleinopathies. Prominent diseases within these categories include Alzheimer's disease (AD), Parkinson's disease (PD), and Huntington's disease (HD) (Dugger and Dickson 2017). The pathology of NDs is characterized by neuronal loss and progressive degeneration in various areas of the nervous system. However, the exact pathogenesis remains unclear, although there is evidence suggesting a complex interplay among genetic, epigenetic, and environmental factors (Fayazi *et al.* 2021; Agnello and Ciaccio 2022).

The clinical manifestations of NDs encompass extrapyramidal and pyramidal movement disorders, as well as cognitive or behavioral disturbances. Patients often present with a combination of these symptoms at the time of diagnosis. Fundamental features of neurodegenerative diseases involve progressive neuronal dysfunction and eventual cell death, which are mediated by processes such as proteotoxic stress, abnormalities in the ubiquitin-proteasomal and autophagosomal/lysosomal systems, oxidative stress, programmed cell death, and neuroinflammation. These diseases are further characterized by the accumulation of specific proteins and vulnerabilities in certain anatomical regions. Moreover, it's important to note that protein abnormalities indicative of NDs may manifest before the onset of clinical symptoms (Dugger and Dickson 2017; Fayazi *et al.* 2021).

Currently, there is no known cure for any neurodegenerative disease. Western medicine primarily focuses on managing symptoms to improve patients' quality of life, which may involve alleviating pain or enhancing mobility. Initial therapies included neurotransmitter-based treatments, enzyme inhibitors, direct receptor agonists, and second messenger modulators. These approaches have been succeeded by various pharmacotherapy groups, many of which have been approved for clinical use over the years. Common drug classes used in the treatment of neurodegenerative diseases

include dopaminergic agents to replace dopamine, acetylcholinesterase inhibitors to hinder the action of cholinesterase, and analgesics for pain relief. Additionally, surgical interventions like deep brain stimulation are employed to address various movement disorders. However, to develop more effective treatments, a thorough understanding of the underlying causes and mechanisms of each disease is essential. Only through this comprehensive understanding can researchers hope to uncover novel therapeutic approaches for neurodegenerative conditions (Gitler *et al.* 2017; Fayazi *et al.* 2021).

2.1.2 Synucleinopathies

Synucleinopathies constitute a group of neurodegenerative disorders characterized by the abnormal aggregation of α-synuclein. This neuronal protein, composed of 140 amino acids, is organized into three distinct domains. The N-terminal domain is notable for its lipid-binding properties, while the central domain, referred to as the non-amyloid-β component or highly amyloidogenic domain, plays a crucial role in α-synuclein aggregation. Conversely, the C-terminal domain contributes to the native unfolded structure of α-synuclein (Dugger and Dickson 2017; Coon and Singer 2020; Koga *et al.* 2021). Synucleinopathies encompass a spectrum of clinically diverse diseases, distinguished by variations in the cellular localization and distribution pattern of α-synuclein deposition. Examples include multiple system atrophy, dementia with Lewy bodies, and Parkinson's disease (Coon and Singer 2020).

PD is classified as a chronic progressive disorder and ranks as the second most common neurodegenerative disease, primarily affecting older individuals in the population. Patients with PD experience a range of clinical symptoms, encompassing both motor and non-motor manifestations. Motor symptoms of PD include resting tremor (typically starting unilaterally), bradykinesia (slow movements), rigidity, shuffling gait, and postural instability. Non-motor symptoms are characterized by cognitive changes, behavioral or neuropsychiatric alterations, symptoms related to autonomic nervous system dysfunction, sensory impairments, and disturbances in sleep patterns. The principal pathological mechanisms underlying PD involve the progressive degeneration of dopaminergic neurons, responsible for producing and transmitting dopamine, in the *substantia nigra pars compacta*—a basal ganglia structure located in the midbrain. Additionally, the development of Lewy Bodies, recognized as a pathologic hallmark, occurs within these affected neurons (Beitz 2014; Gomperts 2016; Lotankar *et al.* 2017; Coon and Singer 2020).

The current treatment of PD is typically categorized into three main approaches: medical therapies, surgical therapies, and experimental therapies. The selection of therapy for an individual patient depends on several factors, including the patient's age, disease stage, predominant symptoms, and the balance of benefits and risks associated with each treatment option. Medical therapies encompass both pharmacological and non-pharmacological interventions. Pharmacotherapy aims to address dopamine deficits and neurotransmitter imbalances, thereby slowing the progression of PD. Non-pharmacological approaches seek to improve certain aspects of the disease or manage its effects through strategies such as exercise programs, educational interventions, participation in support groups, and speech therapy. Surgical therapies, such as deep brain stimulation, are considered when a PD patient begins to experience diminished effectiveness of dopaminergic medications over time. Deep brain stimulation involves the implantation of electrodes in specific brain regions to modulate neural activity and alleviate motor symptoms. Experimental therapies, including gene therapy, are still in the research phase but hold promise as potential treatments for PD. These innovative approaches aim to target underlying disease mechanisms and offer hope for more effective management of this increasingly prevalent condition (Beitz 2014; Coon and Singer 2020).

2.1.3 Trinucleotide repeat disorders

As highlighted earlier, the development of neurodegenerative diseases involves various factors, including genetic components. Within the human DNA sequence, there are repetitive DNA sequences that have the potential to contribute to biodiversity due to variations in their length over evolutionary time. However, many inherited neurological disorders are linked to the expansion of trinucleotide repeat (TNR) sequences. Examples of these disorders include Friedreich's ataxia, spinocerebellar ataxia, and Huntington's disease. The TNR threshold plays a crucial role in the pathogenesis of these diseases. When the number of TNRs exceeds the threshold, genomic protective mechanisms are either overwhelmed or inhibited, leading to a rapid expansion of the repeats and the subsequent development of these inherited neurodegenerative disorders. TNRs, such as CAG repeats, can be found in both coding and non-coding regions of the DNA sequence. In cases where large repeats of the CAG sequence occur in the coding region, the resulting proteins contain expanded polyglutamine tracts, which become toxic. On the other hand, the presence of expanded TNRs in the non-coding region of a gene can

lead to gene silencing or the production of neurotoxic products at the RNA level. These mechanisms contribute to the pathology observed in various neurodegenerative diseases associated with TNR expansions (Wells *et al.* 2005; McMurray 2010; Tan *et al.* 2012; Jain and Vale 2017; Guo *et al.* 2017a; Lai *et al.* 2020).

One of the most extensively studied diseases associated with TNRs is HD. It is an autosomal dominant inherited disorder caused by the expression of a mutant form of the huntingtin protein. Huntingtin is a protein approximately 350 kDa in size, encoded by the *HTT* gene. The first exon of this gene contains uninterrupted trinucleotide CAG repeats, which give rise to the polyglutamine tract in the huntingtin protein. While a healthy individual's *HTT* gene typically contains around 20 CAG repeats, HD occurs when this threshold is exceeded, usually with approximately 40 or more repetitions. Characteristic symptoms of HD include motor abnormalities such as chorea and loss of coordination, as well as psychiatric manifestations like depression, psychosis, and obsessive-compulsive disorder (Matsui and Corey 2012; Jimenez-Sanchez *et al.* 2017; Gusella *et al.* 2021; Fields *et al.* 2021; Tabrizi *et al.* 2022; Alkanli *et al.* 2023). Currently, treatment for HD is primarily symptomatic, focusing on managing the symptoms to improve the patient's quality of life. However, various therapeutic strategies are under investigation in both preclinical models and clinical trials, aiming to target the underlying causes of HD. These approaches encompass pharmacological therapy, stem cell therapy, interventions associated with modifying and degrading mutant *HTT* gene expression, treatments focused on modulating signaling pathways, and strategies aimed at reducing mutant *HTT* gene content. Ongoing research in these areas holds promise for developing more effective treatments for HD in the future (Fields *et al.* 2021; Tabrizi *et al.* 2022; Alkanli *et al.* 2023).

2.1.4 Prion diseases

Prion diseases, also known as transmissible spongiform encephalopathies, represent a group of slowly progressive and fatal neurodegenerative disorders that affect various vertebrate species, including humans. Notably, these diseases can be transmitted between individuals of the same species or even between different species. The pathogenic mechanism underlying these disorders involves the accumulation of a misfolded isoform of the cellular prion protein. This aberrant form of the prion protein, often referred to as the scrapie prion protein, forms aggregates that are partially resistant to protease digestion. Prion diseases are typically categorized into three types: sporadic,

genetic, and acquired. Examples of these diseases include fatal familial insomnia, Gerstmann–Straussler–Scheinker syndrome, and Creutzfeldt-Jakob disease (Geschwind 2015; Kim *et al.* 2018; Carroll and Chesebro 2019; Baiardi *et al.* 2019; Sigurdson *et al.* 2019; Frontzek and Aguzzi 2020; Li *et al.* 2021; Schmitz *et al.* 2022; Appleby *et al.* 2022; Bujdoso *et al.* 2023).

The most prevalent form of prion disease is Creutzfeldt-Jakob disease (CJD), which manifests in various forms caused by different factors:

1. Familial CJD: Caused by genetic factors.
2. Iatrogenic CJD: Results from the human-to-human transmission of misfolded prion protein.
3. Variant CJD: Linked to oral exposure to food contaminated with material from bovine spongiform encephalopathy-affected cattle.
4. Sporadic CJD: Arises from widespread brain deposition of misfolded prion protein.

CJD presents as a neuropsychiatric syndrome characterized by a combination of psychiatric symptoms, such as depression, anxiety, and visual and auditory hallucinations, alongside neurological abnormalities. These neurological features include ataxia, progressive dementia, cerebellar and extrapyramidal signs, myoclonus, and visual disturbances. At present, there is no specific treatment or vaccine available for CJD. However, ongoing research is exploring new approaches, such as neural precursor cell therapy, in hopes of developing effective treatments for this devastating disease (Behan 1982; Will and Zeidler 1996; Armstrong 2006; Baiardi *et al.* 2019; Uttley *et al.* 2020; European Centre for Disease Prevention and Control (ECDC) 2021; Hermann *et al.* 2021; Williams *et al.* 2023).

2.1.5 Motor neuron diseases

Motor neuron diseases rank among the most severe neurodegenerative conditions. These diseases stem from the gradual degeneration of both upper motor neurons in the motor cortex and lower motor neurons in the brainstem and spinal cord. Typically, these conditions provoke weakness without prominent sensory symptoms or pain. Characteristic clinical features of motor neuron diseases include progressive muscle weakness in the extremities, muscle atrophy, fasciculations (muscle twitching), cramping, spasticity, and fatigue. One of the most prevalent disorders in this category is amyotrophic lateral sclerosis (Foster and Salajegheh 2019; Ashford *et al.* 2021).

Spinal muscular atrophy (SMA) is a rarer neurodegenerative motor neuron disease characterized by the degradation of lower alpha spinal motor neurons. Following cystic fibrosis, SMA ranks as the second most common fatal disease with autosomal recessive inheritance. Its primary pathogenic feature is the progressive proximal muscle weakness and paralysis resulting from the degeneration of these motor neurons. Individuals afflicted with SMA, particularly children, also experience weakness in the diaphragm and accessory respiratory muscles, ultimately leading to respiratory insufficiency. SMA is categorized into five types (0-4), distinguished by the highest level of motor function achieved (e.g., sitting or standing) and the age of onset. SMA type 4 represents the mildest form of the disease, typically manifesting in adulthood. Conversely, SMA type 0 presents the most severe form, typically occurring in neonates, often in the prenatal stage, and resulting in a survival rate of fewer than six months for most affected individuals (D'Amico *et al.* 2011; Arnold *et al.* 2015; Kolb and Kissel 2015; Schorling *et al.* 2020; Butterfield 2021; Day *et al.* 2022; Nishio *et al.* 2023).

The molecular basis of SMA lies in the absence of the SMN (survival motor neuron) protein, which is encoded by the *SMN1* gene located on chromosome 5q. In the majority of cases, SMA results from a homozygous deletion of exon 7 within the *SMN1* gene. The severity of SMA is influenced by the presence of the *SMN2* pseudogene, which closely resembles *SMN1* but differs in a few nucleotides. The severity of the disease is largely determined by the copy number of *SMN2*. Since the discovery in 1995 that *SMN1* and *SMN2* genes are responsible for SMA, effective therapies utilizing new drugs, such as nusinersen, onasemnogene abeparvovec, and risdiplam have been integrated into clinical practice. Furthermore, alternative treatment approaches, including gene therapy and stem cell therapy, have been explored. However, the timing and accuracy of SMA diagnosis have become increasingly critical. Consequently, population-based newborn screening programs for SMA, specifically targeting SMA with *SMN1* deletion, have been implemented worldwide, including in the Czech Republic since January 1, 2022. The introduction of newborn SMA screening facilitates the initiation of treatment at a pre-symptomatic stage, maximizing therapeutic effectiveness and improving patient outcomes (D'Amico *et al.* 2011; Arnold *et al.* 2015; Kolb and Kissel 2015; Schorling *et al.* 2020; Butterfield 2021; Day *et al.* 2022; Nishio *et al.* 2023).

2.1.6 Tauopathies

Tauopathies constitute a clinically and pathologically diverse group of neurodegenerative disorders characterized by the intracellular accumulation of abnormal tau protein (for more on tau protein, see Chapter 2.3 Tau protein). There are two main categories of tauopathies: primary and secondary. Primary tauopathies are characterized by the predominant pathology of intracellular deposition of abnormal tau protein. In contrast, secondary tauopathies have another primary cause of disease pathology, with the intracellular accumulation of abnormal tau protein being a secondary feature. The most prevalent tauopathy in the human population is AD, which serves as a classic example of a secondary tauopathy. In AD, the intracellular aggregation of tau protein leads to the formation of neurofibrillary tangles, while extracellular amyloid-β plaques also contribute to disease pathology (for more details, see Chapter 2.2 Alzheimer's disease below). Clinical presentations of tauopathies vary among different disorders, encompassing a spectrum of cognitive and motor impairments (Dugger and Dickson 2017; Riley *et al.* 2022; Islam *et al.* 2022; Creekmore *et al.* 2024).

Currently, there are no approved drugs specifically targeting the underlying pathology of tauopathies. Treatment primarily focuses on managing symptoms to improve patients' quality of life. However, several potential therapeutic agents are undergoing clinical development to address the accumulation of aggregated tau protein, which is a key feature of these disorders. One major area of research involves tau protein inhibitors, aiming to prevent the aggregation and accumulation of abnormal tau protein. Examples of such inhibitors include methylthioninium chloride and Anle138b [5-(1,3-benzodioxol-5-yl)-3-(3-bromophenyl)-1*H*-pyrazole]. Additionally, kinase inhibitors and O-GlcNAcase inhibitors have garnered significant attention. These compounds target processes such as phosphorylation and O-GlcNAcylation, which are common post-translational modifications of tau protein associated with its aggregation. Beyond these approaches, other potential therapies under investigation include gene therapy techniques such as gene silencing, as well as immunotherapy strategies including vaccines and monoclonal antibodies. These interventions aim to target tau protein directly or modulate the immune response against abnormal tau aggregates. While much progress has been made in understanding the underlying mechanisms of tauopathies and developing potential treatments, further research is needed to translate these findings into effective therapies for patients (Islam *et al.* 2022; Cummings *et al.* 2023).

2.2 Alzheimer's disease

2.2.1 Pathogenesis and diagnosis

AD is a prevalent neurodegenerative disorder and ranks as the third most common cause of dementia worldwide. It affects various aspects of human cognition and behavior, including memory loss, cognitive decline, behavioral changes, functional impairment, and difficulties in performing daily tasks. AD is characterized by two distinct forms based on the age of onset. Early-onset AD typically manifests in individuals younger than 65 years of age and is often referred to as familial AD. This form is associated with inherited autosomal mutations in genes responsible for proteins involved in the aggregation of amyloid-β protein. Late-onset AD, on the other hand, occurs in individuals over the age of 65 and is known as sporadic AD. In contrast to familial AD, late-onset AD is primarily influenced by environmental factors rather than a strong family history of the disease (Mantzavinos and Alexiou 2017; Vaz and Silvestre 2020; Scheltens *et al.* 2021; Monteiro *et al.* 2023; Bhole *et al.* 2023).

The progression of AD is typically categorized into four clinical phases (Atri 2019; Breijyeh and Karaman 2020; Scheltens *et al.* 2021):

1. Pre-clinical Stage: This stage is characterized by mild memory loss and early pathological changes in the cerebral cortex and hippocampus. However, individuals in this stage do not exhibit any disruption in daily activities, and no clinical signs of AD are apparent. This phase may persist for several years before the onset of clinical symptoms.
2. Mild or Early Stage: In this stage, individuals may begin to experience difficulties in daily life, including challenges with concentration, memory, orientation in time and place, mood changes, and the development of depression.
3. Moderate Stage: As the disease progresses, it may spread to additional areas of the cerebral cortex, resulting in increased memory loss, difficulties recognizing family and friends, loss of impulse control, and challenges with reading, writing, and speaking.
4. Severe or Late Stage: In the final stage of AD, patients experience progressive functional and cognitive decline. They may no longer recognize their family members, become bedridden, and have difficulty swallowing and

urinating. At this stage, the disease has typically spread throughout the entire cortex, and complications may lead to the patient's death.

The mechanisms driving the progression of Alzheimer's disease (AD) remain incompletely understood. However, the prevailing interpretation of AD pathogenesis involves two primary processes: the extracellular deposition of amyloid β (Aβ) protein in the form of senile plaques and the intracellular deposition of tau protein forming neurofibrillary tangles (NFTs) (**Chyba! Nenalezen zdroj odkazů.**). When both Aβ and tau/phosphorylated tau proteins are detected, the likelihood of AD development increases. Aβ deposits originate from the cleavage of the transmembrane amyloid precursor protein by proteolytic enzymes like α-secretase, β-secretase, and γ-secretase. Aβ protein is known for its propensity to self-aggregate and plays a significant role in neurotoxicity and neural function. Tau protein, on the other hand, is a microtubule-associated protein involved in stabilizing and assembling microtubules, promoting axonal transport, and maintaining dendrite structure. Post-translational modifications, including phosphorylation, regulate its biological activity. Abnormal phosphorylation reduces tau's affinity for microtubules and increases its tendency to aggregate. Consequently, hyperphosphorylated tau loses its normal functions, leading to defects in microtubule assembly, axonal transport disruption, dendritic structural changes, synapse loss, neuronal death, and ultimately dementia. Both tau protein and the prefibrillar aggregates it forms contribute significantly to neurotoxicity, similar to Aβ protein. These processes collectively contribute to the neurodegenerative cascade observed in AD (Šerý *et al.* 2013; Mantzavinos and Alexiou 2017; Vaz and Silvestre 2020; Breijyeh and Karaman 2020; Monteiro *et al.* 2023).

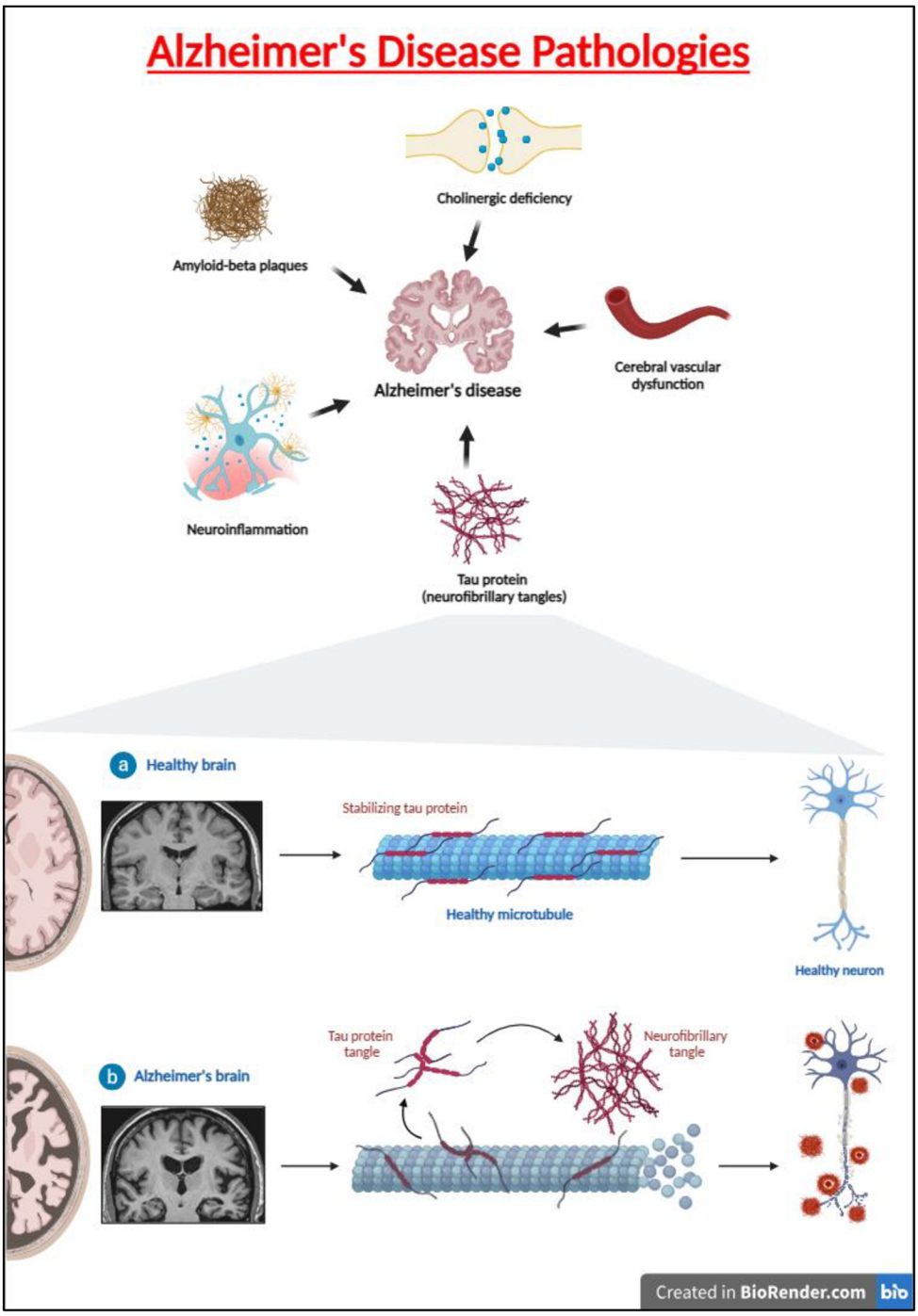

Figure 1: Pathology of Alzheimer´s disease. The hallmark features of extracellular Aβ plaques and intracellular hyperphosphorylated tau-containing NFTs in the brain distinguish AD. Moreover, AD entails cholinergic deficiency, neuroinflammation, and cerebrovascular dysfunction as additional pathological components. Created in Biorender.com (Ref. 1).

The diagnosis of AD typically involves a comprehensive evaluation that includes cognitive testing, neurological examination, magnetic resonance imaging (MRI), and laboratory examinations. However, there is growing interest in identifying the disease before the onset of symptoms using minimally invasive and cost-effective techniques. One approach involves utilizing a combination of cerebrospinal fluid (CSF) biomarkers

and imaging methods, such as amyloid positron emission tomography (PET), to reliably detect AD in its pre-symptomatic stages. CSF biomarkers include markers of neuronal damage, such as tau protein levels, as well as measurements of metabolic activity using fluorodeoxyglucose PET and assessments of brain atrophy using MRI. These diagnostic criteria aim to provide a more accurate and reliable means of identifying AD, particularly in its early stages when intervention may be most beneficial. By integrating multiple biomarkers and imaging modalities, clinicians can achieve a more comprehensive understanding of the underlying pathology and progression of the disease (Hane *et al.* 2017; Khan *et al.* 2020; Breijyeh and Karaman 2020; Scheltens *et al.* 2021; Monteiro *et al.* 2023; Dolphin *et al.* 2024).

AD is associated with several risk factors that can increase an individual's likelihood of developing the disease. Among the primary risk factors is advancing age, with older individuals being at a higher risk of AD compared to younger individuals. Additionally, older patients often contend with other medical conditions, such as cardiovascular disease, obesity, and type II diabetes mellitus, which can further elevate the risk of AD. Psychological factors, including stress and distress, are also recognized as risk factors for AD. Chronic stress and psychological strain have been linked to an increased risk of cognitive decline and AD development. Conversely, certain activities and lifestyle choices can act as protective factors, potentially reducing the risk of AD. Regular physical exercise, including activities such as walking or aerobic exercises, has been shown to have a protective effect against cognitive decline and AD. Additionally, maintaining a healthy diet and engaging in mentally stimulating activities, such as reading, puzzles, or social interactions, may help lower the risk of developing AD. Overall, a combination of factors, including age, comorbidities, stress levels, and lifestyle choices, influences an individual's susceptibility to AD. Adopting healthy lifestyle habits, such as regular exercise, a balanced diet, and engaging in mentally stimulating activities, may help mitigate the risk of developing AD (Robinson *et al.* 2017; Breijyeh and Karaman 2020).

2.2.2 Treatment

The current phase of AD treatment studies encompasses various strategies aimed at counteracting the mechanisms driving disease progression, as there is currently no fully effective cure for AD. Treatment options for AD primarily consist of a few approved drugs, although these therapies predominantly target symptoms, but not the cause of the

disease. These treatment strategies can be categorized into several groups. Initially, treatment approaches were based on the cholinergic hypothesis, which posits that AD patients exhibit a deficiency in the neurotransmitter acetylcholine due to a reduction in the enzyme choline acetyltransferase and subsequent loss of cholinergic neurons in the basal forebrain. To address this deficit, acetylcholinesterase inhibitors were developed to enhance cholinergic transmission, along with modulation of muscarinic and nicotinic acetylcholine receptors. Approved acetylcholinesterase inhibitors include donepezil, rivastigmine, and galantamine, all of which have demonstrated efficacy in treating mild to moderate forms of AD. Although these drugs differ in their pharmacodynamics and pharmacokinetics, their overall efficacy is comparable. Acetylcholinesterase inhibitors are generally well-tolerated, with adverse gastrointestinal effects such as nausea, vomiting, diarrhea, and anorexia being relatively rare. Another drug used in AD treatment is memantine, which is indicated for moderate to severe AD and is often used in combination with acetylcholinesterase inhibitors. Memantine acts as a neuroprotective agent by preventing neuronal loss and improving symptoms through non-competitive blocking of the N-methyl-D-aspartate receptor. While these pharmacological treatments represent the current standard of care for AD, they have modest overall efficacy and do not alter the underlying neurodegenerative process. Nonetheless, they remain valuable in managing symptoms and improving the quality of life for individuals with AD (Mangialasche *et al.* 2010; Briggs *et al.* 2016; Weller and Budson 2018; Vaz and Silvestre 2020; Monteiro *et al.* 2023; Bhole *et al.* 2023).

As previously mentioned, one of the key pathological mechanisms of AD involves the formation of senile plaques due to the extracellular deposition of Aβ protein. The strategy for anti-amyloid therapy involves investigating potential drugs through three approaches: reducing Aβ production, preventing Aβ aggregation, and promoting Aβ clearance. Numerous inhibitors targeting these enzymes have been developed over the years, including verubecestat, lanabecestat, atabecestat, umibecestat, and elenbecestat as β-secretase inhibitors, and semagacestat and avagacestat as γ-secretase inhibitors, with tarenflurbil acting as a modulator. However, none of these drugs have successfully progressed through the final phase of clinical testing. Five drugs categorized as β-secretase inhibitors demonstrated effective reduction of Aβ levels in the cerebrospinal fluid of AD patients; however, cognitive impairment was observed in some cases. Clinical trials of semagacestat had to be halted due to significant clinical deterioration and a higher incidence of skin cancer and infections among patients. Similarly, research

on avagacestat was discontinued due to an increased risk of skin cancer. Regarding tarenflurbil, a phase III clinical trial showed no evidence of cognitive or functional impairment in patients with mild AD. These challenges underscore the complexity of developing effective anti-amyloid therapies for AD and highlight the need for continued research and development in this area. While progress has been made, further investigations are necessary to identify safe and efficacious treatments that target Aβ pathology in AD (Mangialasche *et al.* 2010; Briggs *et al.* 2016; Vaz and Silvestre 2020; Monteiro *et al.* 2023).

The occurrence of AD is also associated with inflammatory processes, which manifest as a specific, targeted, and enhanced immune, biochemical, and hematological response at the local or systemic level. This neuroinflammation is considered desirable and beneficial in the context of the disease, as it activates the immune response. As a result, various forms of immunotherapy are currently being developed to target these inflammatory processes. Immunotherapy can be categorized into passive and active forms. Passive therapy involves the direct administration of antibodies against the targeted protein, while active immunotherapy stimulates the patient's immune system through vaccination to produce antibodies against the targeted protein itself. These approaches aim to modulate the immune response and reduce inflammation in the brain, potentially slowing the progression of AD. Ongoing research in immunotherapy offers promising avenues for the development of effective treatments for AD by targeting the underlying inflammatory mechanisms implicated in the disease (Vaz and Silvestre 2020; Twarowski and Herbet 2023; Bhole *et al.* 2023; Guo *et al.* 2024).

Regarding the elderly population, who are more prone to AD than younger individuals, passive immunization is often considered a preferable treatment option over active immunotherapy. This preference arises from the fact that older adults generally exhibit reduced reactivity to vaccines. Currently, there are two monoclonal antibodies targeting the Aβ protein, aducanumab and lecanemab, that have received approval from the Food and Drug Administration (FDA) for the treatment of AD. Aducanumab, a humanized IgG1 monoclonal antibody, was one of the first drugs approved by the FDA for AD treatment since 2003. However, its approval has been controversial due to the accelerated approval process. While aducanumab has shown the ability to reduce Aβ plaques in the brain, which are believed to contribute to AD, its clinical benefit in terms of improving cognitive function or slowing disease progression has not been definitively demonstrated. Lecanemab, another humanized IgG1 antibody that

specifically binds to Aβ protofibrils, received FDA approval in July 2023. Other anti-amyloid monoclonal antibodies, such as gantenerumab and donanemab, are undergoing various stages of clinical testing. Gantenerumab is notable as the first fully human monoclonal IgG1 anti-Aβ antibody, while donanemab is a humanized IgG1 monoclonal antibody developed from mouse mE8-IgG2a. Furthermore, research groups are investigating monoclonal antibodies targeting the tau protein, although their development in clinical practice is still in its early stages. Several anti-tau monoclonal antibodies, including semorinemab, tilavonemab, gosuranemab, and zagotenemab, have been tested in phase II studies. These efforts reflect the ongoing exploration of immunotherapeutic approaches to address the underlying pathophysiology of AD and hold promise for future treatment options (Vaz and Silvestre 2020; Twarowski and Herbet 2023; Monteiro *et al.* 2023; Cummings *et al.* 2023; Bhole *et al.* 2023; Guo *et al.* 2024; Perneczky *et al.* 2024; Ye *et al.* 2024).

In terms of research strategies targeting tau protein pathology in AD, two primary therapeutic approaches have been described: agents inhibiting tau phosphorylation kinases and agents inhibiting protein aggregation while promoting the disintegration of resulting aggregates. Glycogen synthase kinase 3-beta (GSK-3β) is one of the protein kinases implicated in tau protein phosphorylation and the development of AD. Therefore, inhibiting GSK-3β is considered a promising strategy in AD therapy. Two potential agents have progressed to the clinical phase of drug development: tideglusib, an irreversible GSK-3β inhibitor, and lithium. While research on tideglusib in AD has been discontinued, further studies are needed to elucidate the clinical benefit of lithium salts in AD. Additionally, several compounds are being developed with the potential to serve as drugs for preventing tau aggregation or stabilizing microtubules. Examples include methylthioninium chloride, davunetide, and nicotinamide. These compounds hold promise in targeting tau pathology and potentially mitigating the progression of AD. Continued research and clinical trials will be crucial in determining their efficacy and safety profiles for AD treatment (Mangialasche *et al.* 2010; Briggs *et al.* 2016; Weller and Budson 2018; Vaz and Silvestre 2020; Bhole *et al.* 2023; Ye *et al.* 2024).

2.3 Tau protein

2.3.1 Structure and localization

Tau protein belongs to a family of microtubule-associated proteins present in various animal species. In humans, it is primarily found in neuronal cells but can also be expressed in other cell types, such as glial cells, particularly in pathological conditions, and astrocytes. Under physiological conditions, tau protein is expressed in neurons, predominantly in axons, and to a lesser extent in dendrites and somatodendritic compartments, including the plasma membrane, nucleus, and mitochondria. The distribution of tau protein within a neuron can be polar, with various mechanisms regulating its localization. Tau mRNA contains a specific axonal localization signal, ensuring the localization of tau protein in the axonal compartment. Additionally, cytosolic tau protein can be translocated into the axon through mechanisms such as free diffusion or transport by motor proteins like kinesins. There exists a retrograde barrier within the axon, permitting tau protein entry into the axon but preventing its retrograde transport towards the soma and dendrites (Buee *et al.* 2000; Guo *et al.* 2017b; Pîrscoveanu *et al.* 2017; Tapia-Rojas *et al.* 2019).

The human tau protein is encoded by a single gene known as *MAPT*, located on chromosome 17 at position 17q21, which comprises 16 exons. Alternative splicing of exons 2, 3, and 10 gives rise to six different isoforms of tau protein, ranging from 352 to 441 amino acid residues in length. These isoforms contain an N-terminal part (projection domain), a proline-rich domain, a microtubule-binding domain, and a C-terminal tail, which constitutes the fundamental portion of the protein. The variance among the isoforms arises from the number of repetitive sequences (repeats) in the microtubule-binding domain (3R or 4R) and the presence of inserts at the N-terminal part of the protein (0N, 1N, or 2N) (**Figure**). This diversity in isoforms not only impacts their structural properties but also influences their expression levels. During early (fetal) stages of human development, only one tau isoform is present, characterized by 3R and no N-terminal insertion. Conversely, adults express isoforms with one or two N-terminal insertions and 3R or 4R repeats. The balance between these isoforms is crucial in the adult brain and may significantly contribute to the development of neurodegenerative diseases. In the healthy, mature human brain, the 3R and 4R tau isoforms occur in approximately equal molar ratios, indicating a balanced expression of these isoforms. This equilibrium is essential for maintaining proper

neuronal function and integrity (Friedhoff *et al.* 2000; Avila *et al.* 2004; Kolarova *et al.* 2012; Tapia-Rojas *et al.* 2019; Islam *et al.* 2022; Rawat *et al.* 2022).

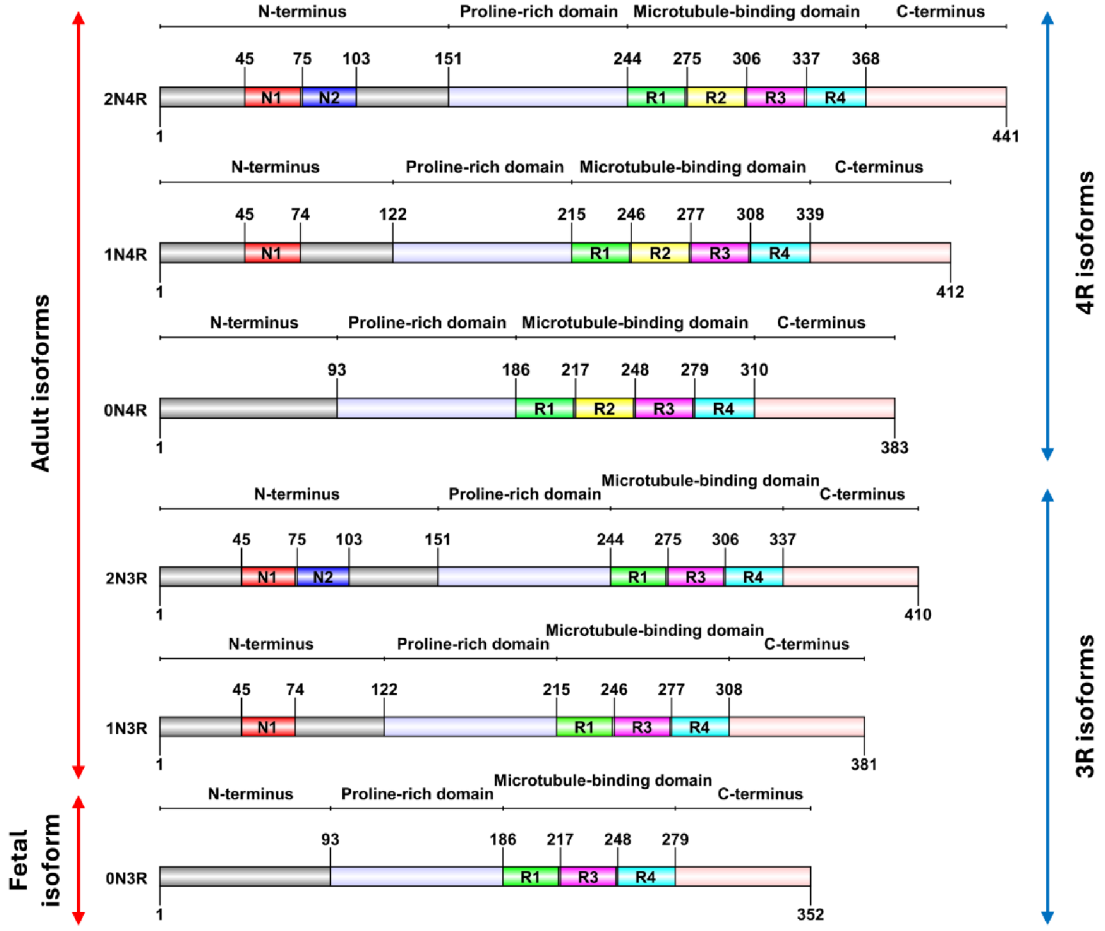

Figure 2: Diagram illustrating the six human CNS tau isoforms. These isoforms comprise an N-terminal region (referred to as the projection domain), a proline-rich domain, a microtubule-binding domain, and a C-terminal tail, serving as the core component of the protein. The distinction among the isoforms arises from variations in the number of repetitive sequences (repeats) within the microtubule-binding domain (3R or 4R) and the presence of inserts at the N-terminal region of the protein (0N, 1N, or 2N). (Adapted from (Pîrscoveanu *et al.* 2017; Nizynski *et al.* 2017).)

2.3.2 Function

As previously stated, tau protein is a member of the microtubule-associated protein family, traditionally known for its role in facilitating microtubule polymerization and stability. Nonetheless, tau protein exhibits multifaceted functionality, serving various roles within the cell (Mietelska-Porowska *et al.* 2014; Tapia-Rojas *et al.* 2019).

The primary and extensively studied function of tau protein revolves around its interaction and binding with microtubules. Tau protein contributes to the assembly and stabilization of microtubules through direct or indirect interactions. Direct interaction relies on the microtubule-binding domain and neighboring regions, which facilitate binding and stabilization, thereby promoting microtubule assembly. Conversely, the projection domain of tau protein is crucial for its indirect interaction by facilitating interactions with other proteins that subsequently interact with microtubules. The binding of tau protein to microtubules at the interface between α/β tubulin dimers is subject to modulation by various mechanisms, with phosphorylation playing a pivotal role. Phosphorylation alters the conformation of tau protein and can neutralize its positive charge, leading to detachment from microtubules. While physiological phosphorylation at specific sites regulates the interaction of tau protein with microtubules, aberrant phosphorylation in pathological conditions diminishes this binding, promoting aggregation and the formation of toxic oligomers. Additionally, specific sequences, including ^{240}KSRLQTAPV^{248}, ^{275}VQINKKLDLS^{285}, are critical for the interaction of tau protein with microtubules. Notably, the latter two sequences are encoded by exon 10, subject to alternative splicing. This phenomenon may elucidate why 3R isoforms of tau protein exhibit weaker interactions with microtubules compared to 4R isoforms (Mietelska-Porowska *et al.* 2014; Tapia-Rojas *et al.* 2019; Barbier *et al.* 2019).

Tau protein's interaction with the end regions of microtubules extends to various classes of proteins involved in cytoskeletal regulation and motor proteins, such as kinesins and dyneins. These interactions are crucial for mediating anterograde and retrograde transport along microtubules, which serve as channels within neurons. By facilitating the binding of motor proteins, tau protein contributes to the regulation of axonal transport, a process vital for maintaining neuronal function. Axonal transport plays a pivotal role in ensuring the proper distribution of organelles, proteins, and lipids between the soma and axons, dendrites, and vice versa. Of particular significance is the transport of mitochondria, which is essential for synaptic function. Pathological

alterations in tau protein can disrupt axonal transport, contributing to neuronal dysfunction. Furthermore, tau protein functions as a scaffold protein, modulating the activity of various proteins, including Src tyrosine kinases. In addition, tau protein plays a role in nuclear localization, where it binds to and protects DNA from denaturation. Under stress conditions, phosphorylated tau facilitates nuclear translocation and contributes to nuclear conformation and the heterochromatinization of ribosomal genes. These diverse functions highlight the multifaceted role of tau protein in neuronal physiology and pathology (Mietelska-Porowska *et al.* 2014; Tapia-Rojas *et al.* 2019; Sinsky *et al.* 2021).

2.3.3 Post-translational modifications

Indeed, tau protein undergoes various post-translational modifications (PTMs) that significantly impact its structure, function, and cellular localization. These modifications play crucial roles in regulating tau's physiological functions within neurons, as well as its involvement in pathological processes observed in neurodegenerative diseases like Alzheimer's disease (Alquezar *et al.* 2021).

Tau protein is predominantly phosphorylated among its various post-translational modifications, with phosphorylation representing the major regulatory mechanism governing its biological activity. In physiological conditions, phosphorylation plays a pivotal role in modulating tau's affinity for microtubules and regulating their stabilization and assembly dynamics. Throughout development, the level of tau protein phosphorylation undergoes significant changes. During embryonic and early stages of human development, tau is highly phosphorylated, with up to eight phosphate groups per molecule. This high phosphorylation level is critical for orchestrating proper neuronal development and cytoskeletal organization during early neuronal differentiation. As development progresses and neurons mature into adulthood, the level of tau phosphorylation diminishes, typically reaching a plateau with only two phosphate groups per molecule. This reduced phosphorylation state optimally facilitates tau's interaction with microtubules, ensuring neuronal cytoskeletal integrity and function. However, during aging, there is a notable resurgence in tau phosphorylation levels, reverting to the heightened state observed during early development. This age-related increase in tau phosphorylation has been implicated in the pathogenesis of neurodegenerative diseases, including Alzheimer's disease, where hyperphosphorylated tau forms insoluble aggregates and neurofibrillary tangles, contributing to neuronal

dysfunction and degeneration. Understanding the intricate regulation of tau phosphorylation throughout development and aging is crucial for unraveling its role in neurodegenerative disorders and may offer insights into therapeutic strategies aimed at mitigating tau pathology and associated cognitive decline (Buee *et al.* 2000; Pîrscoveanu *et al.* 2017; Zabik *et al.* 2017; Tapia-Rojas *et al.* 2019; Alquezar *et al.* 2021; Rawat *et al.* 2022; Ye *et al.* 2024).

In the longest tau isoform (2N4R), tau protein harbors over 80 potential phosphorylation sites on serine, threonine, and tyrosine residues. These sites serve as substrates for various protein kinases, which catalyze the addition of phosphate groups to tau protein. These kinases include proline-directed serine/threonine-protein kinases (such as glycogen synthase kinase-3β, cyclin-dependent kinase 5, and p38 mitogen-activated protein kinase), non-proline-directed serine/threonine-protein kinases (such as Ca^{2+}/calmodulin-dependent protein kinase II and dual-specificity tyrosine-phosphorylation-regulated kinase 1A), and tyrosine protein kinases (such as proline-rich tyrosine kinase 2 and Fyn lymphocyte-specific protein). Conversely, the removal of phosphate groups from tau protein, known as dephosphorylation, is mediated by phosphatases. One of the predominant phosphatases involved in tau dephosphorylation in the brain is protein phosphatase 2A (PP2A). The balance between the activities of kinases and phosphatases is crucial for maintaining the phosphorylation state and function of tau protein (Buee *et al.* 2000; Pîrscoveanu *et al.* 2017; Zabik *et al.* 2017; Tapia-Rojas *et al.* 2019; Alquezar *et al.* 2021; Rawat *et al.* 2022; Ye *et al.* 2024).

Under physiological conditions, tau phosphorylation plays several essential roles. It regulates tau protein localization at various cellular compartments, including the plasma membrane and exocytotic vesicles, as well as at intracellular sites. Additionally, phosphorylation of tau protein is integral to the development of cellular processes, modulating the affinity of tau for microtubules, increasing microtubule dynamics, and contributing to the establishment of neuronal processes and cell polarity. These phosphorylation-mediated processes are essential for maintaining normal neuronal function and cytoskeletal architecture. Indeed, abnormal phosphorylation of tau protein leads to pathological alterations characterized by conformational changes, proteolytic cleavage, and aggregation. In this state, the affinity of tau protein for microtubules is diminished, contributing to the loss of neurons and synapses in the brain, which are hallmark features of neurodegenerative diseases such as AD. The dysregulation of tau phosphorylation is often associated with increased kinase activity, which leads to

hyperphosphorylation of tau protein. Furthermore, this dysregulation can result in decreased dephosphorylation, further exacerbating the accumulation of hyperphosphorylated tau. As a consequence, tau protein loses its ability to interact with microtubules effectively, disrupting cytoskeletal stability and neuronal function. The interplay between abnormal phosphorylation and dysregulated kinase activity underscores the importance of maintaining tau phosphorylation homeostasis for proper neuronal function and preventing the pathological processes associated with neurodegenerative diseases. Therapeutic strategies targeting aberrant tau phosphorylation represent promising avenues for mitigating neurodegeneration and associated cognitive decline (Buee *et al.* 2000; Pîrscoveanu *et al.* 2017; Zabik *et al.* 2017; Tapia-Rojas *et al.* 2019; Alquezar *et al.* 2021; Rawat *et al.* 2022; Ye *et al.* 2024).

Indeed, tau protein undergoes various post-translational modifications (PTMs) besides phosphorylation, including acetylation, ubiquitination, SUMOylation, and truncation. These PTMs are interconnected and collectively contribute to tau pathology and neurodegeneration. Acetylation of tau protein is mediated by histone acetyltransferases (HATs) and can be reversed by histone deacetylases (HDACs). Acetylation regulates tau ubiquitination and neutralizes the charge in the microtubule-binding domain, impairing its ability to bind to microtubules and leading to tau dysfunction. Ubiquitination, SUMOylation, and truncation also play significant roles in tau aggregation and neurodegeneration. Ubiquitination marks tau protein for degradation by the proteasome, but aberrant ubiquitination can lead to the formation of insoluble tau aggregates. SUMOylation, the attachment of small ubiquitin-like modifier (SUMO) proteins, regulates tau protein localization and function. Truncation, involving the cleavage of tau protein into smaller fragments, can promote tau aggregation and toxicity. Overall, the interplay between these PTMs contributes to the pathological accumulation of tau aggregates and the progression of neurodegenerative diseases such as Alzheimer's disease. Understanding the complex network of PTMs on tau protein is crucial for developing targeted therapies aimed at mitigating tau pathology and associated neurodegeneration (Tapia-Rojas *et al.* 2019; Alquezar *et al.* 2021; Islam *et al.* 2022; Rawat *et al.* 2022; Ye *et al.* 2024).

2.3.4 Aggregation, toxicity and spreading

Tau protein, characterized by its internal disorder and high solubility in aqueous solution, can undergo aggregation into various structures, including straight filaments

and paired helical filaments (PHFs), contributing to the formation of NFTs. This aggregation process is facilitated by various mechanisms, including PTMs. Studies have identified two crucial hexapeptide motifs within the R2 and R3 repeat fragments of tau protein, namely ^{275}VQIINK^{280} (PHF6*) in the R2 repeat and ^{306}VQIVYK^{311} (PHF6) in the R3 repeat (**Figure 3**). These motifs play pivotal roles in initiating and stabilizing the formation of cross-β-sheet aggregate structures. While PHF6 is more critical than PHF6* in initiating and stabilizing tau protein aggregation, both sequences are essential for fibrillization. Notably, the presence of the R2 repeat only in the 4R isoforms renders them more prone to aggregation compared to the 3R isoforms. Additionally, the presence of Cys291 and Cys322, which form intermolecular disulfide bridges, further promotes tau protein aggregation. Dysfunction of the PERK (protein kinase R-like endoplasmic reticulum kinase) signaling pathway, identified as one of the genetic risk factors for tauopathies, exacerbates tau aggregation. These factors collectively contribute to the pathological aggregation of tau protein and the development of tauopathies (Guo *et al.* 2017b; Jouanne *et al.* 2017; Brunello *et al.* 2020; Annadurai *et al.* 2022b, 2022a; Islam *et al.* 2022; Park *et al.* 2023; Hernández *et al.* 2023; Hu *et al.* 2023; Ye *et al.* 2024).

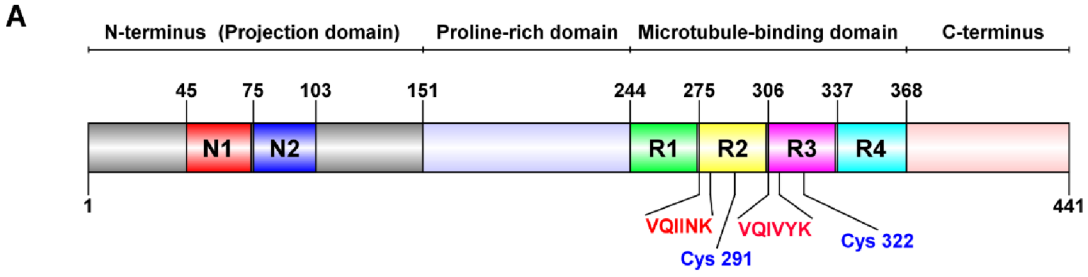

B

R1	^{244}QTAPVPMPDLKNVKSKIGSTENLKHQPGGGK^{274}
R2	^{275}**VQIINK**KLDLSNVQSK**C**GSKDNIKHVPGGGS^{305}
R3	^{306}**VQIVYK**PVDLSKVTSK**C**GSLGNIHHKPGGGQ^{336}
R3 (C322A)	^{306}**VQIVYK**PVDLSKVTSK**A**GSLGNIHHKPGGGQ^{336}
R4	^{337}VEVKSEKLDFKDRVQSKIGSLDNITHVPGGGN^{368}

Figure 3: Structural features and key motifs in the 2N4R tau isoform associated with aggregation. A Schematic representation of the 2N4R tau isoform with motifs that promote tau protein aggregation. **B** Amino acid sequences of tau repeat fragments. The hexapeptide motifs ^{275}VQIINK^{280} (R2 repeat) and ^{306}VQIVYK^{311} (R3 repeat) are important in initiating and stabilizing tau protein aggregation. The presence of Cys291 and Cys322, which form intermolecular disulfide bridges, is also an important factor in the formation of tau protein aggregates.

Indeed, the aberrant PTMs of tau protein disrupt its normal interaction with microtubules, resulting in an accumulation of unbound tau protein within the cytoplasm. This surplus of free tau protein serves as a catalyst for the formation of toxic aggregates, a hallmark of neurodegenerative diseases like AD. These tau aggregates exert detrimental effects on cellular processes, contributing to neuronal dysfunction and cognitive decline in AD. They disrupt cellular metabolism, compromise mitochondrial function, impair synaptic plasticity, and provoke neuroinflammatory responses mediated by glial cells. Consequently, these cascading events exacerbate neurodegeneration, exacerbating cognitive deficits observed in AD. Overall, the dysregulation of tau protein due to abnormal PTMs represents a crucial pathological mechanism underlying AD and related tauopathies, highlighting its significance as a therapeutic target in combating these devastating neurodegenerative disorders (Hu *et al.* 2023; Ye *et al.* 2024).

Tau protein, typically considered an intracellular component, possesses the remarkable ability to be actively released into the extracellular milieu. This phenomenon has significant implications for the pathogenesis of neurodegenerative diseases, including AD and related tauopathies. In these diseases, misfolded and pathological tau proteins propagate through neuroanatomically connected brain regions, reminiscent of prion-like spread. The mechanisms facilitating the spread of abnormal tau species from diseased to healthy cells involve extracellular secretion, intracellular uptake, and direct cell-to-cell transfer. Extracellular secretion of tau protein occurs via various pathways, including exosomes, microvesicles, autophagosomes, and even direct release across the plasma membrane. Once released, pathological tau seeds can initiate and accelerate tau filament formation in recipient cells through seeding mechanisms. In this process, donor cells secrete pathological tau seeds, which are subsequently internalized by recipient cells. Upon internalization, these seeds induce the misfolding and aggregation of endogenous tau proteins within the recipient cells, perpetuating the pathological cascade. Understanding the mechanisms underlying tau propagation is crucial for developing targeted therapeutic interventions aimed at disrupting the spread of pathological tau and halting the progression of neurodegenerative diseases (Fuster-Matanzo *et al.* 2018; Demaegd *et al.* 2018; d'Errico and Meyer-Luehmann 2020; Brunello *et al.* 2020; Annadurai *et al.* 2021; Hu *et al.* 2023).

3 EXPERIMENTAL PART

3.1 Materials

3.1.1 Chemicals, solutions and peptides

Chemicals

Dimethyl sulfoxide (DMSO) (AppliChem, Darmstadt, Germany, #A3672.0250)

Dulbecco's Modified Eagle's medium (DMEM) (Lonza, Basel, Switzerland, #12-604F)

Fetal bovine serum (FBS) (Gibco™, Thermo Fisher Scientific, Waltham, MA, USA, #10270)

150 µM heparin (Sigma Aldrich, Merck, Burlington, MA, USA, #H4784-1G)

Hoechst-33342 nuclear dye (Invitrogen, Thermo Fisher Scientific, Waltham, MA, USA, #H21492)

Lipofectamine™ 3000 Transfection Reagent Kit (P3000™ Reagent, Lipofectamine™ 3000 Reagent) (Invitrogen, Thermo Fisher Scientific, Waltham, MA, USA, #L3000015)

Opti-MEM™ I Reduced Serum Medium (Gibco™, Thermo Fisher Scientific, Waltham, MA, USA, #31985070)

100x penicillin/streptomycin solution (Diagnovum, Marburg, Germany, #D910)

1 mM Thioflavin T (ThT) (Sigma Aldrich, Merck, Burlington, MA, USA, #T3516-5G)

TrypLE™ Express Enzyme (1X), no phenol red (Gibco™, Thermo Fisher Scientific, Waltham, MA, USA, #12604013)

Solutions

Aggregation buffer

20 mM Tris-HCl (pH 7,4), 100 mM NaCl, and 1 mM EDTA were dissolved in sterile H_2O and filtered using a syringe filter.

Complete growth medium

To prepare 500 ml of complete growth medium, FBS was added into D-MEM liquid culture medium (the final concentration of FBS was 10 % (v/v)). Afterward, 5 ml of penicillin/streptomycin solution (antibiotics) was added to the growth medium with FBS to make the final concentration of antibiotics 1 % (v/v). Then, the prepared complete growth medium was filtered using Filter Top 500 rapid Filtermax (0.22 µM). Finally, the bottle was closed with the sterile cap and stored in a cold room (4 °C) (Agrawal *et al.* 2022).

10x PBS

80 g NaCl, 2 g KCl, 32.1 g $Na_2HPO_4.12H_2O$, and 2 g KH_2PO_4 were dissolved in 800 ml sterile H_2O (tissue culture quality), pH was adjusted to 6.8-7.2 1M NaOH or HCl and H_2O added to the final volume (1000 ml). The solution was sterilized by autoclaving (121 °C) and stored in a cold room (4 °C) (Agrawal *et al.* 2022).

1x PBS

100 $ml.l^{-1}$ of 10x PBS was diluted in 900 $ml.l^{-1}$ sterile H_2O.

Peptides

The peptides used for experiments are listed in **Table 1** and were purchased from AnaSpec (Fremont, CA, USA), Genscript Biotech (Piscataway, NJ, USA), and ProteoGenix (Schiltigheim, France). The peptides were reconstituted and stored, as described before (Annadurai *et al.* 2022a).

Table 1: List of peptides used in experiments. The green colour indicates two crucial hexapeptide motifs; the orange colour shows Cys291 and Cys322, and the red colour signifies the Cys-to-Ala substitution.

Peptide	Molecular weight (kDa)	Sequence	Stock concentration (µM)
R2	3.26475	VQIINKKLDLSNVQSKCGSKDNIKHVPGGGS	306.3
R3	3.24776	VQIVYKPVDLSKVTSKCGSLGNIHHKPGGGQ	307.9
R3 C322A	3.21570	VQIVYKPVDLSKVTSKAGSLGNIHHKPGGGQ	307.9
R2R3 (VQ62)	6,4945	VQIINKKLDLSNVQSKCGSKDNIKHVPGGGSV QIVYKPVDLSKVTSKCGSLGNIHHKPGGGQ	237.12
R1R3 (QQ62)	6.48750	QTAPVPMPDLKNVKSKIGSTENLKHQPGGGKV QIVYKPVDLSKVTSKCGSLGNIHHKPGGGQ	154
R3R4 (VT68)	6.69763	VQIVYKPVDLSKVTSKCGSLGNIHHKPGGGQV EVKSEKLDFKDRVQSKIGSLDNITHVPGGGN	154

3.1.2 Cell line

Tau RD P301S FRET Biosensor cells (American Type Culture Collection; ATCC®, Manassas, VA, USA, CRL-3275™)

3.1.3 Drugs

The Prestwick Chemical Library® (stock concentration 10 mM) (GreenPharma, Orléans, France)

3.1.4 Laboratory instruments and equipment

Agilent PlateLoc Thermal Microplate Sealer (Agilent Technologies, Santa Clara, CA USA)

AXIO Observer.D1 Inverted Fluorescence Motorized Phase Contrast Microscope (Zeiss, Oberkochen, Germany)

Biohazard Herasafe KS (Thermo Fisher Scientific, Waltham, MA, USA)

Cell Carrier 384 well plates (PerkinElmer, Waltham, MA, USA)

Cell Voyager CV7000S (Yokogawa, Musashino, Japan)

Centrifuge 5810R (Eppendorf, Hamburg, Germany)

Centrifuge tubes (15 ml, 50 ml) (TPP Techno Plastic Products AG, Trasadingen, Switzerland)

CERTUS FLEX Liquid Dispenser (Fritz Gyger AG, Gwatt, Switzerland)

Echo® 550 (Labcyte, Beckman Coulter, Inc., Brea, CA, USA)

EnSpire® Multimode Plate Reader (PerkinElmer, Waltham, MA, USA)

Filter Top 500 rapid Filtermax (0.22 µM) (TPP Techno Plastic Products AG, Trasadingen, Switzerland)

Heracell 150i CO_2 incubator (Thermo Fisher Scientific, Waltham, MA, USA)

Mini Centrifuge MiniSpin® (Eppendorf, Hamburg, Germany)

Needle 18G (B. Braun Melsungen AG, Melsungen, Germany)

Pipettes (Eppendorf, Hamburg, Germany)

Olympus Ix51 Inverted Microscope (Olympus, Tokyo, Japan)

Primovert Inverted Cell culture Microscope (Zeiss, Oberkochen, Germany)

Rotina 420 R Centrifuge (Hettich Zentrifugen) (Hettich, Tuttlingen, Germany)

Sterile cylinder

Sterile glass bottles

Sterile tips

20ml syringe (B. Braun Melsungen AG, Melsungen, Germany)

Sterile syringe filter (0.22 μM) (TPP Techno Plastic Products AG, Trasadingen, Switzerland)

Tissue culture flasks (T-25 cm^2, T-75 cm^2) (TPP Techno Plastic Products AG, Trasadingen, Switzerland)

Thermo-Shaker PST-60HL (Biosan, Riga, Latvia)

Vi-Cell XR Cell Viability Analyzer (Beckman Coulter Inc., Brea, CA, USA)

Vortex V-1 Plus (Biosan, Riga, Latvia)

3.1.5 Software

DOG 2.0.1 (Domain Graph) (University of Science & Technology, Baohe, Hefei, Anhui, China)

GraphPad Prism 10 (Dotmatics, Boston, MA, USA)

Microsoft Office (Excel, Powerpoint, Word) (Microsoft, Redmond, WA, USA)

ZEN 3.4 (blue edition) (Zeiss, Oberkochen, Germany)

3.2 Methods

3.2.1 Cell culturing

Thawing the frozen cell line

The vial with the frozen cell line was thawed manually in hands (because the temperature of the human body is around 37 °C). Then, the cell suspension from the vial was transferred into the sterile 15ml centrifuge conical tube using the pipette and centrifuged for 5 minutes at 1200 rpm at room temperature (RT). The supernatant was carefully removed from the centrifuge tube, and about 2 ml of the complete DMEM growth medium was added. Then, the pellet of cells was carefully resuspended by repeated pipetting. The cell suspension was transferred into the culture flask (T-25 cm^2), and the complete growth medium was added to the final volume of 5 ml. Finally, the cells were checked under the inverted microscope, and the culture flask was placed in the CO_2 incubator. On the next day, the cells were checked again under the inverted microscope, and if necessary, the complete DMEM growth medium was replaced with a fresh one (Agrawal *et al.* 2022).

Sub-culturing the adherent cell lines

The cell line was maintained in DMEM growth media in the culture flask (T-75 cm^2) in the CO_2 incubator. Every 3-5 days, the cells were checked under the inverted microscope for signs of contamination, debris, or unhealthy cells, and the color of the

growth medium, viscosity, and turbidity were inspected visually. The old DMEM medium was removed and discarded into the waste container containing the disinfection solution. Then, the cells were washed with 10 ml of the sterile 1x PBS twice. Afterward, 1 ml of TrypLE™ was carefully added to the culture flask to remove the cells from its surface. The flask was put in a CO_2 incubator for incubation. After 5 minutes, the cells were observed under the inverted microscope. Then, 5 ml of the fresh DMEM media was added to the flask and mixed well. The cell suspension was transferred to a 50ml centrifuge tube and centrifuged at 1400 rpm for 5 minutes at RT. Subsequently, the supernatant was carefully removed and discarded, and the pellet was resuspended in 5 ml of the fresh DMEM media. The cells were then counted using the Vi-Cell XR Cell Viability Analyzer. Based on the cell count, the appropriate volume of the cell suspension was transferred into the culture flask, and the DMEM growth media was added to the final volume of 15 ml. Finally, the cells were checked using an inverted microscope and placed in the CO_2 incubator. The cells were routinely tested for mycoplasma contaminations monthly (Agrawal *et al.* 2022).

3.2.2 Tau aggregation assay

The primary method utilized in this study was the Thioflavin T binding assay, a widely employed technique for detecting amyloid fibrils both *in vitro* and *ex vivo*. Thioflavin T (ThT) is a cationic benzothiazole dye known for its ability to exhibit enhanced fluorescence upon binding to amyloid fibrils. This phenomenon is characterized by significant shifts in the excitation and emission bands of ThT, resulting in a pronounced increase in fluorescence. Specifically, the excitation maximum occurs at 450 nm, while the emission maximum is observed at 480 nm. Although the precise molecular mechanism underlying Thioflavin-T binding to amyloids remains elusive, two main hypotheses have been proposed. One hypothesis suggests that the enhanced fluorescence arises from the inhibition of free rotation of the benzothiazole and benzamine rings within ThT, which act as a rotor molecule. The ThT binding assay serves as a valuable tool for the identification and structural analysis of various amyloid fibrils, including those formed by proteins such as tau and insulin. Additionally, this assay has applications beyond amyloid detection, including the monitoring of structural changes in DNA (such as abasic sites, gaps, and mismatches) and the recognition of DNA and RNA G-quadruplexes (Khurana *et al.* 2005; Hawe *et al.* 2008; Sabate *et al.*

2013; Girych *et al.* 2016; Schlein 2017; Zhang *et al.* 2018; Verma *et al.* 2021; Chitbankluai *et al.* 2022).

Primary screening

Before starting the preparation, an EnSpire® Multimode Plate Reader was turned on, and the measurement chamber was set to 37° C, and the upper temperature was set to 2 °C warmer than the lower heater temperature to avoid condensation on the sealed plate surface.

First, the aggregation reaction mixtures for R2 and R3 peptides were prepared according to **Table 2**. Using the CERTUS FLEX Liquid Dispenser, 20 µl of the aggregation reaction was added into each well of the Cell Carrier 384 well plate. Then, the plate was placed in an EnSpire® Multimode Plate Reader, and the fluorescence of ThT binding (λ_{exc} = 460–490 nm, λ_{em} = 500–550 nm) to the peptide was recorded. Afterward, 20 nl of drugs from The Prestwick Chemical Library® were added to the plate using Echo® 550; the desired concentration was 10 µM. The plate was sealed using Agilent PlateLoc Thermal Microplate Sealer to prevent evaporation and put into Thermo-Shaker PST-60HL, set to agitation of 1000 rpm and temperature 37 °C. The reading of the fluorescence of ThT binding to the aggregated peptide was repeated three times every 24 h (72 h in total).

Table 2: Composition of the aggregation reaction mixture for R2 and R3 peptides and volume of each component required for one sample

	Stock concentration	**Desired concentration**	**Volume per well (µl)**
Aggregation buffer	-	-	18.36
Heparin	150 µM	5 µM	0.67
ThT	1 mM	15 µM	0.3
R2 peptide	306.3 µM	10 µM	0.65

	Stock concentration	**Desired concentration**	**Volume per well (µl)**
Aggregation buffer	-	-	18.36
Heparin	150 µM	5 µM	0.67
ThT	1 mM	15 µM	0.3
R3 peptide	307.9 µM	10 µM	0.65

Continuous-mode ThT aggregation assay (drug kinetics)

For the continuous-mode ThT aggregation assay, the aggregation mixture for all peptides used was prepared according to **Table 2** and **Table 3**. Then, similarly to the primary screening, 20 µl of the aggregation reaction was added into each well of the Cell Carrier 384 well plate using CERTUS FLEX Liquid Dispenser, and 20 nl of drugs from The Prestwick Chemical Library® were added to the plate using Echo® 550, the desired concentration was 10 µM for R2, R3 and R3 C322A peptides and 20 µM for R2R3, R1R3 and R3R4 peptides. Afterward, the assay plate was sealed using Agilent PlateLoc Thermal Microplate Sealer to prevent evaporation and put into EnSpire® Multimode Plate Reader. The instrument was set to constant agitation of 1000 rpm during the resting period, and the fluorescence of ThT binding to aggregated peptides was recorded every 10 min up to 72 h (Annadurai *et al.* 2021; Agrawal *et al.* 2022).

Table 3: Composition of the aggregation reaction mixture for peptides used (except R2 and R3) and volume of each component required for one sample

	Stock concentration	**Desired concentration**	**Volume per well (µl)**
Aggregation buffer	-	-	17.33
Heparin	150 µM	5 µM	0.67
ThT	1 mM	15 µM	0.30
R2R3 peptide	237.12 µM	20 µM	1.69

	Stock concentration	**Desired concentration**	**Volume per well (µl)**
Aggregation buffer	-	-	16.42
Heparin	150 µM	5 µM	0.67
ThT	1 mM	15 µM	0.30
R1R3/R3R4 peptide	154 µM	20 µM	2.60

	Stock concentration	**Desired concentration**	**Volume per well (µl)**
Aggregation buffer	-	-	18.36
Heparin	150 µM	5 µM	0.67
ThT	1 mM	15 µM	0.30
R3 C322A peptide	307.9 µM	10 µM	0.65

3.2.3 Tau seeding assay

Peptides from the continuous-mode ThT aggregation assay were used for the transfection of cells. Tau RD P301S FRET Biosensor cells were plated in a Cell Carrier 384 well plate at a density of $1x10^6$ cells.ml^{-1} in 50 µl of growth media, and the plate was put into a CO_2 incubator (37 °C, 5 % CO_2). The next day, the transfection reaction mixture was prepared according to **Table 4** and incubated for 15 min at RT. The old growth medium was carefully removed from the wells and replaced by fresh D-MEM medium. Then, 3.5 µl of transfection reaction mixture was added to every well with cells and incubated in a CO_2 incubator for 72 h. The final concentration of peptide aggregates transfected into cells was 100 nM. After 72 h, the biosensor cells were stained with 10 µM Hoechst-33342 nuclear dye for 15 min in a CO_2 incubator (37 °C, 5 % CO_2). Then, the growth medium was replaced with the fresh D-MEM. The cells were imaged on a Cell Voyager CV7000S microscope using a 60x objective. Cells were maintained at 37 °C and 5% CO2/atmospheric air throughout imaging in a live-cell chamber (Annadurai *et al.* 2022a, 2023).

Table 4: Composition of the transfection reaction mixture for peptides used and volume of each component required for one sample

	Volume (µl)		**Volume (µl)**
Opti-MEM™	2.5	Opti-MEM™	2.5
Aggregates (R2/R3) (stock conc. 10 µM)	0.5	Aggregates (R2R3) (stock conc. 20 µM)	0.25
P3000™ Reagent	0.125	P3000TM Reagent	0.125
Lipofectamine™ 3000 Reagent	0.25	Lipofectamine™ 3000 Reagent	0.25

4 RESULTS

4.1 Primary screening of The Prestwick Chemical Library®

The initial analysis involved a primary screening of drugs from The Prestwick Chemical Library®, the list of which is provided in **Table S1** of **Supplement 1**. The ThT binding assay method was used to examine the aggregation changes of R2 and R3 peptides in the presence of individual drugs. The control sample consisted of tau peptide without any drugs. From the obtained ThT fluorescence values after 72 hours, the relative change in peptide aggregation in the presence of drugs compared to the control sample was calculated and divided into four groups: more than 75%, 50-75%, 25-50%, and less than 25%. The results of this analysis, conducted in two replicates, are depicted using heat maps in **Figure 4** and **Figure 5**.

Subsequently, the effectiveness of individual drugs in inhibiting the aggregation of tau peptides was calculated. The obtained values showed that some substances had a significant inhibitory effect on the aggregation of the R2 peptide (higher than 75%, see **Table 5**), while others exhibited a similar effect on the aggregation of the R3 peptide (higher than 60%, see **Table 6**). These results were further analyzed, and the substances were classified into three categories using a Venn diagram (**Figure 6**). **Table 7** displays the list of substances that were evaluated as Dual inhibitors after comparing the effects of R2 and R3 inhibitors. Out of a total of 1280 compounds, 12 R2 inhibitors, 11 R3 inhibitors, and 11 Dual inhibitors were selected from the initial screening for further analysis.

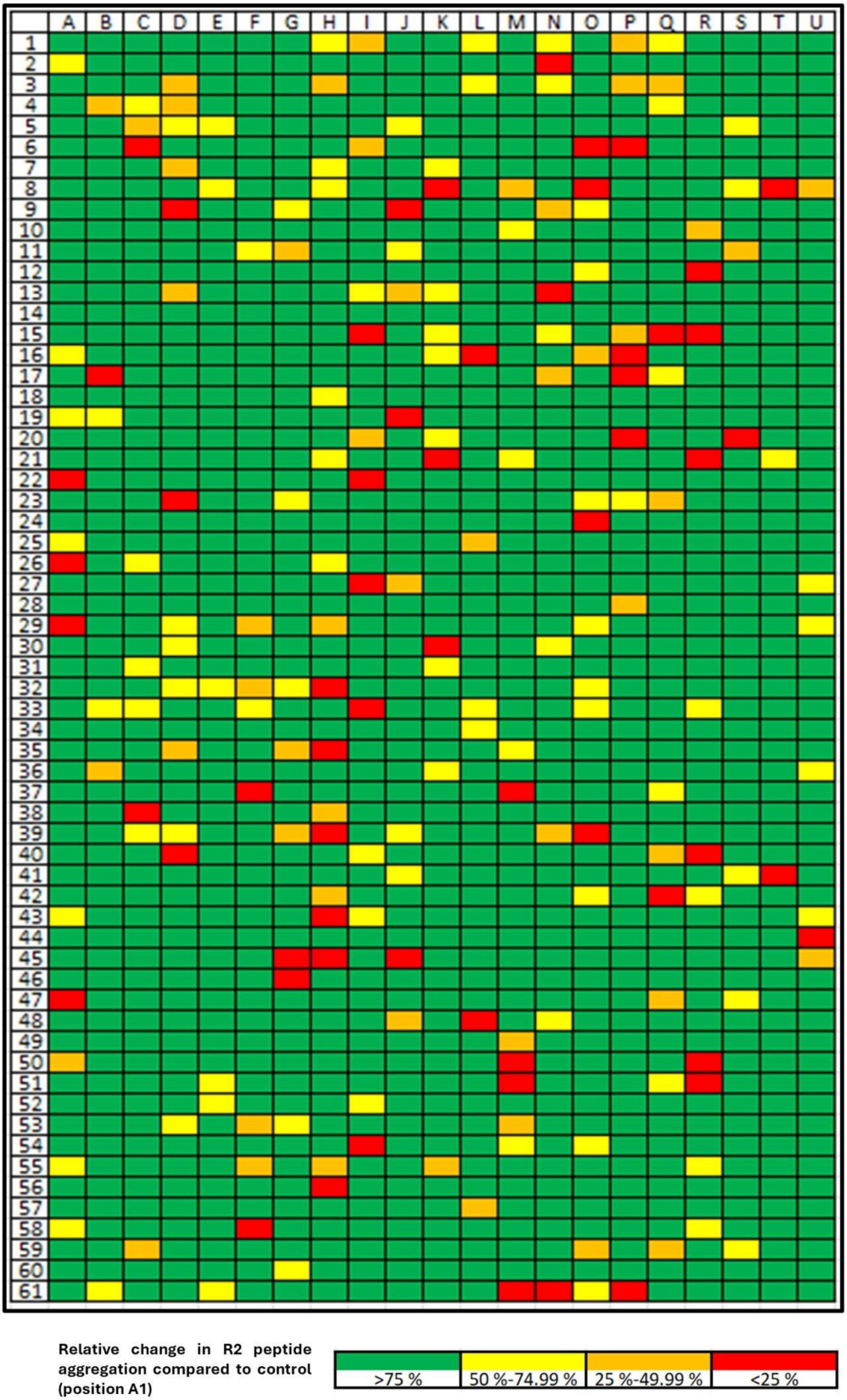

Figure 4: Primary screening of drugs with R2 peptide. Heat map representing the relative change in R2 peptide aggregation in the presence of drugs from The Prestwick Chemical Library® at a concentration of 10 µM after 72 h compared to the control (position A1). Data are represented by two independent experiments.

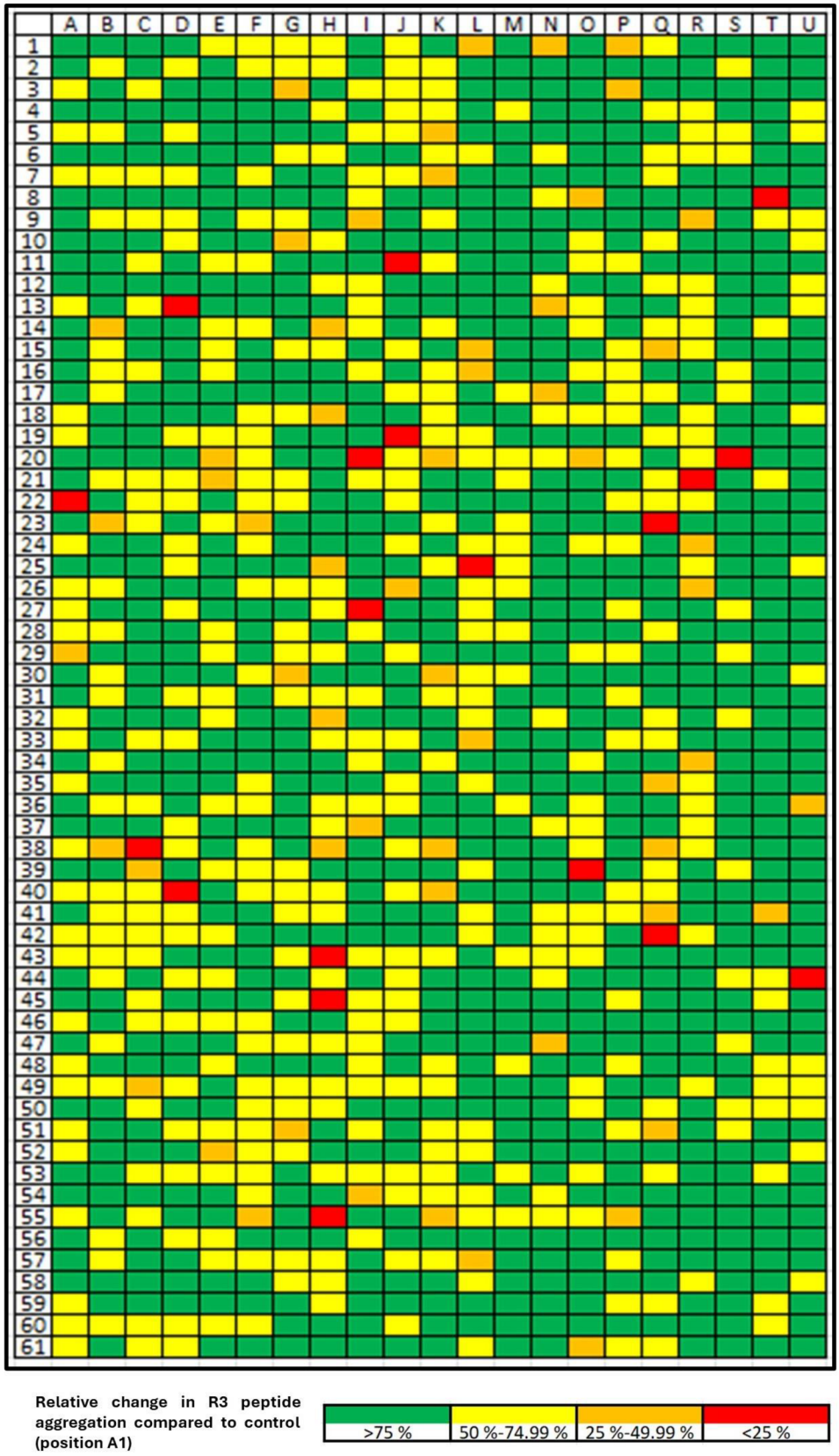

Figure 5: Primary screening of drugs with R3 peptide. Heat map representing the relative change in R3 peptide aggregation in the presence of drugs from The Prestwick Chemical Library® at a concentration of 10 µM after 72 h compared to the control (position A1). Data are represented by two independent experiments.

Table 5: List of R2 inhibitors affecting peptide aggregation more than 75 %. Mean±SEM, n=2

Position	Drug	Effect on R2 (%)	Effect on R3 (%)
Q15	Epirubicin hydrochloride	99±0	62±13
J19	Doxorubicin hydrochloride	98±0	100±0
U44	Pyrvinium pamoate	98±0	89±0
A22	R(-) Apomorphine hydrochloride hemihydrate	97±1	92±1
I27	Daunorubicin hydrochloride	97±0	79±1
N13	Nisoldipine	97±0	60±9
O39	Benserazide hydrochloride	96±0	84±3
M37	Tyloxapol	96±0	23±51
H43	Chicago sky blue 6B	96±0	91±2
B17	Nifedipine	94±0	39±18
O8	Merbromin	94±1	72±5
I15	Alfacalcidol	92±5	0±1
I54	Rifapentine	92±1	68±1
H45	Cyclosporin A	92±1	76±4
S20	Verteporfin	92±5	93±2
A29	Dantrolene sodium salt	91±1	66±2
F58	Thiostrepton	90±1	0±38
K21	Etretinate	89±2	0±6
M51	Simvastatin	89±1	17±12
N61	Aprepitant	89±2	20±18
P20	Ethaverine hydrochloride	89±0	40±18
A47	Antimycin A	88±1	1±26
Q42	(-)-Eseroline fumarate salt	80±6	79±12

Table 6: List of R3 inhibitors affecting peptide aggregation more than 60 %. Mean±SEM, n=2

Position	Drug	Effect on R2 (%)	Effect on R3 (%)
J19	Doxorubicin hydrochloride	98±0	100±0
S20	Verteporfin	92±5	93±2
A22	R(-) Apomorphine hydrochloride hemihydrate	97±1	92±1
H43	Chicago sky blue 6B	96±0	91±2
U44	Pyrvinium pamoate	98±0	89±0
L25	Phenazopyridine hydrochloride	66±3	87±4
R21	Methacycline hydrochloride	77±5	86±1
H55	Methyldopa (L,-)	70±1	84±3
O39	Benserazide hydrochloride	96±0	84±3
D40	Oxytetracycline dihydrate	75±4	81±5
D13	Levodopa	73±3	80±7
Q23	Dopamine hydrochloride	74±1	79±3
I27	Daunorubicin hydrochloride	97±0	79±1
Q42	(-)-Eseroline fumarate salt	80±6	79±12
I20	Meclocycline sulfosalicylate	65±2	77±9
J11	Oxantel pamoate	37±2	76±1
H45	Cyclosporin A	92±1	76±4
B14	Flufenamic acid	17±1	73±1
K7	Sulfasalazine	36±2	73±8
O8	Merbromin	94±1	72±5
Q15	Epirubicin hydrochloride	99±0	62±13
H18	Carbidopa	47±2	61±4

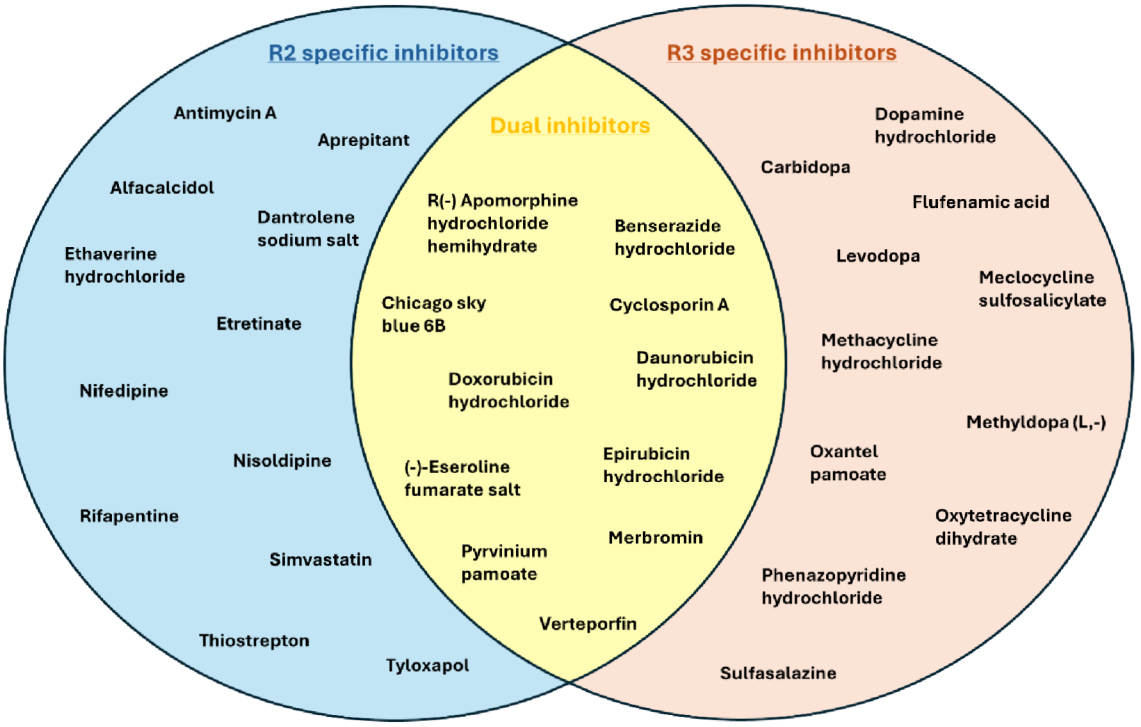

Figure 6: Drugs classification. Venn diagram showing the classification of drugs (listed in **Table 5** and **Table 6**) into three categories.

Table 7: List of Dual inhibitors having the highest effect on R2 and R3 peptide aggregation. Mean±SEM, n=2

Position	Drug	Effect on R2 (%)	Effect on R3 (%)
J19	Doxorubicin hydrochloride	98±0	100±0
A22	R(-) Apomorphine hydrochloride hemihydrate	97±1	92±1
H43	Chicago sky blue 6B	96±0	91±2
U44	Pyrvinium pamoate	98±0	89±0
S20	Verteporfin	92±5	93±2
O39	Benserazide hydrochloride	96±0	84±3
I27	Daunorubicin hydrochloride	97±0	79±1
H45	Cyclosporin A	92±1	76±4
O8	Merbromin	94±1	72±5
Q15	Epirubicin hydrochloride	99±0	62±13
Q42	(-)-Eseroline fumarate salt	80±6	79±12

4.2 Continuous-mode ThT aggregation assay (drug kinetics)

The subsequent analysis encompassed the continuous-mode ThT aggregation assay, facilitating the examination of the kinetics of the chosen drugs. Throughout this assessment, ThT fluorescence, binding to aggregated peptides, was assessed at ten-minute intervals spanning 72 hours. The acquired data underwent normalization based on the lowest and highest relative fluorescence intensity values within the dataset. The resultant graphs for the five most effective drugs are depicted in **Figure 7** (for R2 inhibitors), **Figure 8** (for R3 inhibitors), and **Figure 9** (for Dual inhibitors). These findings were later quantified employing the area under the curve (**Table 8**, **Table 9**, and **Table 10**), which serves as an integrated gauge of a measurable impact or occurrence. It is utilized as a cumulative measure of drug efficacy in pharmacokinetics and as a method for comparing peaks in chromatography.

Among the substances with the greatest inhibitory effect on the aggregation of the R2 peptide were Dantrolene sodium salt, Etretinate, Nifedipine, Nisoldipine, and Rifapentine (**Figure 7A**). Surprisingly, all of these drugs exhibited an inhibitory effect on the aggregation of the R3 peptide as well (**Figure 7B**), despite being characterized as R2 inhibitors, indicating that they should not inhibit the aggregation of R3 peptide. On the other hand, in the case of the combination of these R2 inhibitors with the R1R3 peptide, which lacks the R2 repeat motif in its structure, no inhibitory effect on aggregation was observed (**Figure 7C**).

Figure 8 displays graphs obtained from the analysis of the kinetics of R3 inhibitors in combination with R2, R3, R2R3, and R3 mut peptides. It was expected that these substances, characterized as R3 inhibitors, would not affect the aggregation of the R2 peptide. However, in **Figure 8A**, it is possible to observe that some drugs indeed inhibited the aggregation of the R2 peptide. As anticipated, an inhibitory effect on the aggregation of the R3 peptide was observed for all R3 inhibitors in each case (**Figure 8B**). Significant reduction in the aggregation of the R3 peptide can be observed, for instance, with Oxytetracycline dihydrate or Meclocycline sulfosalicylate. From the graphs illustrating the kinetics of R3 inhibitors in combination with the R2R3 peptide, substances exhibiting the greatest impact on inhibiting the aggregation of this combined peptide can be identified, such as Phenazopyridine hydrochloride or Oxytetracycline dihydrate (**Figure 8C**). Also noteworthy are the results of the analysis for the R3 mut peptide (**Figure 8D**), which aimed to determine whether the presence of cysteine at

position 322 is crucial for the antifibrillization effect of the selected drugs. It is evident that, since the aggregation of the R3 mut peptide was inhibited in all cases, it can be inferred that the studied drugs interact with the R3 peptide in regions not containing Cys322, thus indicating that the presence of this amino acid is not essential for the antifibrillization effect of the studied drugs.

The last group of compounds consisted of so-called Dual Inhibitors, which were expected to exhibit inhibitory effects on the aggregation of all peptides used: R2, R3, R3 mut, and R2R3. As observed in the individual graphs (**Figure 9A-D**), most of the studied Dual Inhibitors yielded the expected results. Consequently, the majority of these drugs were selected for further analysis.

Within the selected drugs used for subsequent analysis via tau seeding assay, certain groups of compounds were characterized based on their structure. Examples of these are displayed in **Table 11**.

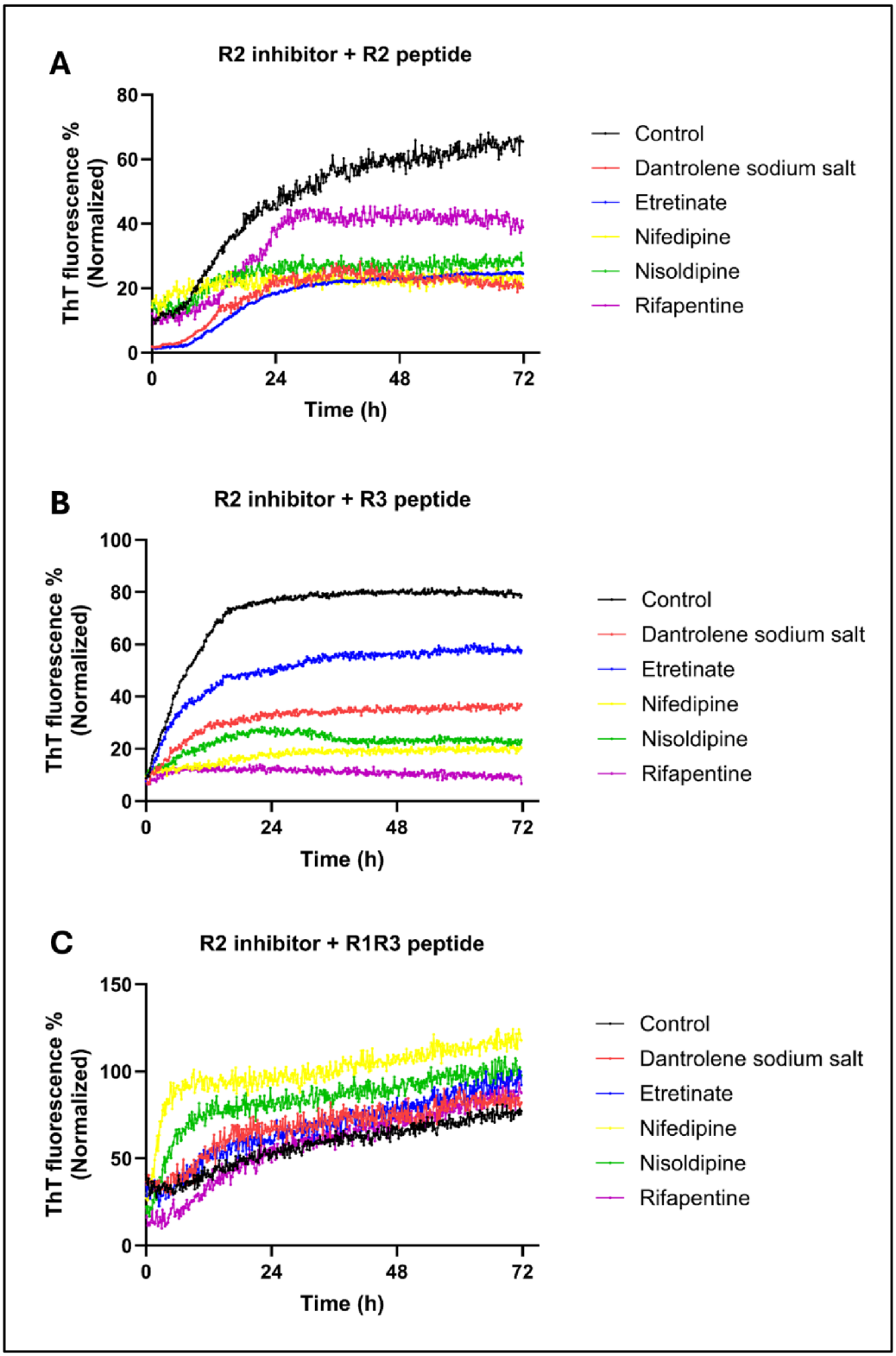

Figure 7: Impact of R2 inhibitors on tau peptide aggregation. A Graph showing the effect of selected R2 inhibitors at a single concentration of 10 µM on R2 peptide. **B** Graph showing the effect of selected R2 inhibitors at a single concentration of 10 µM on R3 peptide. **C** Graph showing the effect of selected R2 inhibitors at a single concentration of 20 µM on R1R3 peptide. The raw data (ThT fluorescence) were normalised to the lower and higher relative fluorescence intensity values in the data set.

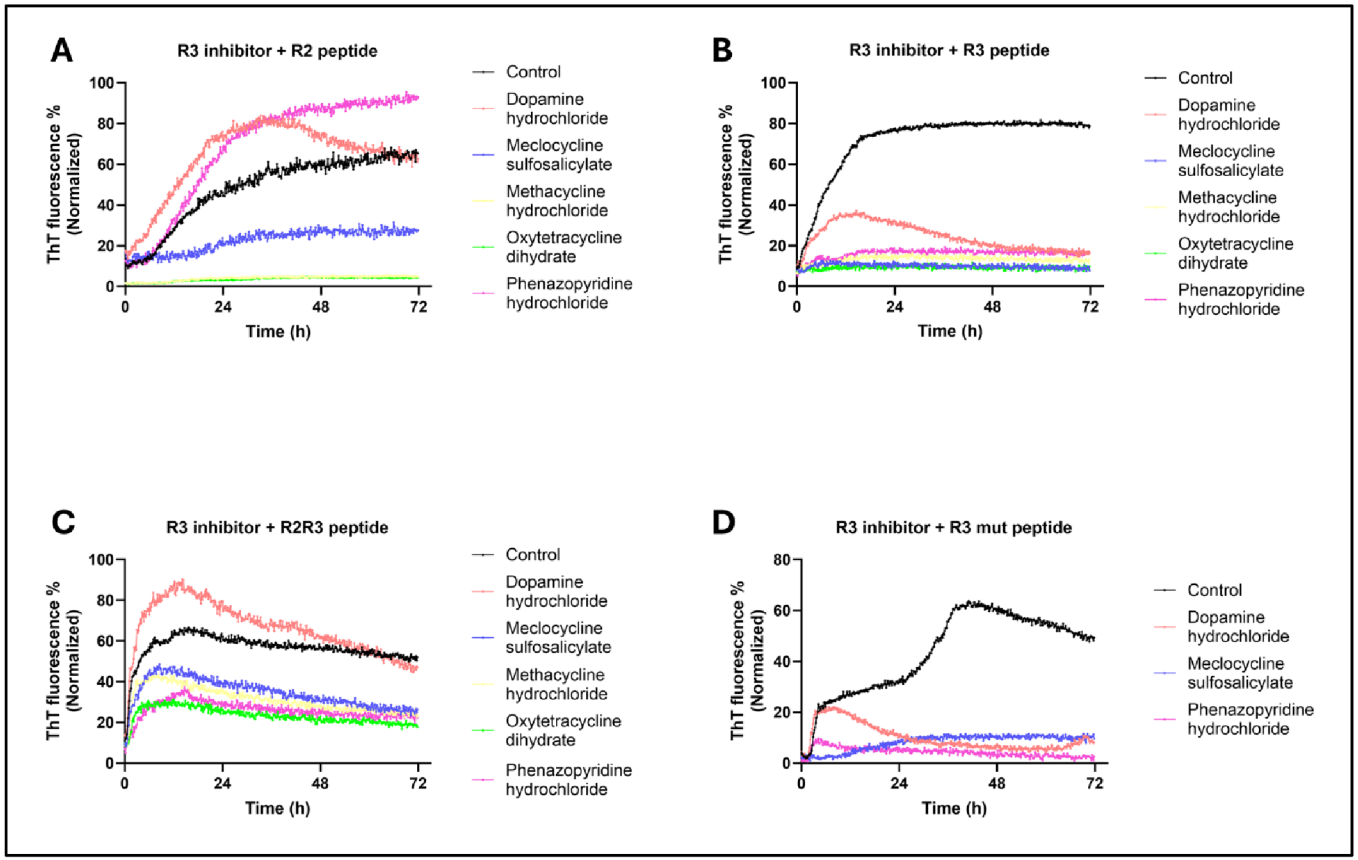

Figure 8: Impact of R3 inhibitors on tau peptide aggregation. A Graph showing the effect of selected R3 inhibitors at a single concentration of 10 µM on R2 peptide. **B** Graph showing the effect of selected R3 inhibitors at a single concentration of 10 µM on R3 peptide. **C** Graph showing the effect of selected R3 inhibitors at a single concentration of 20 µM on R2R3 peptide. **D** Graph showing the effect of selected R3 inhibitors on at a single concentration of 10 µM R3 mut peptide. The raw data (ThT fluorescence) were normalised to the lower and higher relative fluorescence intensity values in the data set.

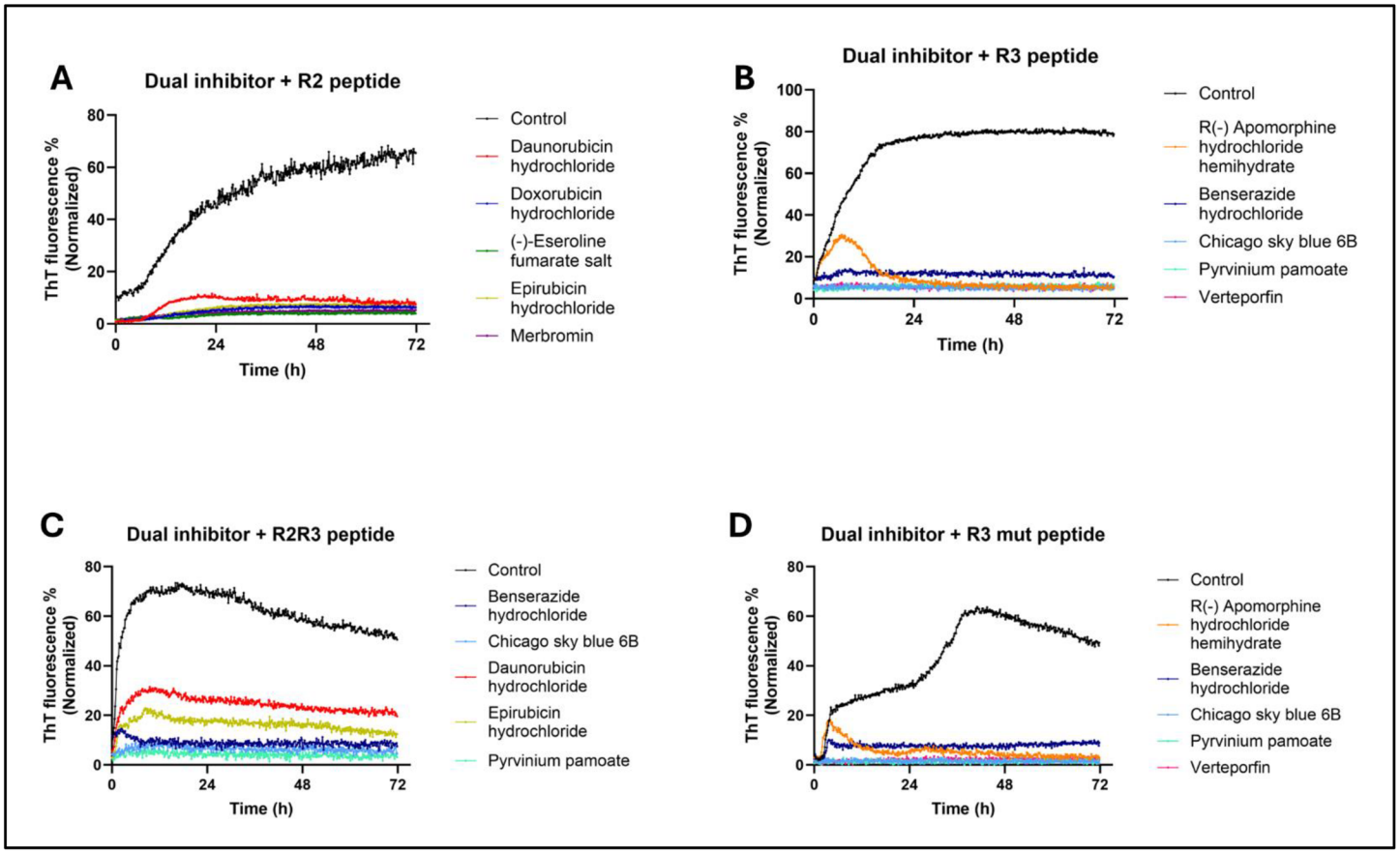

Figure 9: Impact of Dual inhibitors on tau peptide aggregation. **A** Graph showing the effect of selected Dual inhibitors at a single concentration of 10 µM on R2 peptide. **B** Graph showing the effect of selected Dual inhibitors at a single concentration of 10 µM on R3 peptide. **C** Graph showing the effect of selected Dual inhibitors at a single concentration of 20 µM on R2R3 peptide. **D** Graph showing the effect of selected Dual inhibitors on at a single concentration of 10 µM R3 mut peptide. The raw data (ThT fluorescence) were normalised to the lower and higher relative fluorescence intensity values in the data set.

Table 8: Quantification of Impact of TOP5 R2 inhibitors on tau peptide aggregation. Mean±SEM, n=2

Type	Drug	Area under the curve (AUC)	Relative AUC
R2 inhibitor + R2 peptide	Control	3474±53.16	100 %
	Etretinate	1292±35.68	37.19 %
	Dandrolene sodium salt	1358±22.83	39.09 %
	Nifedipine	1580±27.56	45.48 %
	Nisoldipine	1781±25.99	51.27 %
	Rifapentine	2467±41.47	71.01 %
R2 inhibitor + R3 peptide	Control	5147±44.90	100 %
	Rifapentine	786.3±7.22	15.28 %
	Nifedipine	1263±10.62	24.54 %
	Nisoldipine	1636±60.13	31.79 %
	Dandrolene sodium salt	2276±21.85	44.22 %
	Etretinate	3598±24.36	69.90 %
R2 inhibitor + R1R3 peptide	Control	4135±26.64	100 %
	Rifapentine	4207±25.27	101.74 %
	Dandrolene sodium salt	4862±38.46	117.58 %
	Etretinate	4909±37.53	118.72 %
	Nisoldipine	6002±42.81	145.15 %
	Nifedipine	7200±56.27	174.12 %

Table 9: Quantification of Impact of TOP5 R3 inhibitors on tau peptide aggregation. Mean±SEM, n=2

Type	Drug	Area under the curve (AUC)	Relative AUC
R3 inhibitor + R3 peptide	Control	5147±44.90	100 %
	Oxytetracycline dihydrate	667.4±8.32	12.97 %
	Meclocycline sulfosalicylate	721.5±7.14	14.02 %
	Methacycline hydrochloride	956.9±10.50	18.59 %
	Phenazopyridine hydrochloride	1155±8.01	22.44 %
	Dopamine hydrochloride	1753±25.59	34.06 %
R3 inhibitor + R2 peptide	Control	3474±53.16	100 %
	Oxytetracycline dihydrate	260.9±5.48	7.51 %
	Methacycline hydrochloride	289.9±7.21	8.34 %
	Meclocycline sulfosalicylate	1622±18.94	46.69 %
	Dopamine hydrochloride	4605±97.33	132.56 %
	Phenazopyridine hydrochloride	4910±158.1	141.34 %
R3 inhibitor + R2R3 peptide	Control	4072±45.58	100 %
	Oxytetracycline dihydrate	1677±27.88	41.18 %
	Phenazopyridine hydrochloride	1874±32.35	46.02 %
	Methacycline hydrochloride	2249±30.21	55.23 %
	Meclocycline sulfosalicylate	2488±22.99	61.10 %
	Dopamine hydrochloride	4766±86.15	117.04 %
R3 inhibitor + R3 mut peptide	Control	3110±83.50	100 %
	Phenazopyridine hydrochloride	315.1±2.91	10.13 %
	Meclocycline sulfosalicylate	591.3±20.43	19.01 %
	Dopamine hydrochloride	718.0±13.96	23.09 %

Table 10: Quantification of Impact of TOP5 Dual inhibitors on tau peptide aggregation. Mean±SEM, n=2

Type	Drug	Area under the curve (AUC)	Relative AUC
Dual inhibitor + R2 peptide	Control	3474±53.16	100 %
	(-)-Eseroline fumarate salt	251.2±5.07	7.23 %
	Merbromin	308.2±6.45	8.87 %
	Doxorubicin hydrochloride	372.2±10.35	10.71 %
	Epirubicin hydrochloride	416.5±5.72	11.99 %
	Daunorubicin hydrochloride	581.5±9.02	16.74 %
Dual inhibitor + R3 peptide	Control	5147±44.90	100 %
	Chicago sky blue 6B	384.0±4.90	7.46 %
	Verteporfin	400.8±7.12	7.79 %
	Pyrvinium pamoate	408.8±7.10	7.94 %
	R(-) Apomorphine hydrochloride hemihydrate	722.6±11.22	14.04 %
	Benserazide hydrochloride	841.6±14.19	16.35 %
Dual inhibitor + R2R3 peptide	Control	4419±50.27	100 %
	Pyrvinium pamoate	292.7±4.78	6.62 %
	Chicago sky blue 6B	467.3±5.85	10.57 %
	Benserazide hydrochloride	647.4±6.25	14.65 %
	Epirubicin hydrochloride	1175±17.20	26.59 %
	Daunorubicin hydrochloride	1758±33.11	39.78 %
Dual inhibitor + R3 mut peptide	Control	3110±83.50	100 %
	Pyrvinium pamoate	2.48±0.20	0.08 %
	Chicago sky blue 6B	110.7±1.94	3.56 %
	Verteporfin	144.9±1.94	4.66 %
	R(-) Apomorphine hydrochloride hemihydrate	403.7±5.37	12.98 %
	Benserazide hydrochloride	556.5±3.42	17.89 %

Table 11: Examples of the most effective drugs selected for the tau seeding assay classified into three groups based on their structure. The structures of the compounds were taken from ChemSpider (Ref. 2)

Group	Drug	Structure
Catechols	R(-) Apomorphine hydrochloride hemihydrate	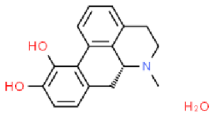 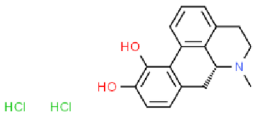
	Benserazide hydrochloride	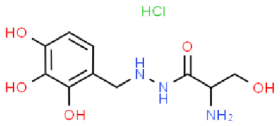
	Dopamine hydrochloride	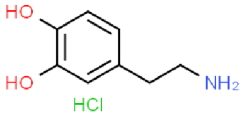
	Levodopa	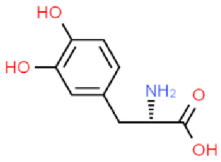
	Methyldopa (L,-)	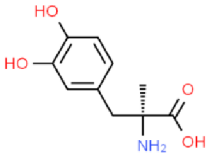
Anthraquinones/Terpenoids/Tetracyclines	Daunorubicin hydrochloride	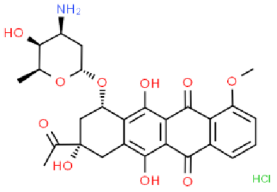
	Doxorubicin hydrochloride	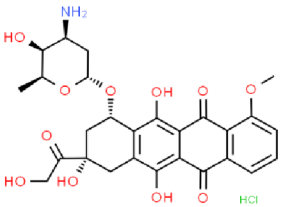
	Epirubicin hydrochloride	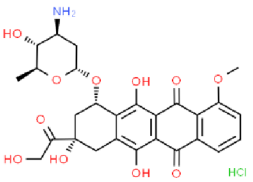

Table 12: Examples of the most effective drugs selected for the tau seeding assay classified into three groups based on their structure. The structures of the compounds were taken from ChemSpider (Ref. 2) *(continued)*

Group	Drug	Structure
Anthraquinones/Terpenoids /Tetracyclines	Methacycline hydrochloride	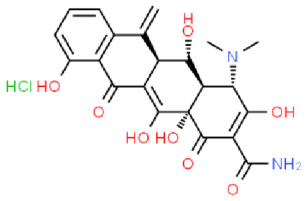
	Oxytetracycline dihydrate	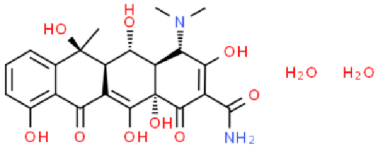
Others	Chicago sky blue 6B	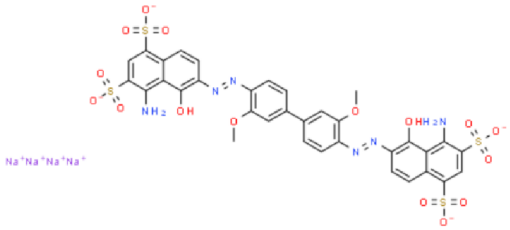
	Dantrolene sodium salt	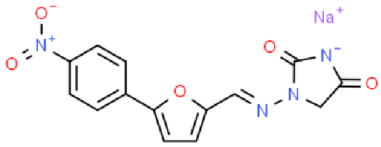
	Pyrvinium pamoate	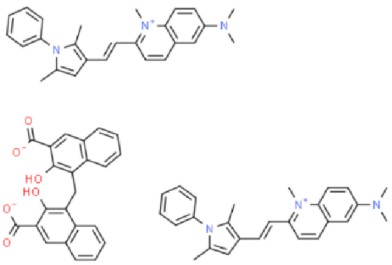
	Rifapentine	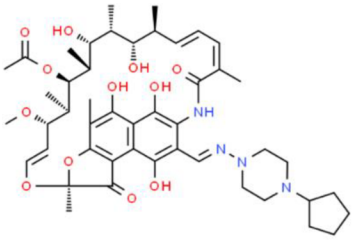
	Verteporfin	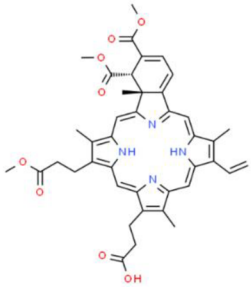

4.3 Tau seeding assay

A seeding assay was performed using biosensor cells and samples obtained from the continuous-mode ThT aggregation assay. The aim of this experiment was to determine whether the selected compounds could prevent the formation of intracellular aggregates that occur during the accumulation of exogenous seeds in the cell. A transfection reaction mixture without peptides and drugs was used as a negative control, while a peptide without drugs served as a positive control.

Figure 10 shows graphs representing the number of seeded intracellular aggregates for the 2-4 most effective drugs from each category. Rifapentine and Dandrolene sodium salt were tested as R2 inhibitors. However, none of these drugs showed inhibitory effects in the formation of intracellular aggregates (**Figure 10A**). On the other hand, some compounds, such as Methacycline hydrochloride (**Figure 10B**) or Chicago sky blue 6B (**Figure 10C**), inhibited the formation of intracellular aggregates induced by R2 and R3 peptides to the level of the negative control. However, no inhibition occurred in the formation of intracellular aggregates induced by the combined R2R3 peptide.

From **Figure 10**, it is evident that among the effective compounds inhibiting the formation of intracellular aggregates are Chicago sky blue 6B, Methacycline hydrochloride, and Dopamine hydrochloride.

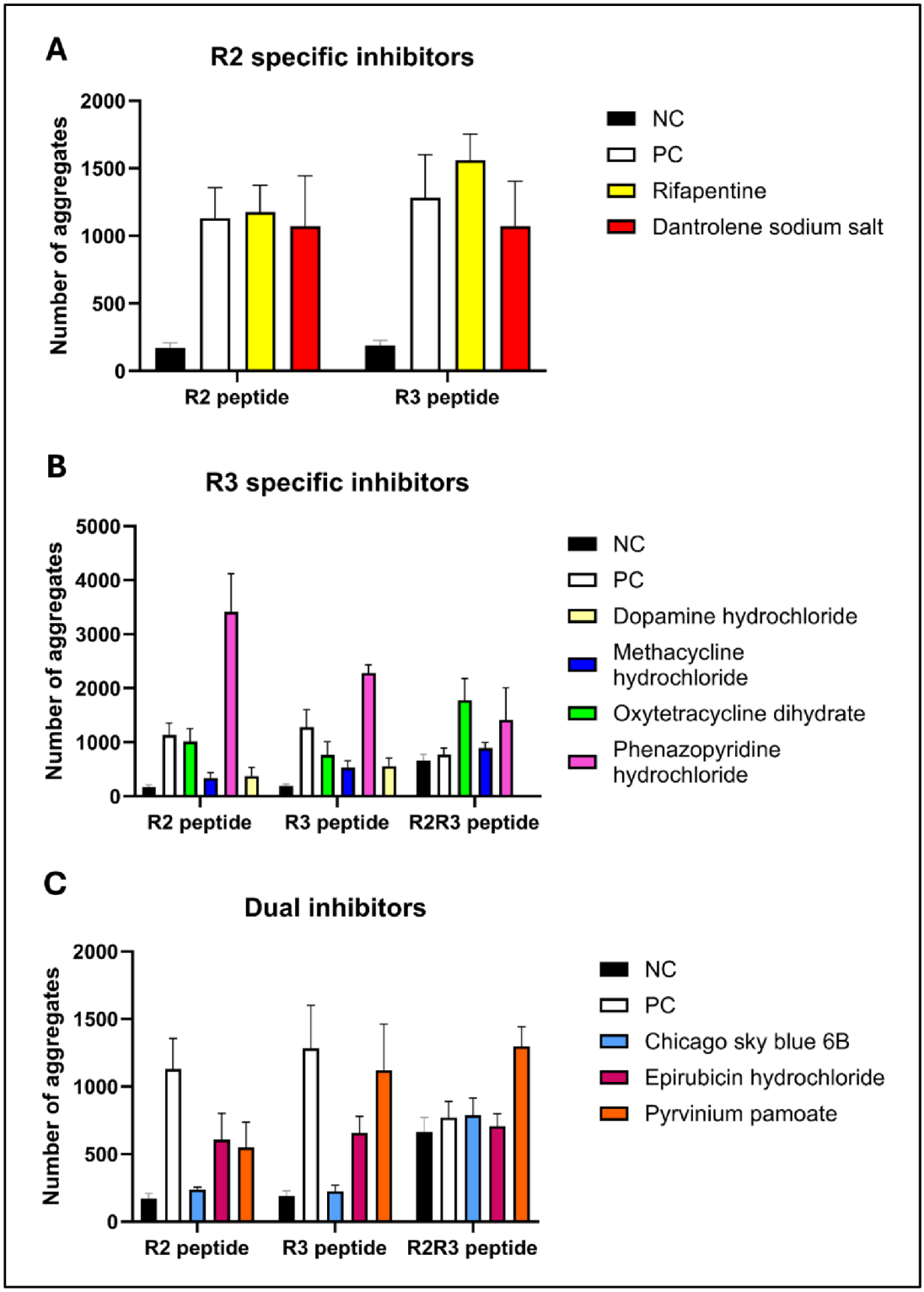

Figure 10: Cellular seeding assay. A-C The number of seeded intracellular Tau RD P301S aggregates in biosensor cells after 72 h of treatment with 100 nM R2, R3, or R2R3 samples in the presence of 2-4 most effective drugs from continuous-mode ThT aggregation assay. NC = Negative Control, PC = Positive Control. Mean±SEM, n=2.

5 DISCUSSION

Despite significant advances in scientific research and medical practice, many diseases still lack effective treatments, including neurodegenerative disorders like Alzheimer's disease. The development of new medications is a lengthy process, spanning from the initial concept to FDA approval, which can take anywhere from 10 to 25 years (Trajanoska *et al.* 2023). Leveraging existing drugs for the treatment of different conditions than those they were initially approved for could streamline the development process for treating various diseases. This approach would spare scientists the arduous phases of developing and synthesizing new compounds.

The objective of this study was to identify compounds stored within the Prestwick chemical library® that could potentially modulate the aggregation and propagation of tau protein, offering alternative therapeutic options for Alzheimer's disease. Initially, a primary screening of all compounds was conducted using R2 and R3 peptides. These peptides were chosen based on previous research highlighting their significance in tau protein aggregation, seeding, and propagation (Annadurai *et al.* 2022a). The specific hexapeptide motifs within these regions (^{275}VQIINK^{280} and ^{306}VQIVYK^{311}) play critical roles in initiating and stabilizing the formation of cross-β-sheet aggregates, which are pivotal in tau pathology and neurodegenerative mechanisms (Von Bergen *et al.* 2000, 2001). Additionally, these regions harbor sites susceptible to various post-translational modifications implicating in tau pathology and neurodegeneration, such as phosphorylation, acetylation, and ubiquitination (Caballero *et al.* 2021; Man *et al.* 2023; Ye *et al.* 2024).

The identified compounds were subsequently categorized into three groups: R2-specific inhibitors, R3-specific inhibitors, and Dual inhibitors. Utilizing Dual inhibitors in the treatment of Alzheimer's disease could yield significant benefits. Similar to cholinesterase inhibitors (Ballard 2002), it's conceivable that compounds inhibiting both R2 and R3 simultaneously might exhibit superior clinical efficacy compared to those targeting only R2 or R3. Moreover, it's known that the adult human brain harbors tau isoforms with 3R and 4R variations, distinguished by the presence or absence of the R2 region in the microtubule-binding domain (Tapia-Rojas *et al.* 2019). Dual inhibitors could effectively target all existing isoforms in the human brain, obviating the need for prescribing combinations of R2 and R3 inhibitors. This approach could reduce the risk of drug interactions and toxicity associated with dosage constraints (Roy *et al.* 2023).

For subsequent analysis using the continuous-mode ThT aggregation assay, wherein the kinetics of drugs were observed over 72 hours, bi-repeat peptides R2R3, R1R3, and R3R4 were included alongside simple peptides R2 and R3. Previous studies have demonstrated the aggregation capability of these peptides under *in vitro* conditions (Jayan *et al.* 2021; Sahayaraj *et al.* 2023; Longhini *et al.* 2024). Utilizing shorter protein constructs is expected to facilitate faster and more homogeneous fiber formation compared to full-length proteins (Jayan *et al.* 2021). The aim of using the R3 mut peptide (R3 C322A peptide) was to determine whether the presence of cysteine at position 322 is crucial for the antifibrillization effect of the selected drugs (Annadurai *et al.* 2022b).

Upon analyzing the results of these experiments, it was surprisingly uncovered that certain drugs, designated as specific inhibitors, exerted inhibitory effects on the aggregation of both peptides. This suggests a potential misclassification of compounds into predefined categories. On the other hand, in instances where R2 inhibitors targeted the R3 peptide, no inhibition of R1R3 peptide aggregation was observed. This prompts a hypothesis that both peptides may share a common or similar domain to which the tested substance binds, with the presence of the R1 region potentially impeding the inhibitory effect of substances. However, this hypothesis lacks experimental validation, necessitating further investigation. To explore this conjecture, employing simulations of drug-peptide interactions via molecular dynamics simulation is proposed (Annadurai *et al.* 2022b).

In this study, which aimed to identify suitable candidates as specific pharmacological modulators of tau protein aggregation and spreading for Alzheimer's disease therapy, three substances emerged as promising candidates for their notable inhibitory effects on R3 and R2R3 peptide aggregation, along with their ability to prevent intracellular aggregate formation.

The first compound of interest is Chicago sky blue 6B. Prior research has highlighted its neuroprotective and anti-inflammatory properties in animal models (Pomierny *et al.* 2024). Therefore, early administration of this drug in AD could potentially curtail extensive neuroinflammation, a contributing factor to AD pathology. Additionally, Chicago sky blue 6B has shown inhibitory effects on α-synuclein aggregation, a hallmark of synucleinopathies like Parkinson's disease (Min *et al.* 2022). Further investigations could explore its potential as a universal protein aggregation inhibitor, offering therapeutic benefits across various neurodegenerative diseases.

The second compound, Methacycline hydrochloride, belonging to the tetracycline group, has garnered attention for its significant inhibitory and disaggregating effects on the Aβ protein, as demonstrated in previous studies (Xu *et al.* 2020). If it proves effective against the aggregation of both Aβ and tau proteins implicated in AD, Methacycline hydrochloride could be classified as a Dual-Targeting inhibitor, potentially enhancing its efficacy in AD treatment.

Lastly, Dopamine hydrochloride, a catechol compound, has shown promise as an inhibitor of ataxin-3 protein aggregation, a characteristic feature of Machado-Joseph disease, a type of spinocerebellar ataxia. This finding suggests the potential for repurposing Dopamine hydrochloride for the treatment of neurodegenerative diseases beyond its conventional use (Figueiredo *et al.* 2023).

Overall, these compounds offer promising avenues for therapeutic intervention in AD and other neurodegenerative disorders, presenting opportunities for further exploration and development in the quest for effective treatments.

Nevertheless, the study identified a few shortcomings that warrant attention for enhancing its validity and reliability. Firstly, the replicate number in the experiments was insufficient, potentially compromising the robustness of the statistical analyses and the reliability of the conclusions drawn. To address this issue, efforts have been initiated to increase the replicate number for all experiments, thereby bolstering the statistical power of the results. Additionally, the initial selection of drugs in the study lacked strong statistical analysis, which may have introduced biases and inaccuracies in identifying promising candidates. Currently, the data are undergoing rigorous statistical analysis to refine the selection process for pharmacological agents. These analytical efforts aim to ensure that only the most promising candidates progress to further investigation.

6 CONCLUSION

The objective of this master's thesis was to identify potential candidates as specific pharmacological modulators of tau protein aggregation and spreading for the treatment of Alzheimer's disease (AD). Initially, a primary screening of the Prestwick Chemical Library was conducted using the ThT aggregation assay. Out of the 1280 compounds screened, 34 promising candidates were selected and categorized into three groups: R2-specific inhibitors, R3-specific inhibitors, and Dual inhibitors. These compounds were subsequently subjected to a continuous-mode ThT aggregation assay to assess their kinetics over 72 hours. The most effective compounds were then further evaluated using a tau seeding assay in biosensor cells.

Through this comprehensive analysis, three compounds—Chicago sky blue 6B, Methacycline hydrochloride, and Dopamine hydrochloride—emerged as potential inhibitors capable of preventing the formation and propagation of intracellular aggregates, thus holding promise for AD therapy. However, to substantiate this hypothesis, additional investigations employing biochemical methods (e.g., Native Page or Western blot) or structural analyses (e.g., molecular dynamics simulation) are warranted. Furthermore, exploring the application of a 3D spheroid cultivation system is advisable, as it mimics a physicochemical environment closer to *in vivo* conditions, facilitating enhanced cell-matrix interactions and potentially overcoming the limitations associated with traditional monolayer cell cultures.

7 REFERENCES

7.1 Scientific literature

Agnello, L., and Ciaccio, M. 2022. Neurodegenerative Diseases: From Molecular Basis to Therapy. Int J Mol Sci **23**(21): 12854. doi:10.3390/ijms232112854.

Agrawal, K., Bouchal, J., Das, V., Drábek, J., Džubák, P., Hajdúch, M., Koberna, K., Ligasová, A., Mistrík, M., De Sanctis, J.B., Srovnal, J., Janošťáková, A., Kudlová, N., Stránská, J., Buriánová, R., Kotulová, J., Schadich, E., Ondra, M., Kubíčková, A., Gurská, S., Flodrová, P., Flodr, P., Kurfürstová, D., Kořínková, G., Gachechiladze, M., Buchtová, T., Trojanec, R., Šporiková, Z., Řehulka, J., Ligasová, A., Koberna, K., Stanková, J., Frydrych, I., Lacey, M., Škrott, Z., Mašek, V., Medvedíková, M., Gurský, J., Hrubá, L., Václavková, J., Holub, D., Oždian, T., Jakoubková, M., Petřík, M., Nový, Z., Annadurai, N., Carazo, A., Lišková, B., Koudeláková, V., Uniyal, V., Macečková, Z., Slavík, H., Řehulková, A., Bartáková, K., and Slavkovský, R. 2022. Laboratory Techniques in Cellular and Molecular Medicine. *In* 1st edition. Univerzita Palackého v Olomouci, Křížkovského 8, 771 47 Olomouc. doi:10.5507/lf.22.24460499.

Alkanli, S.S., Alkanli, N., Ay, A., and Albeniz, I. 2023. CRISPR/Cas9 Mediated Therapeutic Approach in Huntington's Disease. Mol Neurobiol **60**(3): 1486–1498. doi:10.1007/s12035-022-03150-5.

Alquezar, C., Arya, S., and Kao, A.W. 2021. Tau Post-translational Modifications: Dynamic Transformers of Tau Function, Degradation, and Aggregation. Front Neurol **11**: 595532. doi:10.3389/fneur.2020.595532.

Annadurai, N., De Sanctis, J.B., Hajdúch, M., and Das, V. 2021. Tau secretion and propagation: Perspectives for potential preventive interventions in Alzheimer's disease and other tauopathies. Experimental Neurology **343**: 113756. doi:10.1016/j.expneurol.2021.113756.

Annadurai, N., Hrubý, J., Kubíčková, A., Malina, L., Hajdúch, M., and Das, V. 2023. Time- and dose-dependent seeding tendency of exogenous tau R2 and R3 aggregates in cells. Biochemical and Biophysical Research Communications **653**: 102–105. doi:10.1016/j.bbrc.2023.02.057.

Annadurai, N., Malina, L., Malohlava, J., Hajdúch, M., and Das, V. 2022a. Tau R2 and R3 are essential regions for tau aggregation, seeding and propagation. Biochimie **200**: 79–86. doi:10.1016/j.biochi.2022.05.013.

Annadurai, N., Malina, L., Salmona, M., Diomede, L., Bastone, A., Cagnotto, A., Romeo, M., Šrejber, M., Berka, K., Otyepka, M., Hajdúch, M., and Das, V. 2022b. Antitumour drugs targeting tau R3 VQIVYK and Cys322 prevent seeding of endogenous tau aggregates by exogenous seeds. The FEBS Journal **289**(7): 1929–1949. doi:10.1111/febs.16270.

Appleby, B.S., Shetty, S., and Elkasaby, M. 2022. Genetic aspects of human prion diseases. Front Neurol **13**: 1003056. doi:10.3389/fneur.2022.1003056.

Armstrong, R.A. 2006. Creutzfeldt-Jakob disease and vision. Clinical and Experimental Optometry **89**(1): 3–9. doi:10.1111/j.1444-0938.2006.00001.x.

Arnold, W.D., Kassar, D., and Kissel, J.T. 2015. Spinal Muscular Atrophy: Diagnosis and Management in a New Therapeutic Era. Muscle Nerve **51**(2): 157–167. doi:10.1002/mus.24497.

Ashford, B.A., Boche, D., Cooper-Knock, J., Heath, P.R., Simpson, J.E., and Highley, J.R. 2021. Review: Microglia in motor neuron disease. Neuropathology and Applied Neurobiology **47**(2): 179–197. doi:10.1111/nan.12640.

Atri, A. 2019. The Alzheimer's Disease Clinical Spectrum. Medical Clinics of North America **103**(2): 263–293. doi:10.1016/j.mcna.2018.10.009.

Avila, J., Lucas, J.J., Pérez, M., and Hernández, F. 2004. Role of Tau Protein in Both Physiological and Pathological Conditions. Physiological Reviews **84**(2): 361–384. doi:10.1152/physrev.00024.2003.

Baiardi, S., Rossi, M., Capellari, S., and Parchi, P. 2019. Recent advances in the histo-molecular pathology of human prion disease. Brain Pathol **29**(2): 278–300. doi:10.1111/bpa.12695.

Ballard, C.G. 2002. Advances in the Treatment of Alzheimer's Disease: Benefits of Dual Cholinesterase Inhibition. Eur Neurol **47**(1): 64–70. doi:10.1159/000047952.

Barbier, P., Zejneli, O., Martinho, M., Lasorsa, A., Belle, V., Smet-Nocca, C., Tsvetkov, P.O., Devred, F., and Landrieu, I. 2019. Role of Tau as a Microtubule-Associated Protein: Structural and Functional Aspects. Front. Aging Neurosci. **11**: 204. doi:10.3389/fnagi.2019.00204.

Behan, P.O. 1982. Creutzfeldt-Jakob disease. British Medical Journal (Clinical research ed.) **284**(6330): 1658. BMJ Publishing Group. doi:10.1136/bmj.284.6330.1658-a.

Beitz, J.M. 2014. Parkinson's disease: a review. FBS **6**(1): 65–74. IMR Press. doi:10.2741/S415.

Bhole, R.P., Chikhale, R.V., and Rathi, K.M. 2023. Current biomarkers and treatment strategies in Alzheimer disease: An overview and future perspectives. IBRO Neurosci Rep **16**: 8–42. doi:10.1016/j.ibneur.2023.11.003.

Breijyeh, Z., and Karaman, R. 2020. Comprehensive Review on Alzheimer's Disease: Causes and Treatment. Molecules **25**(24): 5789. doi:10.3390/molecules25245789.

Briggs, R., Kennelly, S.P., and O'Neill, D. 2016. Drug treatments in Alzheimer's disease. Clin Med **16**(3): 247–253. doi:10.7861/clinmedicine.16-3-247.

Brunello, C.A., Merezhko, M., Uronen, R.-L., and Huttunen, H.J. 2020. Mechanisms of secretion and spreading of pathological tau protein. Cell. Mol. Life Sci. **77**(9): 1721–1744. doi:10.1007/s00018-019-03349-1.

Buee, L., Bussiere, T., Buee-Scherrer, V., Delacourte, A., and Hof, P.R. 2000. Tau protein isoforms, phosphorylation and role in neurodegenerative disorders. Brain Research Reviews.

Bujdoso, R., Smith, A., Fleck, O., Spiropoulos, J., Andréoletti, O., and Thackray, A.M. 2023. Prion disease modelled in Drosophila. Cell Tissue Res **392**(1): 47–62. doi:10.1007/s00441-022-03586-0.

Butterfield, R.J. 2021. Spinal muscular atrophy treatments, newborn screening, and the creation of a neurogenetics urgency. Semin Pediatr Neurol **38**: 100899. doi:10.1016/j.spen.2021.100899.

Caballero, B., Bourdenx, M., Luengo, E., Diaz, A., Sohn, P.D., Chen, X., Wang, C., Juste, Y.R., Wegmann, S., Patel, B., Young, Z.T., Kuo, S.Y., Rodriguez-Navarro, J.A., Shao, H., Lopez, M.G., Karch, C.M., Goate, A.M., Gestwicki, J.E., Hyman, B.T., Gan, L., and Cuervo, A.M. 2021. Acetylated tau inhibits chaperone-mediated autophagy and promotes tau pathology propagation in mice. Nat Commun **12**: 2238. doi:10.1038/s41467-021-22501-9.

Carroll, J.A., and Chesebro, B. 2019. Neuroinflammation, Microglia, and Cell-Association during Prion Disease. Viruses **11**(1): 65. doi:10.3390/v11010065.

Chitbankluai, K., Thavarungkul, P., Kanatharana, P., Kaewpet, M., and Buranachai, C. 2022. Newly found K+-Thioflavin T competitive binding to DNA G-quadruplexes and the development of a label-free fluorescent biosensor with extra low detection limit for K+ determination in urine samples. Spectrochimica Acta Part A: Molecular and Biomolecular Spectroscopy **276**: 121244. doi:10.1016/j.saa.2022.121244.

Coon, E.A., and Singer, W. 2020. Synucleinopathies. Continuum (Minneap Minn) **26**(1): 72–92. doi:10.1212/CON.0000000000000819.

Creekmore, B.C., Watanabe, R., and Lee, E.B. 2024. Neurodegenerative Disease Tauopathies. Annual Review of Pathology: Mechanisms of Disease **19**(1): 345–370. doi:10.1146/annurev-pathmechdis-051222-120750.

Cummings, J.L., Gonzalez, M.I., Pritchard, M.C., May, P.C., Toledo-Sherman, L.M., and Harris, G.A. 2023. The therapeutic landscape of tauopathies: challenges and prospects. Alzheimers Res Ther **15**: 168. doi:10.1186/s13195-023-01321-7.

D'Amico, A., Mercuri, E., Tiziano, F.D., and Bertini, E. 2011. Spinal muscular atrophy. Orphanet J Rare Dis **6**: 71. doi:10.1186/1750-1172-6-71.

Day, J.W., Howell, K., Place, A., Long, K., Rossello, J., Kertesz, N., and Nomikos, G. 2022. Advances and limitations for the treatment of spinal muscular atrophy. BMC Pediatr **22**: 632. doi:10.1186/s12887-022-03671-x.

Demaegd, K., Schymkowitz, J., and Rousseau, F. 2018. Transcellular Spreading of Tau in Tauopathies. Chembiochem **19**(23): 2424–2432. doi:10.1002/cbic.201800288.

Dolphin, H., Dyer, A.H., Morrison, L., Shenkin, S.D., Welsh, T., and Kennelly, S.P. 2024. New horizons in the diagnosis and management of Alzheimer's Disease in older adults. Age Ageing **53**(2): afae005. doi:10.1093/ageing/afae005.

Dugger, B.N., and Dickson, D.W. 2017. Pathology of Neurodegenerative Diseases. Cold Spring Harb Perspect Biol **9**(7): a028035. doi:10.1101/cshperspect.a028035.

d'Errico, P., and Meyer-Luehmann, M. 2020. Mechanisms of Pathogenic Tau and Aβ Protein Spreading in Alzheimer's Disease. Front Aging Neurosci **12**: 265. doi:10.3389/fnagi.2020.00265.

European Centre for Disease Prevention and Control (ECDC). 2021. The risk of variant Creutzfeldt-Jakob disease transmission via blood and plasma-derived medicinal products. RISK ASSESSMENT: 1–21.

Fayazi, N., Sheykhhasan, M., Soleimani Asl, S., and Najafi, R. 2021. Stem Cell-Derived Exosomes: a New Strategy of Neurodegenerative Disease Treatment. Mol Neurobiol **58**(7): 3494–3514. doi:10.1007/s12035-021-02324-x.

Fields, E., Vaughan, E., Tripu, D., Lim, I., Shrout, K., Conway, J., Salib, N., Lee, Y., Dhamsania, A., Jacobsen, M., Woo, A., Xue, H., and Cao, K. 2021. Gene targeting techniques for Huntington's disease. Ageing Res Rev **70**: 101385. doi:10.1016/j.arr.2021.101385.

Figueiredo, F., Sárkány, Z., Silva, A., Vilasboas-Campos, D., Maciel, P., Teixeira-Castro, A., Martins, P.M., and Macedo-Ribeiro, S. 2023. Drug repurposing of dopaminergic drugs to inhibit ataxin-3 aggregation. Biomedicine & Pharmacotherapy **165**: 115258. doi:10.1016/j.biopha.2023.115258.

Foster, L.A., and Salajegheh, M.K. 2019. Motor Neuron Disease: Pathophysiology, Diagnosis, and Management. The American Journal of Medicine **132**(1): 32–37. doi:10.1016/j.amjmed.2018.07.012.

Friedhoff, P., von Bergen, M., Mandelkow, E.-M., and Mandelkow, E. 2000. Structure of tau protein and assembly into paired helical filaments. Biochimica et Biophysica Acta (BBA) - Molecular Basis of Disease **1502**(1): 122–132. doi:10.1016/S0925-4439(00)00038-7.

Frontzek, K., and Aguzzi, A.A. 2020. Recent developments in antibody therapeutics against prion disease. Emerging Topics in Life Sciences **4**(2): 169–173. Portland Press. doi:10.1042/etls20200002.

Fuster-Matanzo, A., Hernández, F., and Ávila, J. 2018. Tau Spreading Mechanisms; Implications for Dysfunctional Tauopathies. Int J Mol Sci **19**(3): 645. doi:10.3390/ijms19030645.

Geschwind, M.D. 2015. Prion Diseases. Continuum (Minneap Minn) **21**(6 NEUROINFECTIOUS DISEASE): 1612–1638. doi:10.1212/CON.0000000000000251.

Girych, M., Gorbenko, G., Maliyov, I., Trusova, V., Mizuguchi, C., Saito, H., and Kinnunen, P. 2016. Combined thioflavin T–Congo red fluorescence assay for amyloid fibril detection. Methods Appl. Fluoresc. **4**(3): 034010. doi:10.1088/2050-6120/4/3/034010.

Gitler, A.D., Dhillon, P., and Shorter, J. 2017. Neurodegenerative disease: models, mechanisms, and a new hope. Dis Model Mech **10**(5): 499–502. doi:10.1242/dmm.030205.

Gomperts, S.N. 2016. Lewy Body Dementias: Dementia With Lewy Bodies and Parkinson Disease Dementia. Continuum (Minneap Minn) **22**(2 Dementia): 435–463. doi:10.1212/CON.0000000000000309.

Guo, J., Chen, L., and Li, G.-M. 2017a. DNA mismatch repair in trinucleotide repeat instability. Sci China Life Sci **60**(10): 1087–1092. doi:10.1007/s11427-017-9186-7.

Guo, T., Noble, W., and Hanger, D.P. 2017b. Roles of tau protein in health and disease. Acta Neuropathol **133**(5): 665–704. doi:10.1007/s00401-017-1707-9.

Guo, X., Yan, L., Zhang, D., and Zhao, Y. 2024. Passive immunotherapy for Alzheimer's disease. Ageing Research Reviews **94**: 102192. doi:10.1016/j.arr.2024.102192.

Gusella, J.F., Lee, J.-M., and MacDonald, M.E. 2021. Huntington's disease: nearly four decades of human molecular genetics. Hum Mol Genet **30**(R2): R254–R263. doi:10.1093/hmg/ddab170.

Hane, F.T., Robinson, M., Lee, B.Y., Bai, O., Leonenko, Z., and Albert, M.S. 2017. Recent Progress in Alzheimer's Disease Research, Part 3: Diagnosis and Treatment. Journal of Alzheimer's Disease **57**(3): 645–665. IOS Press. doi:10.3233/JAD-160907.

Hawe, A., Sutter, M., and Jiskoot, W. 2008. Extrinsic Fluorescent Dyes as Tools for Protein Characterization. Pharm Res **25**(7): 1487–1499. doi:10.1007/s11095-007-9516-9.

Heemels, M.-T. 2016. Neurodegenerative diseases. Nature **539**(7628): 179–179. Nature Publishing Group. doi:10.1038/539179a.

Hermann, P., Appleby, B., Brandel, J.-P., Caughey, B., Collins, S., Geschwind, M., Green, A., Haïk, S., Kovacs, G.G., Ladogana, A., Llorens, F., Mead, S., Nishida, N., Pal, S., Parchi, P., Pocchiari, M., Satoh, K., Zanusso, G., and Zerr, I. 2021. Biomarkers and diagnostic guidelines for sporadic Creutzfeldt-Jakob disease. The Lancet. Neurology **20**(3): 235. NIH Public Access. doi:10.1016/S1474-4422(20)30477-4.

Hernández, F., Ferrer, I., Pérez, M., Zabala, J.C., Del Rio, J.A., and Avila, J. 2023. Tau Aggregation. Neuroscience **518**: 64–69. doi:10.1016/j.neuroscience.2022.04.024.

Hu, J., Sha, W., Yuan, S., Wu, J., and Huang, Y. 2023. Aggregation, Transmission, and Toxicity of the Microtubule-Associated Protein Tau: A Complex Comprehension. Int J Mol Sci **24**(19): 15023. doi:10.3390/ijms241915023.

Islam, M., Shen, F., Regmi, D., and Du, D. 2022. Therapeutic Strategies for Tauopathies and Drug Repurposing as a Potential Approach. Biochem Pharmacol **198**: 114979. doi:10.1016/j.bcp.2022.114979.

Jain, A., and Vale, R.D. 2017. RNA Phase Transitions in Repeat Expansion Disorders. Nature **546**(7657): 243–247. doi:10.1038/nature22386.

Jayan, P., Vahid, A.A., Kizhakkeduth, S.T., Muhammed, S.O.H., Shibina, A.B., and Vijayan, V. 2021. Direct Observation of the Self-Aggregation of R3R4 Bi-repeat of Tau Protein. ChemBioChem **22**(12): 2093–2097. doi:10.1002/cbic.202100013.

Jimenez-Sanchez, M., Licitra, F., Underwood, B.R., and Rubinsztein, D.C. 2017. Huntington's Disease: Mechanisms of Pathogenesis and Therapeutic Strategies. Cold Spring Harb Perspect Med **7**(7): a024240. doi:10.1101/cshperspect.a024240.

Jouanne, M., Rault, S., and Voisin-Chiret, A.-S. 2017. Tau protein aggregation in Alzheimer's disease: An attractive target for the development of novel therapeutic agents. European Journal of Medicinal Chemistry **139**: 153–167. doi:10.1016/j.ejmech.2017.07.070.

Khan, S., Barve, K.H., and Kumar, M.S. 2020. Recent Advancements in Pathogenesis, Diagnostics and Treatment of Alzheimer's Disease. Curr Neuropharmacol **18**(11): 1106–1125. doi:10.2174/1570159X18666200528142429.

Khurana, R., Coleman, C., Ionescu-Zanetti, C., Carter, S.A., Krishna, V., Grover, R.K., Roy, R., and Singh, S. 2005. Mechanism of thioflavin T binding to amyloid fibrils. Journal of Structural Biology **151**(3): 229–238. doi:10.1016/j.jsb.2005.06.006.

Kim, M.-O., Takada, L.T., Wong, K., Forner, S.A., and Geschwind, M.D. 2018. Genetic PrP Prion Diseases. Cold Spring Harb Perspect Biol **10**(5): a033134. doi:10.1101/cshperspect.a033134.

Koga, S., Sekiya, H., Kondru, N., Ross, O.A., and Dickson, D.W. 2021. Neuropathology and molecular diagnosis of Synucleinopathies. Mol Neurodegener **16**: 83. doi:10.1186/s13024-021-00501-z.

Kolarova, M., García-Sierra, F., Bartos, A., Ricny, J., and Ripova, D. 2012. Structure and Pathology of Tau Protein in Alzheimer Disease. International Journal of Alzheimer's Disease **2012**: 1–13. doi:10.1155/2012/731526.

Kolb, S.J., and Kissel, J.T. 2015. Spinal Muscular Atrophy. Neurol Clin **33**(4): 831–846. doi:10.1016/j.ncl.2015.07.004.

Lai, Y., Beaver, J.M., Laverde, E., and Liu, Y. 2020. Trinucleotide repeat instability via DNA base excision repair. DNA Repair (Amst) **93**: 102912. doi:10.1016/j.dnarep.2020.102912.

Li, B., Chen, M., and Zhu, C. 2021. Neuroinflammation in Prion Disease. Int J Mol Sci **22**(4): 2196. doi:10.3390/ijms22042196.

Longhini, A.P., DuBose, A., Lobo, S., Vijayan, V., Bai, Y., Rivera, E.K., Sala-Jarque, J., Nikitina, A., Carrettiero, D.C., Unger, M.T., Sclafani, O.R., Fu, V., Beckett, E.R., Vigers, M., Buée, L., Landrieu, I., Shell, S., Shea, J.E., Han, S., and Kosik, K.S. 2024. Precision

proteoform design for 4R tau isoform selective templated aggregation. Proc Natl Acad Sci U S A **121**(15): e2320456121. doi:10.1073/pnas.2320456121.

Lotankar, S., Prabhavalkar, K.S., and Bhatt, L.K. 2017. Biomarkers for Parkinson's Disease: Recent Advancement. Neurosci Bull **33**(5): 585–597. doi:10.1007/s12264-017-0183-5.

Man, V.H., He, X., Gao, J., and Wang, J. 2023. Phosphorylation of Tau R2 Repeat Destabilizes Its Binding to Microtubules: A Molecular Dynamics Simulation Study. ACS Chem Neurosci **14**(3): 458–467. doi:10.1021/acschemneuro.2c00611.

Mangialasche, F., Solomon, A., Winblad, B., Mecocci, P., and Kivipelto, M. 2010. Alzheimer's disease: clinical trials and drug development. The Lancet Neurology **9**(7): 702–716. doi:10.1016/S1474-4422(10)70119-8.

Mantzavinos, V., and Alexiou, A. 2017. Biomarkers for Alzheimer's Disease Diagnosis. CAR **14**(11). doi:10.2174/1567205014666170203125942.

Matsui, M., and Corey, D.R. 2012. Allele-selective inhibition of trinucleotide repeat genes. Drug Discov Today **17**(9–10): 443–450. doi:10.1016/j.drudis.2012.01.006.

McMurray, C.T. 2010. Mechanisms of trinucleotide repeat instability during human development. Nat Rev Genet **11**(11): 786–799. doi:10.1038/nrg2828.

Mietelska-Porowska, A., Wasik, U., Goras, M., Filipek, A., and Niewiadomska, G. 2014. Tau Protein Modifications and Interactions: Their Role in Function and Dysfunction. Int J Mol Sci **15**(3): 4671–4713. doi:10.3390/ijms15034671.

Min, J.-O., Strohäker, T., Jeong, B.-C., Zweckstetter, M., and Lee, S.-J. 2022. Chicago sky blue 6B inhibits α-synuclein aggregation and propagation. Mol Brain **15**(27). doi:10.1186/s13041-022-00913-y.

Monteiro, A.R., Barbosa, D.J., Remião, F., and Silva, R. 2023. Alzheimer's disease: Insights and new prospects in disease pathophysiology, biomarkers and disease-modifying drugs. Biochemical Pharmacology **211**: 115522. doi:10.1016/j.bcp.2023.115522.

Nishio, H., Niba, E.T.E., Saito, T., Okamoto, K., Takeshima, Y., and Awano, H. 2023. Spinal Muscular Atrophy: The Past, Present, and Future of Diagnosis and Treatment. Int J Mol Sci **24**(15): 11939. doi:10.3390/ijms241511939.

Nizynski, B., Dzwolak, W., and Nieznanski, K. 2017. Amyloidogenesis of Tau protein. Protein Sci **26**(11): 2126–2150. doi:10.1002/pro.3275.

Park, G., Xu, K., Chea, L., Kim, K., Safarta, L., Song, K.-H., Wu, J., Park, S., Min, H., Hiramatsu, N., Han, J., and Lin, J.H. 2023. Neurodegeneration risk factor, EIF2AK3 (PERK), influences tau protein aggregation. J Biol Chem **299**(2): 102821. doi:10.1016/j.jbc.2022.102821.

Perneczky, R., Dom, G., Chan, A., Falkai, P., and Bassetti, C.L.A. 2024. Anti-amyloid antibody treatments for Alzheimer's disease. European journal of neurology **31**(2): e16049. Wiley.

Pîrscoveanu, D.F.V., Pirici, I., and Tudoric, V. 2017. Tau protein in neurodegenerative diseases – a review. **58**(4): 1141–1150.

Pomierny, B., Krzyżanowska, W., Skórkowska, A., Jurczyk, J., Budziszewska, B., and Pera, J. 2024. Chicago sky blue 6B exerts neuroprotective and anti-inflammatory effects on focal cerebral ischemia. Biomedicine & Pharmacotherapy **170**: 116102. doi:10.1016/j.biopha.2023.116102.

Rawat, P., Sehar, U., Bisht, J., Selman, A., Culberson, J., and Reddy, P.H. 2022. Phosphorylated Tau in Alzheimer's Disease and Other Tauopathies. Int J Mol Sci **23**(21): 12841. doi:10.3390/ijms232112841.

Riley, K.J., Graner, B.D., and Veronesi, M.C. 2022. The tauopathies: Neuroimaging characteristics and emerging experimental therapies. J Neuroimaging **32**(4): 565–581. doi:10.1111/jon.13001.

Robinson, M., Lee, B.Y., and Hane, F.T. 2017. Recent Progress in Alzheimer's Disease Research, Part 2: Genetics and Epidemiology. Journal of Alzheimer's Disease **57**(2): 317–330. IOS Press. doi:10.3233/JAD-161149.

Roy, R., Ria, T., RoyMahaPatra, D., and Sk, U.H. 2023. Single Inhibitors versus Dual Inhibitors: Role of HDAC in Cancer. ACS Omega **8**(19): 16532–16544. American Chemical Society. doi:10.1021/acsomega.3c00222.

Sabate, R., Rodriguez-Santiago, L., Sodupe, M., Saupe, S.J., and Ventura, S. 2013. Thioflavin-T excimer formation upon interaction with amyloid fibers. Chem. Commun. **49**(51): 5745. doi:10.1039/c3cc42040j.

Sahayaraj, A.E., Viswanathan, R., Pinhero, F., Abdul Vahid, A., and Vijayan, V. 2023. Sequence-Dependent Conformational Properties of PGGG Motif in Tau Repeats: Insights from Molecular Dynamics Simulations of Narrow Pick Filament. ACS Chem. Neurosci. **14**(1): 136–147. American Chemical Society. doi:10.1021/acschemneuro.2c00602.

Scheltens, P., Strooper, B.D., Kivipelto, M., Holstege, H., Chételat, G., Teunissen, C.E., Cummings, J., and van der Flier, W.M. 2021. Alzheimer's disease. Lancet **397**(10284): 1577–1590. doi:10.1016/S0140-6736(20)32205-4.

Schlein, M. 2017. Insulin Formulation Characterization—the Thioflavin T Assays. AAPS J **19**(2): 397–408. doi:10.1208/s12248-016-0028-6.

Schmitz, M., Villar-Piqué, A., Hermann, P., Escaramís, G., Calero, M., Chen, C., Kruse, N., Cramm, M., Golanska, E., Sikorska, B., Liberski, P.P., Pocchiari, M., Lange, P., Stehmann, C., Sarros, S., Martí, E., Baldeiras, I., Santana, I., Žáková, D., Mitrová, E., Dong, X.-P., Collins, S., Poleggi, A., Ladogana, A., Mollenhauer, B., Kovacs, G.G., Geschwind, M.D., Sánchez-Valle, R., Zerr, I., and Llorens, F. 2022. Diagnostic accuracy of cerebrospinal fluid biomarkers in genetic prion diseases. Brain **145**(2): 700–712. doi:10.1093/brain/awab350.

Schorling, D.C., Pechmann, A., and Kirschner, J. 2020. Advances in Treatment of Spinal Muscular Atrophy – New Phenotypes, New Challenges, New Implications for Care. J Neuromuscul Dis **7**(1): 1–13. doi:10.3233/JND-190424.

Šerý, O., Povová, J., Míšek, I., Pešák, L., and Janout, V. 2013. Molecular mechanisms of neuropathological changes in Alzheimer's disease: a review. fn **1**: 1–9. doi:10.5114/fn.2013.34190.

Sigurdson, C.J., Bartz, J.C., and Glatzel, M. 2019. Cellular and Molecular Mechanisms of Prion Disease. Annu Rev Pathol **14**: 497–516. doi:10.1146/annurev-pathmechdis-012418-013109.

Sinsky, J., Pichlerova, K., and Hanes, J. 2021. Tau Protein Interaction Partners and Their Roles in Alzheimer's Disease and Other Tauopathies. Int J Mol Sci **22**(17): 9207. doi:10.3390/ijms22179207.

Tabrizi, S.J., Estevez-Fraga, C., van Roon-Mom, W.M.C., Flower, M.D., Scahill, R.I., Wild, E.J., Muñoz-Sanjuan, I., Sampaio, C., Rosser, A.E., and Leavitt, B.R. 2022. Potential disease modifying therapies for Huntington's disease, lessons learned and future opportunities. Lancet Neurol **21**(7): 645–658. doi:10.1016/S1474-4422(22)00121-1.

Tan, H., Xu, Z., and Jin, P. 2012. Role of noncoding RNAs in trinucleotide repeat neurodegenerative disorders. Experimental Neurology **235**(2): 469–475. doi:10.1016/j.expneurol.2012.01.019.

Tapia-Rojas, C., Cabezas-Opazo, F., Deaton, C.A., Vergara, E.H., Johnson, G.V.W., and Quintanilla, R.A. 2019. It's all about tau. Prog Neurobiol **175**: 54–76. doi:10.1016/j.pneurobio.2018.12.005.

Trajanoska, K., Bhérer, C., Taliun, D., Zhou, S., Richards, J.B., and Mooser, V. 2023. From target discovery to clinical drug development with human genetics. Nature **620**(7975): 737–745. Nature Publishing Group. doi:10.1038/s41586-023-06388-8.

Twarowski, B., and Herbet, M. 2023. Inflammatory Processes in Alzheimer's Disease—Pathomechanism, Diagnosis and Treatment: A Review. Int J Mol Sci **24**(7): 6518. doi:10.3390/ijms24076518.

Uttley, L., Carroll, C., Wong, R., Hilton, D.A., and Stevenson, M. 2020. Creutzfeldt-Jakob disease: a systematic review of global incidence, prevalence, infectivity, and incubation. Lancet Infect Dis **20**(1): e2–e10. doi:10.1016/S1473-3099(19)30615-2.

Vaquer-Alicea, J., and Diamond, M.I. 2019. Propagation of Protein Aggregation in Neurodegenerative Diseases. Annual Review of Biochemistry **88**(1): 785–810. doi:10.1146/annurev-biochem-061516-045049.

Vaz, M., and Silvestre, S. 2020. Alzheimer's disease: Recent treatment strategies. European Journal of Pharmacology **887**: 173554. doi:10.1016/j.ejphar.2020.173554.

Verma, S., Ravichandiran, V., and Ranjan, N. 2021. Beyond amyloid proteins: Thioflavin T in nucleic acid recognition. Biochimie **190**: 111–123. doi:10.1016/j.biochi.2021.06.003.

Von Bergen, M., Barghorn, S., Li, L., Marx, A., Biernat, J., Mandelkow, E.-M., and Mandelkow, E. 2001. Mutations of Tau Protein in Frontotemporal Dementia Promote Aggregation of Paired Helical Filaments by Enhancing Local β-Structure. Journal of Biological Chemistry **276**(51): 48165–48174. doi:10.1074/jbc.M105196200.

Von Bergen, M., Friedhoff, P., Biernat, J., Heberle, J., Mandelkow, E.-M., and Mandelkow, E. 2000. Assembly of τ protein into Alzheimer paired helical filaments depends on a local sequence motif (306VQIVYK311) forming β structure. Proc Natl Acad Sci U S A **97**(10): 5129–5134.

Weller, J., and Budson, A. 2018. Current understanding of Alzheimer's disease diagnosis and treatment. F1000Res **7**: 1161. doi:10.12688/f1000research.14506.1.

Wells, R.D., Dere, R., Hebert, M.L., Napierala, M., and Son, L.S. 2005. Advances in mechanisms of genetic instability related to hereditary neurological diseases. Nucleic Acids Res **33**(12): 3785–3798. doi:10.1093/nar/gki697.

Will, R., and Zeidler, M. 1996. Diagnosing Creutzfeldt-Jakob disease. BMJ : British Medical Journal **313**(7061): 833. BMJ Publishing Group. doi:10.1136/bmj.313.7061.833.

Williams, K., Foliaki, S.T., Race, B., Smith, A., Thomas, T., Groveman, B.R., and Haigh, C.L. 2023. Neural cell engraftment therapy for sporadic Creutzfeldt-Jakob disease restores neuroelectrophysiological parameters in a cerebral organoid model. Stem Cell Res Ther **14**: 348. doi:10.1186/s13287-023-03591-2.

Xu, J., Zhao, C., Huang, X., and Du, W. 2020. Tetracycline derivatives resist the assembly behavior of human islet amyloid polypeptide. Biochimie **174**: 95–106. doi:10.1016/j.biochi.2020.04.012.

Ye, J., Wan, H., Chen, S., and Liu, G.-P. 2024. Targeting tau in Alzheimer's disease: from mechanisms to clinical therapy. Neural Regeneration Research **19**(7): 1489–1498. doi:10.4103/1673-5374.385847.

Zabik, N.L., Imhof, M.M., and Martic-Milne, S. 2017. Structural evaluations of tau protein conformation: methodologies and approaches. Biochem Cell Biol **95**(3): 338–349. doi:10.1139/bcb-2016-0227.

Zhang, X.F., Xu, H.M., Han, L., Li, N.B., and Luo, H.Q. 2018. A Thioflavin T-induced G-Quadruplex Fluorescent Biosensor for Target DNA Detection. ANAL. SCI. **34**(2): 149–153. doi:10.2116/analsci.34.149.

7.2 Website references and hyperlinks

Ref. 1: BioRender https://biorender.com/

Ref. 2: ChemSpider https://www.chemspider.com/

8 LIST OF SYMBOLS AND ABBREVIATIONS

Aβ	Amyloid β
AD	Alzheimer's disease
CJD	Creuztfeld-Jakob disease
D-MEM	Dulbecco's Modified Eagle's medium
FBS	Fetal bovine serum
FDA	Food and Drug Administration
HD	Huntington's disease
MRI	Magnetic resonance imaging
NDs	Neurodegenerative diseases
NFTs	Neurofibrillary tangles
PD	Parkinson's disease
PET	Amyloid positron emission tomography
PHFs	Paired helical filaments
PTMs	Post-translational modifications
RT	Room temperature
SMA	Spinal muscular atrophy
ThT	Thioflavin T
TNR	Trinucleotide repeat

9 LIST OF FIGURES

10 LIST OF TABLES

11 LIST OF APPENDICES

Supplement 1: List of drugs used in the primary screening of The Prestwick Chemical Library®

Supplement 1: List of drugs used in the primary screening of The Prestwick Chemical Library®

Table S1: Drugs used in the primary screening

Position	Drug	Position	Drug
A1	Control	A41	Thalidomide
A2	Azaguanine-8	A42	Moxisylyte hydrochoride
A3	Isoniazid	A43	Tiratricol, 3,3',5-triiodothyroacetic acid
A4	Meticrane	A44	Carbamazepine
A5	Tranexamic acid	A45	Pyrantel tartrate
A6	Sulfaphenazole	A46	Homatropine hydrobromide (R,S)
A7	Ampyrone	A47	Antimycin A
A8	Chloramphenicol	A48	Imipramine hydrochloride
A9	Midodrine hydrochloride	A49	Scopolamin-N-oxide hydrobromide
A10	Procaine hydrochloride	A50	Fulvestrant
A11	Ranitidine hydrochloride	A51	Flavoxate hydrochloride
A12	Mupirocin	A52	Zimelidine dihydrochloride monohydrate
A13	Piroxicam	A53	Diphenidol hydrochloride
A14	Morantel tartrate	A54	Amoxapine
A15	Norfloxacin	A55	Triprolidine hydrochloride
A16	Todralazine hydrochloride	A56	Metolazone
A17	Etodolac	A57	Indomethacin
A18	Metronidazole	A58	Amfepramone hydrochloride
A19	Mexiletine hydrochloride	A59	Fenoterol hydrobromide
A20	Khellin	A60	Loxapine succinate
A21	Chlorothiazide	A61	Trazodone hydrochloride
A22	R(-) Apomorphine hydrochloride hemihydrate	B1	Dipyridamole
A23	Ethisterone	B2	Lincomycin hydrochloride
A24	Naloxone hydrochloride	B3	Chloroxine
A25	Vincamine	B4	Flunarizine dihydrochloride
A26	Bromocryptine mesylate	B5	Acetazolamide
A27	Fludrocortisone acetate	B6	Chlorzoxazone
A28	Glipizide	B7	Hydroflumethiazide
A29	Dantrolene sodium salt	B8	Tranylcypromine hydrochloride
A30	Verapamil hydrochloride	B9	Sulfadiazine
A31	Lisinopril	B10	Pargyline hydrochloride
A32	Erythromycin	B11	Diprophylline
A33	Ifenprodil tartrate	B12	Oxolinic acid
A34	Allantoin	B13	Betazole hydrochloride
A35	Pentylenetetrazole	B14	Flufenamic acid
A36	Benzonatate	B15	Triflupromazine hydrochloride
A37	Etofylline	B16	Fenspiride hydrochloride
A38	Panthenol (D)	B17	Nifedipine
A39	Levamisole hydrochloride	B18	Xylometazoline hydrochloride
A40	Epirizole	B19	Sulindac

Table S2: Drugs used in the primary screening *(continued)*

Position	Drug	Position	Drug
B20	Hyoscyamine (L)	B60	Prednisolone
B21	Edrophonium chloride	B61	Tioconazole
B22	Bufexamac	C1	Diethylcarbamazine citrate
B23	Azacyclonol	C2	Diltiazem hydrochloride
B24	Norethindrone	C3	Pimethixene maleate
B25	Cyproheptadine hydrochloride	C4	Loperamide hydrochloride
B26	Doxepin hydrochloride	C5	Econazole nitrate
B27	Ciprofloxacin hydrochloride monohydrate	C6	Josamycin
B28	Cortisone	C7	Enalapril maleate
B29	Dehydrocholic acid	C8	Atracurium besylate
B30	Homochlorcyclizine dihydrochloride	C9	Ethosuximide
B31	Hydroxyzine dihydrochloride	C10	Heptaminol hydrochloride
B32	Glafenine hydrochloride	C11	Aceclofenac
B33	Chlorhexidine	C12	Thiamphenicol
B34	Telenzepine dihydrochloride	C13	Aztreonam
B35	Didanosine	C14	Dapsone
B36	Trifluoperazine dihydrochloride	C15	Asenapine maleate
B37	Metformin hydrochloride	C16	Naproxen
B38	Ornidazole	C17	Tolfenamic acid
B39	Sulfacetamide sodic hydrate	C18	Acetohexamide
B40	Alverine citrate salt	C19	Mefexamide hydrochloride
B41	Norethynodrel	C20	Diphenhydramine hydrochloride
B42	Methocarbamol	C21	Nifenazone
B43	Triamterene	C22	Adiphenine hydrochloride
B44	Nimesulide	C23	Carmofur
B45	Isoxicam	C24	Baclofen (R,S)
B46	Flumequine	C25	Dropropizine (R,S)
B47	Mefenamic acid	C26	Lynestrenol
B48	Gemfibrozil	C27	Niflumic acid
B49	Chlorpromazine hydrochloride	C28	Danazol
B50	Oxymetazoline hydrochloride	C29	Dimenhydrinate
B51	Amitryptiline hydrochloride	C30	Haloperidol
B52	Chlorphensin carbamate	C31	Fenofibrate
B53	Moroxidine hydrochloride	C32	Perphenazine
B54	Glutethimide, para-amino	C33	Chenodiol
B55	Azathioprine	C34	Methotrexate
B56	Nortriptyline hydrochloride	C35	Pergolide mesylate
B57	Famotidine	C36	Chlortetracycline hydrochloride
B58	Dyclonine hydrochloride	C37	Bupivacaine hydrochloride
B59	Ampicillin trihydrate	C38	Paclitaxel

Table S3: Drugs used in the primary screening *(continued)*

Position	Drug	Position	Drug
C39	Minocycline hydrochloride	D18	Metaraminol bitartrate
C40	Isoflupredone acetate	D19	Ticlopidine hydrochloride
C41	Mafenide hydrochloride	D20	Tibolone
C42	Sulfathiazole	D21	Benoxinate hydrochloride
C43	Iproniazide phosphate	D22	Mebendazole
C44	Cimetidine	D23	Miconazole
C45	Cloxacillin sodium salt	D24	Clemizole hydrochloride
C46	Troleandomycin	D25	Prednisone
C47	Pentoxifylline	D26	Ofloxacin
C48	Naphazoline hydrochloride	D27	Diazoxide
C49	Meclofenamic acid sodium salt monohydrate	D28	Albendazole
C50	Sulpiride	D29	Disulfiram
C51	Tiapride hydrochloride	D30	Retinoic acid
C52	Minaprine dihydrochloride	D31	Pioglitazone
C53	Griseofulvin	D32	Clotrimazole
C54	Dibucaine	D33	Chlorpheniramine maleate
C55	Dilazep dihydrochloride	D34	Labetalol hydrochloride
C56	Acyclovir	D35	Isoconazole
C57	Pinacidil	D36	Oxybutynin chloride
C58	Guanabenz acetate	D37	Clindamycin hydrochloride
C59	Isotretinoin	D38	Benzydamine hydrochloride
C60	Nicorandil	D39	Nicergoline
C61	Disopyramide	D40	Oxytetracycline dihydrate
D1	Naltrexone hydrochloride dihydrate	D41	Gallamine triethiodide
D2	Bumetanide	D42	Guanethidine sulfate
D3	Mefloquine hydrochloride	D43	Amprolium hydrochloride
D4	Perhexiline maleate	D44	Nitrofurantoin
D5	Astemizole	D45	Idoxuridine
D6	Acemetacin	D46	Mephenesin
D7	Tamoxifen citrate	D47	Ethambutol dihydrochloride
D8	Clemastine fumarate	D48	Pentolinium bitartrate
D9	Ivermectin	D49	Hexamethonium dibromide dihydrate
D10	Glibenclamide	D50	Salbutamol
D11	Amiloride hydrochloride dihydrate	D51	Dicyclomine hydrochloride
D12	Riluzole hydrochloride	D52	Trimethoprim
D13	Levodopa	D53	Oxethazaine
D14	Sulfamethoxazole	D54	Fenbufen
D15	Doxylamine succinate	D55	Isoxsuprine hydrochloride
D16	Catharanthine	D56	Tropicamide
D17	Pyrimethamine	D57	Thioridazine hydrochloride

Table S4: Drugs used in the primary screening *(continued)*

Position	Drug	Position	Drug
D58	Lomefloxacin hydrochloride	E38	Pirenzepine dihydrochloride
D59	Amidopyrine	E39	Pyrilamine maleate
D60	Clonidine hydrochloride	E40	Cefotaxime sodium salt
D61	Acetylsalicylsalicylic acid	E41	Mifepristone
E1	Antazoline hydrochloride	E42	Thioproperazine dimesylate
E2	Nomifensine maleate	E43	Amodiaquin dihydrochloride dihydrate
E3	Vinpocetine	E44	Dihydrostreptomycin sulfate
E4	Nalbuphine hydrochloride	E45	Clofilium tosylate
E5	Cinnarizine	E46	Sulfaguanidine
E6	Spironolactone	E47	Phenelzine sulfate
E7	Spiperone	E48	Minoxidil
E8	Terfenadine	E49	Flutamide
E9	Fipexide hydrochloride	E50	Antipyrine, 4-hydroxy
E10	Canrenoic acid potassium salt	E51	Tolbutamide
E11	Pimozide	E52	Niclosamide
E12	Neomycin sulfate	E53	Camptothecine (S,+)
E13	Quinacrine dihydrochloride hydrate	E54	Lidocaine hydrochloride
E14	Hydrochlorothiazide	E55	Fenbendazole
E15	Hydralazine hydrochloride	E56	Tolazoline hydrochloride
E16	Captopril	E57	Indapamide
E17	Phenformin hydrochloride	E58	Tolnaftate
E18	Antipyrine	E59	Phentolamine hydrochloride
E19	Aminopurine, 6-benzyl	E60	Trimethobenzamide hydrochloride
E20	Diflunisal	E61	Proglumide
E21	Prilocaine hydrochloride	F1	Pindolol
E22	Amyleine hydrochloride	F2	Alprenolol hydrochloride
E23	Metoclopramide monohydrochloride	F3	Nocodazole
E24	Pheniramine maleate	F4	Praziquantel
E25	Ketoprofen	F5	Oxandrolone
E26	Acebutolol hydrochloride	F6	Fendiline hydrochloride
E27	Nefopam hydrochloride	F7	Triamcinolone
E28	Diphemanil methylsulfate	F8	Quinidine hydrochloride monohydrate
E29	Orphenadrine hydrochloride	F9	Dexamethasone acetate
E30	Busulfan	F10	Sulfinpyrazone
E31	Bupropion hydrochloride	F11	Tetracycline hydrochloride
E32	Mianserine hydrochloride	F12	Diperodon hydrochloride
E33	Ethacrynic acid	F13	Dihydroergotamine tartrate
E34	Dizocilpine maleate	F14	Mebeverine hydrochloride
E35	Clomipramine hydrochloride	F15	Gentamicine sulfate
E36	Picotamide monohydrate	F16	Fluphenazine dihydrochloride
E37	Methylprednisolone, 6-alpha	F17	Streptomycin sulfate

Table S5: Drugs used in the primary screening *(continued)*

Position	Drug	Position	Drug
F18	Serotonin hydrochloride	F55	Dobutamine hydrochloride
F19	Tremorine dihydrochloride	F56	Iohexol
F20	Metixene hydrochloride	F57	Betamethasone
F21	Furosemide	F58	Thiostrepton
F22	Vigabatrin hydrochloride	F59	Debrisoquin sulfate
F23	Chlorthalidone	F60	Grepafloxacin
F24	Fluoxetine hydrochloride	F61	Betaxolol hydrochloride
F25	Bambuterol hydrochloride	G1	Probenecid
F26	Lofexidine	G2	Ketanserin tartrate hydrate
F27	Ketotifen fumarate	G3	Selegiline hydrochloride
F28	Pirenperone	G4	Haloprogin
F29	Lidoflazine	G5	Mevastatin
F30	Ciclopirox ethanolamine	G6	Amifostine
F31	Terbutaline hemisulfate	G7	Mometasone furoate
F32	Hexetidine	G8	Zotepine
F33	Testosterone propionate	G9	Camylofine chlorhydrate
F34	Ziprasidone Hydrochloride	G10	Corticosterone
F35	Androsterone	G11	Etofenamate
F36	Tetracaïne hydrochloride	G12	Clobutinol hydrochloride
F37	Suloctidil	G13	Tizanidine hydrochloride
F38	Reboxetine mesylate	G14	Stanozolol
F39	Pefloxacine	G15	Fenipentol
F40	Emedastine	G16	Cefixime
F41	Estradiol-17 beta	G17	Amisulpride
F42	Tranilast	G18	Itopride
F43	Alizapride hydrochloride	G19	Dipivefrin hydrochloride
F44	Loracarbef	G20	Chlorpropamide
F45	Tropisetron hydrochloride	G21	Rofecoxib
F46	Mizolastine	G22	Zidovudine, AZT
F47	Vatalanib	G23	Omeprazole
F48	Alendronate sodium	G24	Desipramine hydrochloride
F49	Alfuzosin hydrochloride	G25	Cetirizine dihydrochloride
F50	Cefotiam hydrochloride	G26	Moclobemide
F51	Practolol	G27	Norcyclobenzaprine
F52	Nitrofural	G28	Colchicine
F53	Methapyrilene hydrochloride	G29	Miglitol
F54	Biperiden hydrochloride	G30	Amethopterin (R,S)

Table S6: Drugs used in the primary screening *(continued)*

Position	Drug	Position	Drug
G31	Phenacetin	H12	Yohimbine hydrochloride
G32	Nicardipine hydrochloride	H13	Cefadroxil
G33	Betahistine mesylate	H14	Diclofenac sodium
G34	Hemicholinium bromide	H15	Oxcarbazepine
G35	Pentamidine isethionate	H16	Butenafine Hydrochloride
G36	Thyroxine (L)	H17	Linezolid
G37	Pyridostigmine iodide	H18	Carbidopa
G38	Carbarsone	H19	Niridazole
G39	Troglitazone	H20	Mercaptopurine
G40	Carisoprodol	H21	Fentiazac
G41	Papaverine hydrochloride	H22	Tomoxetine hydrochloride
G42	Cyanocobalamin	H23	Ascorbic acid
G43	Zaleplon	H24	Cefaclor hydrate
G44	Gabazine bromide	H25	Zaprinast
G45	Zafirlukast	H26	Terconazole
G46	Calcipotriene	H27	Clenbuterol hydrochloride
G47	Diosmin	H28	Metaproterenol sulfate, orciprenaline sulfate
G48	Metrizamide	H29	Hycanthone
G49	Pyridoxine hydrochloride	H30	Trimethadione
G50	Cefotetan	H31	Brinzolamide
G51	Thiorphan	H32	Rifampicin
G52	Phenylpropanolamine hydrochloride	H33	Methiothepin maleate
G53	Benperidol	H34	Methoxamine hydrochloride
G54	Sulfisoxazole	H35	Mitoxantrone dihydrochloride
G55	Propylthiouracil	H36	Tetramisole hydrochloride
G56	Clorgyline hydrochloride	H37	Amikacin hydrate
G57	Etifenin	H38	Nifuroxazide
G58	Clopamide	H39	Pepstatin A
G59	Pyrazinamide	H40	Atropine sulfate monohydrate
G60	Metergoline	H41	Modafinil
G61	Tiabendazole	H42	Tenatoprazole
H1	Methylergometrine maleate	H43	Chicago sky blue 6B
H2	Atovaquone	H44	Voriconazole
H3	Probucol	H45	Cyclosporin A
H4	Tobramycin	H46	Exemestane
H5	Kanamycin A sulfate	H47	Cyclobenzaprine hydrochloride
H6	Tolazamide	H48	Carbadox
H7	Idebenone	H49	Mebhydroline 1,5-naphtalenedisulfonate
H8	Pentobarbital	H50	(-)-Emtricitabine
H9	Amlodipine	H51	Tosufloxacin hydrochloride
H10	Dacarbazine	H52	Cytarabine
H11	Cephalosporanic acid, 7-amino	H53	Brompheniramine maleate

Table S7: Drugs used in the primary screening *(continued)*

Position	Drug	Position	Drug
H54	Aceclidine Hydrochloride	I37	Piracetam
H55	Methyldopa (L,-)	I38	Carbetapentane citrate
H56	Colistin sulfate	I39	Molsidomine
H57	Chlormezanone	I40	Clomiphene citrate (Z,E)
H58	Tiaprofenic acid	I41	Dirithromycin
H59	Maprotiline hydrochloride	I42	Adamantamine fumarate
H60	Sisomicin sulfate	I43	Itraconazole
H61	Adenosine 5'-monophosphate monohydrate	I44	Lamivudine
I1	Lovastatin	I45	Escitalopram oxalate
I2	Ambroxol hydrochloride	I46	Dibenzepine hydrochloride
I3	Ethionamide	I47	Cilostazol
I4	Clofazimine	I48	Digoxin
I5	(S)-(-)-Atenolol	I49	Temozolomide
I6	GBR 12909 dihydrochloride	I50	Hydrocortisone base
I7	Pregnenolone	I51	Eburnamonine (-)
I8	Etoposide	I52	Meclozine dihydrochloride
I9	Mirtazapine	I53	Quipazine dimaleate salt
I10	Delavirdine	I54	Rifapentine
I11	Eserine hemisulfate salt	I55	Folic acid
I12	Bacampicillin hydrochloride	I56	Progesterone
I13	Acetopromazine maleate salt	I57	Levetiracetam
I14	Buflomedil hydrochloride	I58	Zoxazolamine
I15	Alfacalcidol	I59	Dosulepin hydrochloride
I16	Digitoxigenin	I60	N6-methyladenosine
I17	Fomepizole	I61	Artemisinin
I18	Carteolol hydrochloride	J1	Chlorprothixene hydrochloride
I19	Rimantadine Hydrochloride	J2	Acenocoumarol
I20	Meclocycline sulfosalicylate	J3	Pemirolast potassium
I21	Demecarium bromide	J4	Budesonide
I22	Efavirenz	J5	Bepridil hydrochloride
I23	Racecadotril	J6	Triflusal
I24	Primaquine diphosphate	J7	Bezafibrate
I25	Penciclovir	J8	Phenindione
I26	Cefoperazone dihydrate	J9	Dequalinium dichloride
I27	Daunorubicin hydrochloride	J10	Chloroquine diphosphate
I28	Procainamide hydrochloride	J11	Oxantel pamoate
I29	Vancomycin hydrochloride	J12	Gliclazide
I30	Thioguanosine	J13	Butoconazole nitrate
I31	Sibutramine hydrochloride	J14	Acarbose
I32	Amoxicillin	J15	Biotin
I33	Nystatine	J16	Ropinirole hydrochloride
I34	Benfluorex	J17	Roxatidine Acetate hydrochloride
I35	Tenoxicam	J18	Galanthamine hydrobromide
I36	Nafronyl oxalate	J19	Doxorubicin hydrochloride

Table S8: Drugs used in the primary screening *(continued)*

Position	Drug	Position	Drug
J20	Xylazine	K2	Domperidone
J21	Hydroxytacrine maleate (R,S)	K3	Ethamivan
J22	Oxibendazol	K4	Clozapine
J23	Melatonin	K5	Cyclizine hydrochloride
J24	Acipimox	K6	Droperidol
J25	Neostigmine bromide	K7	Sulfasalazine
J26	Benazepril hydrochloride	K8	Benzbromarone
J27	Felodipine	K9	Trolox
J28	Dexfenfluramine hydrochloride	K10	Clebopride maleate
J29	Tacrine hydrochloride	K11	Clorsulon
J30	Ceftazidime pentahydrate	K12	Fusidic acid sodium salt
J31	Guanfacine hydrochloride	K13	Parthenolide
J32	Propafenone hydrochloride	K14	Hesperidin
J33	Ritodrine hydrochloride	K15	Prenylamine lactate
J34	Bromperidol	K16	Amphotericin B
J35	Dextromethorphan hydrobromide monohydrate	K17	Nicotinamide
J36	Imipenem	K18	Erlotinib
J37	Meloxicam	K19	Argatroban
J38	Mesoridazine besylate	K20	Cisapride
J39	Nefazodone hydrochloride	K21	Etretinate
J40	Thiocolchicoside	K22	Epiandrosterone
J41	Ketoconazole	K23	Zopiclone
J42	Trimetazidine dihydrochloride	K24	Dicloxacillin sodium salt hydrate
J43	Prochlorperazine dimaleate	K25	Hydroxychloroquine sulfate
J44	DO 897/99	K26	Dinoprost trometamol
J45	Amiodarone hydrochloride	K27	Acamprosate calcium
J46	Entacapone	K28	Ceforanide
J47	Bisacodyl	K29	Dimethisoquin hydrochloride
J48	Lacidipine	K30	Closantel
J49	Valacyclovir hydrochloride	K31	Sertindole
J50	Azelastine hydrochloride	K32	Sulmazole
J51	Carbimazole	K33	Carbinoxamine maleate salt
J52	Celiprolol hydrochloride	K34	Glimepiride
J53	Pilocarpine nitrate	K35	Auranofin
J54	Ipsapirone	K36	Pranlukast
J55	Butalbital	K37	Azlocillin sodium salt
J56	Diflorasone Diacetate	K38	Dydrogesterone
J57	Niridazole	K39	Butacaine
J58	Aniracetam	K40	Pranoprofen
J59	Raclopride	K41	Olanzapine
J60	Etoricoxib	K42	Tylosin
J61	Bisoprolol fumarate	K43	Paroxetine Hydrochloride
K1	Iobenguane sulfate	K44	Trihexyphenidyl-D,L Hydrochloride

Table S9: Drugs used in the primary screening *(continued)*

Position	Drug	Position	Drug
K45	Gabapentin	L24	Abacavir Sulfate
K46	Sulfabenzamide	L25	Phenazopyridine hydrochloride
K47	Iopamidol	L26	Monobenzone
K48	Althiazide	L27	Sulfapyridine
K49	Niacin	L28	Thioperamide maleate
K50	Sulfaquinoxaline sodium salt	L29	Leflunomide
K51	Cortisol acetate	L30	S(-)Eticlopride hydrochloride
K52	Nadide	L31	Podophyllotoxin
K53	Hymecromone	L32	Bretylium tosylate
K54	Terazosin hydrochloride	L33	Propidium iodide
K55	(+)-Isoproterenol (+)-bitartrate salt	L34	Toremifene
K56	Butamben	L35	Flunisolide
K57	Nizatidine	L36	Pyrithyldione
K58	Alclometasone dipropionate	L37	Mepenzolate bromide
K59	Propofol	L38	Bucladesine sodium salt
K60	Clobetasol propionate	L39	Zileuton
K61	Pentetic acid	L40	Sulfamonomethoxine
L1	(R) -Naproxen sodium salt	L41	Opipramol dihydrochloride
L2	Crotamiton	L42	Ifosfamide
L3	Gefitinib	L43	Pempidine tartrate
L4	Methazolamide	L44	Nafcillin sodium salt monohydrate
L5	Picrotoxinin	L45	Promazine hydrochloride
L6	Cromolyn disodium salt	L46	Liothyronine
L7	D,L-Penicillamine	L47	Famprofazone
L8	Clidinium bromide	L48	Ciclesonide
L9	Sumatriptan succinate	L49	Dipyrone
L10	Cefoxitin sodium salt	L50	Theophylline monohydrate
L11	Secnidazole	L51	Phenethicillin potassium salt
L12	Trimeprazine tartrate	L52	Digoxigenin
L13	Citalopram Hydrobromide	L53	Metoprolol-(+,-) (+)-tartrate salt
L14	Nylidrin	L54	Felbinac
L15	Succinylsulfathiazole	L55	Medrysone
L16	Raloxifene hydrochloride	L56	Diloxanide furoate
L17	Benzocaine	L57	Demeclocycline hydrochloride
L18	Iopromide	L58	2-Aminobenzenesulfonamide
L19	Isopyrin hydrochloride	L59	Meclofenoxate hydrochloride
L20	Bemegride	L60	Xamoterol hemifumarate
L21	Streptozotocin	L61	Norgestrel-(-)-D
L22	Flubendazol	M1	Primidone
L23	Sulfamethizole	M2	Clofibric acid

Table S10: Drugs used in the primary screening *(continued)*

Position	Drug	Position	Drug
M3	Pralidoxime chloride	M44	Oxacillin sodium
M4	Cloperastine hydrochloride	M45	Zolmitriptan
M5	(R)-(+)-Atenolol	M46	Ibutilide fumarate
M6	N-Acetyl-DL-homocysteine Thiolactone	M47	Amiprilose hydrochloride
M7	Spectinomycin dihydrochloride	M48	Venlafaxine
M8	Benfotiamine	M49	Beclomethasone dipropionate
M9	Cefsulodin sodium salt	M50	Methyl benzethonium chloride
M10	Loratadine	M51	Simvastatin
M11	Benzthiazide	M52	Sulfachloropyridazine
M12	Nalidixic acid sodium salt	M53	Reserpine
M13	Novobiocin sodium salt	M54	Deferoxamine mesylate
M14	Mirabegron	M55	Dolasetron mesilate
M15	Procyclidine hydrochloride	M56	Flecainide acetate
M16	Sulfamerazine	M57	Aminohippuric acid
M17	Roxithromycin	M58	Spiramycin
M18	Bromopride	M59	Urapidil hydrochloride
M19	Methylhydantoin-5-(D)	M60	Piperacillin sodium salt
M20	Isosorbide dinitrate	M61	Lorglumide sodium salt
M21	Theobromine	N1	Ethoxyquin
M22	Sulfamethoxypyridazine	N2	Thonzonium bromide
M23	Meglumine	N3	Sulfamethazine sodium salt
M24	Flumethasone	N4	(-)-MK 801 hydrogen maleate
M25	Butylparaben	N5	Dicumarol
M26	Flunixin meglumine	N6	Salmeterol
M27	Metyrapone	N7	Isocarboxazid
M28	Fenoprofen calcium salt dihydrate	N8	Florfenicol
M29	Estrone	N9	Oxiconazole Nitrate
M30	Furaltadone hydrochloride	N10	Trimipramine maleate salt
M31	Rolipram	N11	Lanatoside C
M32	Fluocinonide	N12	Suprofen
M33	Flucytosine	N13	Nisoldipine
M34	Bendroflumethiazide	N14	Oxalamine citrate salt
M35	Phenoxybenzamine hydrochloride	N15	Beta-Escin
M36	Eucatropine hydrochloride	N16	Indoprofen
M37	Tyloxapol	N17	Tigecycline
M38	Flurandrenolide	N18	Ethynylestradiol 3-methyl ether
M39	Piromidic acid	N19	Ethotoin
M40	Halcinonide	N20	Tolmetin sodium salt dihydrate
M41	Fosfosal	N21	Chlorcyclizine hydrochloride
M42	Tetraethylenepentamine pentahydrochloride	N22	Azacytidine-5
M43	Trichlormethiazide	N23	Pramoxine hydrochloride

Table S11: Drugs used in the primary screening *(continued)*

Position	Drug	Position	Drug
N24	Bicalutamide	O1	S-(+)-ibuprofen
N25	Mephentermine hemisulfate	O2	Chlorotrianisene
N26	Clioquinol	O3	Flurbiprofen
N27	Cefazolin sodium salt	O4	Guanadrel sulfate
N28	N-Acetyl-L-leucine	O5	Quinapril hydrochloride
N29	Glycopyrrolate	O6	Alexidine dihydrochloride
N30	Fluspirilen	O7	Dehydroisoandosterone 3-acetate
N31	Diethylstilbestrol	O8	Merbromin
N32	Nitrendipine	O9	Prazosin hydrochloride
N33	Tinidazole	O10	Methotrimeprazine maleat salt
N34	Idazoxan hydrochloride	O11	Deoxycorticosterone
N35	Guaifenesin	O12	Nilvadipine
N36	Bephenium hydroxynaphthoate	O13	Furazolidone
N37	Methimazole	O14	Suxibuzone
N38	Altretamine	O15	Nadolol
N39	Lithocholic acid	O16	Acitretin
N40	Megestrol acetate	O17	Viloxazine hydrochloride
N41	Rebamipide	O18	Tazobactam
N42	Chloropyramine hydrochloride	O19	Iocetamic acid
N43	Benzamil hydrochloride	O20	Estropipate
N44	Deflazacort	O21	Iodixanol
N45	Acefylline	O22	Tetrahydrozoline hydrochloride
N46	Propantheline bromide	O23	Doxazosin mesylate
N47	Thiamine hydrochloride	O24	Benzethonium chloride
N48	Carbenoxolone disodium salt	O25	Acetaminophen
N49	Tramadol hydrochloride	O26	Fluorometholone
N50	(-) -Levobunolol hydrochloride	O27	Ioversol
N51	3-alpha-Hydroxy-5-beta-androstan-17-one	O28	Sulfadimethoxine
N52	(+) -Levobunolol hydrochloride	O29	Promethazine hydrochloride
N53	Diphenylpyraline hydrochloride	O30	Folinic acid calcium salt
N54	Paromomycin sulfate	O31	Dioxybenzone
N55	Finasteride	O32	Monensin sodium salt
N56	Scopolamine hydrochloride	O33	Ethynodiol diacetate
N57	Liranaftate	O34	Ribostamycin sulfate salt
N58	Oxybenzone	O35	Nimodipine
N59	Trimetozine	O36	Vidarabine
N60	Pipemidic acid	O37	Nilutamide
N61	Aprepitant	O38	Proadifen hydrochloride

Table S12: Drugs used in the primary screening *(continued)*

Position	Drug	Position	Drug
O39	Benserazide hydrochloride	P15	Pinaverium bromide
O40	Hexylcaine hydrochloride	P16	Sulconazole nitrate
O41	Timolol maleate salt	P17	Avermectin B1a
O42	Dienestrol	P18	Aminophylline
O43	Urosiol	P19	Irsogladine maleate
O44	Etanidazole	P20	Ethaverine hydrochloride
O45	Dichlorphenamide	P21	Warfarin
O46	6-Furfurylaminopurine	P22	Ethopropazine hydrochloride
O47	Moxalactam disodium salt	P23	Irinotecan hydrochloride trihydrate
O48	Zonisamide	P24	Equilin
O49	Dimethadione	P25	Cefmetazole sodium salt
O50	Ibandronate sodium	P26	Methylhydantoin-5-(L)
O51	Ganciclovir	P27	Doxofylline
O52	Butylscopolammonium (n-) bromide	P28	Luteolin
O53	Clinafloxacin	P29	Cefuroxime sodium salt
O54	Hexestrol	P30	Carbachol
O55	Fluvastatin sodium salt	P31	Balsalazide Sodium
O56	Trioxsalen	P32	Esmolol hydrochloride
O57	Phthalylsulfathiazole	P33	Ebselen
O58	Cephalothin sodium salt	P34	Methylatropine nitrate
O59	Rabeprazole Sodium salt	P35	Mevalonic-D, L acid lactone
O60	Sulfanilamide	P36	Nisoxetine hydrochloride
O61	Diacerein	P37	Pipenzolate bromide
P1	Levonordefrin	P38	L(-)-vesamicol hydrochloride
P2	Adrenosterone	P39	Isopropamide iodide
P3	Isoetharine mesylate salt	P40	Protriptyline hydrochloride
P4	Nabumetone	P41	Cinoxacin
P5	Methacholine chloride	P42	Allopurinol
P6	Bacitracin	P43	Cycloheximide
P7	Sulfameter	P44	Stavudine
P8	Ketorolac tromethamine	P45	Amrinone
P9	Zomepirac sodium salt	P46	Aminocaproic acid
P10	Iodipamide	P47	Denatonium benzoate
P11	Drofenine hydrochloride	P48	Buspirone hydrochloride
P12	(+,-)-Octopamine hydrochloride	P49	Remoxipride Hydrochloride
P13	Pridinol methanesulfonate salt	P50	Acetylcysteine
P14	Proparacaine hydrochloride	P51	Nitrocaramiphen hydrochloride

Table S13: Drugs used in the primary screening *(continued)*

Position	Drug	Position	Drug
P52	Famciclovir	Q30	Nifekalant
P53	Gliquidone	Q31	Bosentan
P54	5-fluorouracil	Q32	Articaine hydrochloride
P55	Alfadolone acetate	Q33	Moxifloxacin
P56	Clofibrate	Q34	Tridihexethyl chloride
P57	Flucloxacillin sodium	Q35	Silodosin
P58	Topotecan	Q36	Iopanoic acid
P59	Isradipine	Q37	Ezetimibe
P60	Gatifloxacin	Q38	Ioxaglic acid
P61	Halofantrine hydrochloride	Q39	Donepezil hydrochloride
Q1	Imatinib	Q40	Lansoprazole
Q2	Etomidate	Q41	Pidotimod
Q3	Nelfinavir mesylate	Q42	(-)-Eseroline fumarate salt
Q4	Moricizine hydrochloride	Q43	Anagrelide
Q5	Ipriflavone	Q44	Ranolazine
Q6	Phensuximide	Q45	Indinavir sulfate
Q7	(R)-Duloxetine hydrochloride	Q46	Fexofenadine hydrochloride
Q8	Imidurea	Q47	Loteprednol etabonate
Q9	Aminacrine	Q48	Procarbazine hydrochloride
Q10	(S)-propranolol hydrochloride	Q49	Pemetrexed disodium
Q11	Cefuroxime axetil	Q50	Enilconazole
Q12	Spaglumic acid	Q51	Doxycycline hydrochloride
Q13	Irbesartan	Q52	Pirlindole mesylate
Q14	Perindopril	Q53	Bromhexine hydrochloride
Q15	Epirubicin hydrochloride	Q54	Dimaprit dihydrochloride
Q16	Mecamylamine hydrochloride	Q55	Cefdinir
Q17	Cisatracurium besylate	Q56	Ribavirin
Q18	Canrenone	Q57	Mitotane
Q19	Anastrozole	Q58	Azapropazone
Q20	THIP Hydrochloride	Q59	Aripiprazole
Q21	Melengestrol acetate	Q60	Deptropine citrate
Q22	Nandrolone	Q61	Azithromycin
Q23	Dopamine hydrochloride	R1	Isometheptene mucate
Q24	Pizotifen malate	R2	Gemcitabine
Q25	Mesna	R3	Nomegestrol acetate
Q26	Alfaxalone	R4	Formoterol fumarate
Q27	Cyclophosphamide	R5	Penbutolol sulfate
Q28	Trapidil	R6	Trimebutine
Q29	Atorvastatin	R7	Pivmecillinam hydrochloride

Table S14: Drugs used in the primary screening *(continued)*

Position	Drug	Position	Drug
R8	Rizatriptan benzoate	R51	Saquinavir mesylate
R9	Naftifine hydrochloride	R52	Ceftibuten
R10	1,8-Dihydroxyanthraquinone	R53	Floxuridine
R11	Bethanechol chloride	R54	Fleroxacin
R12	Benidipine hydrochloride	R55	Naftopidil dihydrochloride
R13	Isosorbide mononitrate	R56	Amcinonide
R14	Clopidogrel	R57	Guaiacol
R15	Misoprostol	R58	Celecoxib
R16	Terbinafine	R59	Fluvoxamine maleate
R17	4-aminosalicylic acid	R60	Triclosan
R18	Tolterodine tartrate	R61	Apramycin
R19	Viomycin sulfate	S1	Fluocinolone acetonide
R20	Raltitrexed	S2	Ethamsylate
R21	Methacycline hydrochloride	S3	Losartan
R22	Sulbactam	S4	Letrozole
R23	Pronethalol hydrochloride	S5	Racepinephrine hydrochloride
R24	Anethole-trithione	S6	Molindone hydrochloride
R25	Oxfendazol	S7	Pravastatin
R26	Carprofen	S8	Sertaconazole nitrate
R27	Cyclopenthiazide	S9	Doxapram hydrochloride
R28	Ambrisentan	S10	Piperidolate hydrochloride
R29	Meptazinol hydrochloride	S11	Pantoprazole sodium
R30	Ethinylestradiol	S12	Milrinone
R31	Sertraline	S13	Nateglinide
R32	Ibudilast	S14	(R)-Propranolol hydrochloride
R33	Nifurtimox	S15	Cefpiramide
R34	Olmesartan	S16	Topiramate
R35	Pancuronium bromide	S17	Phenothiazine
R36	Rufloxacin	S18	Cyclopentolate hydrochloride
R37	Prednicarbate	S19	Rasagiline
R38	Nevirapine	S20	Verteporfin
R39	Levopropoxyphene napsylate	S21	Ampiroxicam
R40	Tegaserod maleate	S22	Ronidazole
R41	Meprylcaine hydrochloride	S23	Valsartan
R42	Nitazoxanide	S24	Sotalol hydrochloride
R43	Cyproterone acetate	S25	Clavulanate potassium salt
R44	Perospirone	S26	Tracazolate hydrochloride
R45	Levalbuterol hydrochloride	S27	Caffeine
R46	Benzoxiquine	S28	Proscillaridin A
R47	Sulfadoxine	S29	Candesartan
R48	Histamine dihydrochloride	S30	Prothionamide
R49	Clonixin Lysinate	S31	Enoxacin
R50	Lomerizine hydrochloride	S32	Darunavir

Table S15: Drugs used in the primary screening *(continued)*

Position	Drug	Position	Drug
S33	Sparfloxacin	T9	Zalcitabine
S34	Moxonidine	T10	Rivastigmine
S35	Benztropine mesylate	T11	Piretanide
S36	Arbutin	T12	Amorolfine hydrochloride
S37	Montelukast	T13	Oxprenolol hydrochloride
S38	Alcuronium chloride	T14	Tolcapone
S39	Rosiglitazone Hydrochloride	T15	Ticarcillin sodium
S40	Repaglinide	T16	Algestone acetophenide
S41	Amlexanox	T17	Formestane
S42	Trifluridine	T18	Adapalene
S43	Tegafur	T19	Nelarabine
S44	Methantheline bromide	T20	Pregabalin
S45	Avobenzone	T21	(-)-Isoproterenol hydrochloride
S46	Ciprofibrate	T22	Lofepramine
S47	Fenoldopam	T23	Ramipril
S48	D-cycloserine	T24	Risedronic acid monohydrate
S49	Enalaprilat dihydrate	T25	Azaperone
S50	Estriol	T26	Triclabendazole
S51	Flumethasone pivalate	T27	Decamethonium bromide
S52	Meropenem	T28	Mepivacaine hydrochloride
S53	Alosetron hydrochloride	T29	Memantine Hydrochloride
S54	Dorzolamide hydrochloride	T30	Methenamine
S55	Milnacipran hydrochloride	T31	Norgestimate
S56	Gestrinone	T32	Cladribine
S57	Valproic acid	T33	Zuclopenthixol dihydrochloride
S58	Zardaverine	T34	Granisetron
S59	Carvedilol	T35	Gabexate mesilate
S60	Pramipexole dihydrochloride	T36	Clarithromycin
S61	Fludarabine	T37	Alprostadil
T1	Fluticasone propionate	T38	Telmisartan
T2	Olopatadine hydrochloride	T39	Benzathine benzylpenicillin
T3	Fursultiamine Hydrochloride	T40	Cilnidipine
T4	Desloratadine	T41	Methyldopate hydrochloride
T5	Etilefrine hydrochloride	T42	Sildenafil
T6	Vecuronium bromide	T43	Piperacetazine
T7	Tocainide hydrochloride	T44	Enrofloxacin
T8	Docetaxel	T45	Ondansetron Hydrochloride

Table S16: Drugs used in the primary screening *(continued)*

Position	Drug	Position	Drug
T46	Altrenogest	U24	Nialamide
T47	Thiethylperazine dimalate	U25	Besifloxacin hydrochloride
T48	Actarit	U26	Rifabutin
T49	Benzylpenicillin sodium	U27	Oxymetholone
T50	Diatrizoic acid dihydrate	U28	Clocortolone pivalate
T51	(+,-)-Synephrine	U29	Desonide
T52	Homoveratrylamine	U30	Indatraline hydrochloride
T53	Sarafloxacin	U31	Estradiol Valerate
T54	Valdecoxib	U32	Piribedil hydrochloride
T55	Mephenytoin	U33	Diclazuril
T56	Palonosetron hydrochloride	U34	Phenylbutazone
T57	Cefepime hydrochloride	U35	Fluconazole
T58	Brimonidine L-Tartrate	U36	Lymecycline
T59	Darifenacin hydrobromide	U37	Lamotrigine
T60	Rifaximin	U38	Lodoxamide
T61	Ozagrel hydrochloride	U39	Tulobuterol
U1	Phentermine hydrochloride	U40	Rimexolone
U2	Chlormadinone acetate	U41	Bifonazole
U3	Vardenafil	U42	Torsemide
U4	Proguanil hydrochloride	U43	Fosinopril
U5	Anthralin	U44	Pyrvinium pamoate
U6	Pivampicillin	U45	Hexachlorophene
U7	Tripelennamine hydrochloride	U46	Quinethazone
U8	Tribenoside	U47	Troxipide
U9	Nalmefene hydrochloride	U48	Oxaprozin
U10	Risperidone	U49	Estramustine
U11	Imiquimod	U50	Vorinostat
U12	Levocabastine hydrochloride	U51	Azatadine maleate
U13	Acetylsalicylic acid	U52	Methiazole
U14	Oxyphenbutazone	U53	Phenprobamate
U15	Ubenimex	U54	Homosalate
U16	Propoxycaine hydrochloride	U55	Cefpodoxime proxetil
U17	Felbamate	U56	Toltrazuril
U18	Mesalamine	U57	Ritonavir
U19	Ethoxzolamide	U58	Parbendazole
U20	Methicillin sodium	U59	Latanoprost
U21	Dofetilide	U60	Nadifloxacin
U22	(S)-(-)-Cycloserine	U61	Cefprozil
U23	Zoledronic acid hydrate		